

this document downloaded from

# vulcanhammer.info

the website about  
Vulcan Iron Works  
Inc. and the pile  
driving equipment it  
manufactured

Visit our companion site  
<http://www.vulcanhammer.org>

## Terms and Conditions of Use:

All of the information, data and computer software ("information") presented on this web site is for general information only. While every effort will be made to insure its accuracy, this information should not be used or relied on for any specific application without independent, competent professional examination and verification of its accuracy, suitability and applicability by a licensed professional. Anyone making use of this information does so at his or her own risk and assumes any and all liability resulting from such use. The entire risk as to quality or usability of the information contained within is with the reader. In no event will this web page or webmaster be held liable, nor does this web page or its webmaster provide insurance against liability, for any damages including lost profits, lost savings or any other incidental or consequential damages arising from the use or inability to use the information contained within.

This site is not an official site of Prentice-Hall, Pile Buck, or Vulcan Foundation Equipment. All references to sources of software, equipment, parts, service or repairs do not constitute an endorsement.

US-CE-C

Property of the United States Government

S-75-5



TECHNICAL REPORT S-75-5

# WAVE EQUATION ANALYSES OF PILE DRIVING

by

D. Michael Holloway

Soils and Pavements Laboratory

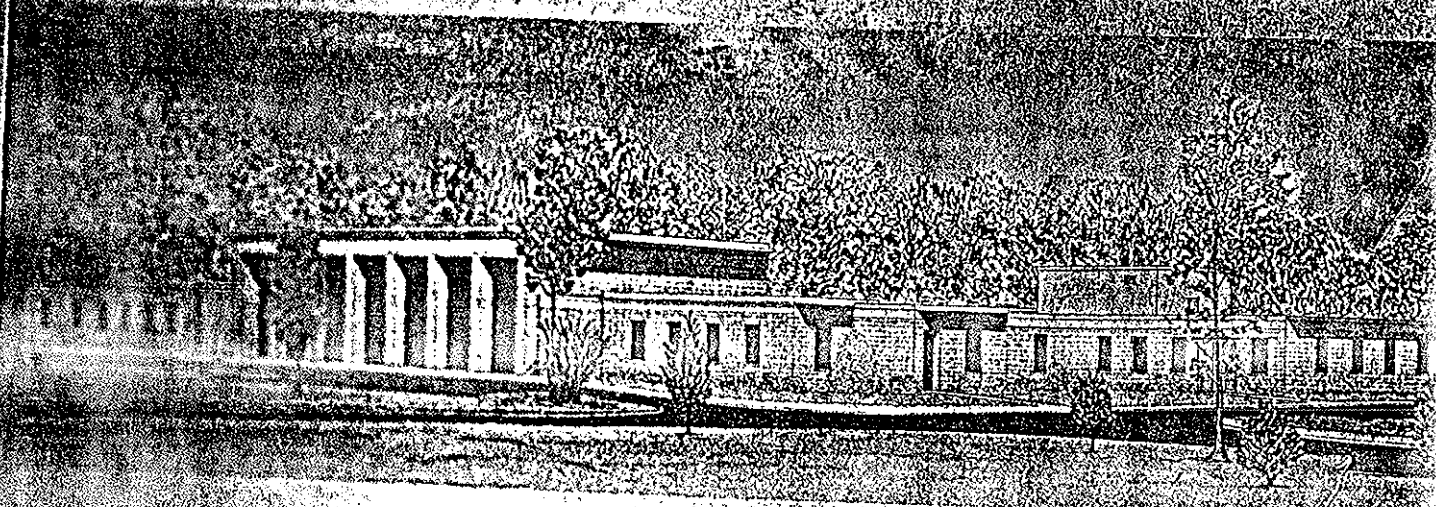
U. S. Army Engineer Waterways Experiment Station  
P. O. Box 631, Vicksburg, Miss. 39180

June 1975

Final Report

AD B604-8544

Distribution limited to U. S. Government agencies only; computer program documentation  
June 1975. Other requests for this document must be referred to U. S. Army Engineer  
Waterways Experiment Station.



Prepared for Office, Chief of Engineers, U. S. Army  
Washington, D. C. 20314

Under Project No. 4A161102B52E,  
Task 04, Work Unit 010

LIBRARY BRANCH  
TECHNICAL INFORMATION CENTER





Unclassified

SECURITY CLASSIFICATION OF THIS PAGE (When Data Entered)

REPORT DOCUMENTATION PAGE		READ INSTRUCTIONS BEFORE COMPLETING FORM
1. REPORT NUMBER Technical Report S-75-5	2. GOVT ACCESSION NO.	3. RECIPIENT'S CATALOG NUMBER
4. TITLE (and Subtitle)  WAVE EQUATION ANALYSES OF PILE DRIVING		5. TYPE OF REPORT & PERIOD COVERED  Final report
		6. PERFORMING ORG. REPORT NUMBER
7. AUTHOR(s)  D. Michael Holloway		8. CONTRACT OR GRANT NUMBER(s)
9. PERFORMING ORGANIZATION NAME AND ADDRESS U. S. Army Engineer Waterways Experiment Station Soils and Pavements Laboratory P. O. Box 631, Vicksburg, Miss. 39180		10. PROGRAM ELEMENT, PROJECT, TASK AREA & WORK UNIT NUMBERS Project 4A161102B52E Task 04, Work Unit 010
11. CONTROLLING OFFICE NAME AND ADDRESS  Office, Chief of Engineers, U. S. Army Washington, D. C. 20314		12. REPORT DATE June 1975
		13. NUMBER OF PAGES 105
14. MONITORING AGENCY NAME & ADDRESS (if different from Controlling Office)		15. SECURITY CLASS. (of this report)  Unclassified
		15a. DECLASSIFICATION/DOWNGRADING SCHEDULE
16. DISTRIBUTION STATEMENT (of this Report)  Distribution limited to U. S. Government agencies only; computer program documentation; June 1975. Other requests for this document must be re- ferred to U. S. Army Engineer Waterways Experiment Station.		
17. DISTRIBUTION STATEMENT (of the abstract entered in Block 20, if different from Report)		
18. SUPPLEMENTARY NOTES		
19. KEY WORDS (Continue on reverse side if necessary and identify by block number)  Cohesive soils Pile driving Wave equations		
20. ABSTRACT (Continue on reverse side if necessary and identify by block number)  The one-dimensional wave equation analysis has been found to be superior to dynamic formulae and other available numerical techniques for analyzing impact pile-driving behavior. The results are usually acceptable for selection of efficient hammer-pile-soil systems; somewhat limited success has been attained in predicting pile bearing capacity, particularly for piles in cohesive soils. The most successful applications of wave equation solutions have involved the (Continued)		

Unclassified

SECURITY CLASSIFICATION OF THIS PAGE(When Data Entered)

20. ABSTRACT (Continued).

selection of compatible driving equipment and determination of pile driveability. Evaluation of peak driving stresses has reduced the incidence of pile breakage. Computer programs from Texas A&M University were adapted to computer facilities at the U. S. Army Engineer Waterways Experiment Station. The wave equation theory was reviewed, and analytical solutions based on one-dimensional theory were described. Examples of wave equation applications to practical engineering problems are presented. A time-sharing version of the Texas A&M design-oriented computer program is listed and usage guidelines are provided.

Unclassified

SECURITY CLASSIFICATION OF THIS PAGE(When Data Entered)

CATEGORY B

ELECTRONIC COMPUTER PROGRAM ABSTRACT			
TITLE OF PROGRAM Wave Equation Analyses of Pile Driving (TAMFOR)		PROGRAM NO. 741-F3-R0007	
PREPARING AGENCY U. S. Army Engineer Waterways Experiment Station, Geotechnical Laboratory, P. O. Box 631, Vicksburg, MS 39180			
AUTHOR(S) D. Michael Holloway	DATE PROGRAM COMPLETED June 1975	STATUS OF PROGRAM	
		PHASE Init	STAGE Op
A. PURPOSE OF PROGRAM  One-dimensional wave equation analysis for analyzing impact pile-driving behavior.			
B. PROGRAM SPECIFICATIONS  Written in standard time-sharing FORTRAN.			
C. METHODS  Program adapted from Texas A&M University programs and converted to a time-sharing mode.			
D. EQUIPMENT DETAILS  G-635 computer with time-sharing capability.			
E. INPUT-OUTPUT  See documentation described below.			
F. ADDITIONAL REMARKS  Documentation contained in WES TR S-75-5, "Wave Equation Analyses of Pile Driving," by D. M. Holloway, June 1975.			



## PREFACE

The work reported herein was conducted at the U. S. Army Engineer Waterways Experiment Station (WES) under the sponsorship of the Directorate of Military Construction, Office, Chief of Engineers, under Research in Military Engineering and Construction, Project 4A161102B52E, Task 04, Work Unit No. 010, Study of Pile-Driving Stresses by the Wave Equation.

This study was conducted and the report was prepared by Mr. D. M. Holloway of the Soil Mechanics Division (SMD) under the direction of Mr. C. L. McAnear, Chief, SMD, Soils and Pavements Laboratory (S&PL). Mr. J. P. Sale was Chief, S&PL.

BG E. D. Peixotto, CE, and COL G. H. Hilt, CE, were Directors of WES during the course of this investigation and the preparation of this report. Mr. F. R. Brown was Technical Director.



## CONTENTS

	Page
PREFACE . . . . .	1
CONVERSION FACTORS, U. S. CUSTOMARY TO METRIC (SI) UNITS OF MEASUREMENT . . . . .	3
PART I: INTRODUCTION . . . . .	4
PART II: WAVE EQUATION THEORY . . . . .	6
One-Dimensional Wave Equation . . . . .	6
Assumptions . . . . .	10
PART III: MATHEMATICAL MODELS . . . . .	12
Finite Difference Method . . . . .	12
Smith's Numerical Model . . . . .	14
Electronic Analog Method . . . . .	23
Finite Element Method . . . . .	27
PART IV: MATERIAL BEHAVIOR REPRESENTATIONS . . . . .	32
Hammers . . . . .	32
Driving Accessories . . . . .	36
Piling . . . . .	38
Pile-Soil Interaction . . . . .	39
PART V: WAVE EQUATION APPLICATIONS . . . . .	45
Finite Difference Wave Equation Computer Program . . . . .	45
Basic Concepts . . . . .	47
Equipment Selection . . . . .	50
Bearing Capacity Prediction . . . . .	52
Example Problems . . . . .	59
PART VI: CONCLUSIONS AND RECOMMENDATIONS . . . . .	69
REFERENCES . . . . .	71
TABLES 1-9	
APPENDIX A: WAVE EQUATION COMPUTER PROGRAM TAMFOR . . . . .	A1
Basic Parameters . . . . .	A2
Problem Parameters . . . . .	A5
APPENDIX B: NOTATION . . . . .	B1

# CONVERSION FACTORS, U. S. CUSTOMARY TO METRIC (SI) UNITS OF MEASUREMENT

U. S. customary units of measurement used in this report can be converted to metric (SI) units as follows:

<u>Multiply</u>	<u>By</u>	<u>To Obtain</u>
inches	2.54	centimeters
feet	0.3048	meters
square inches	6.4516	square centimeters
inches per second	2.54	centimeters per second
inches per second per second	2.54	centimeters per second per second
feet per second	0.3048	meters per second
feet per second per second	0.3048	meters per second per second
cubic feet per minute	0.02831685	cubic meters per minute
pounds (mass)	0.4535924	newtons
pounds (force)	4.448222	newtons
kips (1000 pounds)	4448.222	kilograms
pounds per inch	175.1268	newtons per meter
pounds per square inch	6894.757	pascals
pounds per cubic foot	16.0185	kilograms per cubic meter
tons per square foot	9764.86	kilograms per square meter
kips per square inch	6894757	kilopascals
pound-seconds <sup>2</sup> per inch <sup>4</sup>	0.10693	newton-seconds <sup>2</sup> per centimeter <sup>4</sup>
pound-seconds per feet <sup>4</sup>	515.4369	newton-seconds per meter <sup>4</sup>
pound-seconds per inch	1.751268	newton-seconds per meter
foot-pounds	1.355818	joules
seconds per foot	3.2808398	seconds per meter

## WAVE EQUATION ANALYSES OF PILE DRIVING

### PART I: INTRODUCTION

1. The selection of compatible and economical pile-driving equipment, the prevention of pile damage in driving, and the prediction of pile bearing capacity from driving data are often major considerations in pile-driving problems.

2. The application of stress wave propagation theory to pile-driving problems has provided the only rational method for analyzing an extremely complex engineering problem. The development of high-speed digital computers has made numerical solutions to wave equation problems the most versatile method for studying pile-driving behavior.

3. The purpose of this study is to examine wave equation solutions to pile-driving problems and to present particular applications of the methods that have significant practical value to the Corps of Engineers. Computer programs from Texas A&M University (TAMU) publications have been adapted for use on computer facilities at the U. S. Army Engineer Waterways Experiment Station (WES), and a condensed version of the design-oriented TAMU program has been modified for time-sharing usage.

4. Wave equation theory is discussed in Part II. The one-dimensional wave equation is derived in detail based upon the equilibrium equation of motion at a point on a rod. The necessary initial conditions and boundary conditions are described, and the inherent assumptions generated by the problem formulation are emphasized in this part.

5. Direct solutions to the differential (wave) equation are extremely difficult except for a few special cases. The general pile-soil interaction behavior is far too complicated to solve by closed-form solution techniques, as a rule. The mathematical models which may be employed in obtaining practical (approximate) solutions to the wave equation problems are described in detail in Part III. Finite difference (lumped parameter) methods are given particular attention. An electronic analog computer method is described in some detail, and

finally, applications of finite element methods to pile foundation behavior are briefly discussed.

6. Part IV focuses on the material behavior representations that may be applied in the solutions of pile-driving problems. Hammer assembly components and piling materials have been thoroughly studied to determine necessary behavior parameters for use in wave equation analyses. Pile-soil interaction properties at the pile tip and along the shaft have received considerable attention in the literature. The work of various investigators in ascertaining these data is described in this part.

7. Part V contains detailed descriptions of wave equation applications to practical engineering problems. The finite difference computer programs developed at TAMU are described in some detail. A version of the design-oriented TAMU program has been adapted for use on time-sharing computer facilities at WES. The file name for the time-sharing program is TAMFOR, a FORTRAN program, and a printout of TAMFOR is included in Appendix A. Several basic concepts of pile-driving behavior have been delineated as a result of wave equation applications. Use of the wave equation methods in equipment selection, pile-driving performance, and bearing capacity prediction are described. Example problems solved using TAMFOR complete Part V.

8. Part VI discusses several conclusions and recommendations that can be drawn from this research effort.

9. Impact pile driving involves a multitude of essential variables in describing the mechanical behavior of the hammer-pile-soil system. The dynamic interaction of the component parts of the physical system includes nonlinear and inelastic material deformations, complex energy losses, foundation nonhomogeneity, deformation and deformation rate-dependent soil response, and transient phenomena such as pore pressure dissipation and consolidation. A mathematical model which can incorporate any and all of the system variables for a driven pile has yet to be developed.

## PART II: WAVE EQUATION THEORY

10. The basis of the dynamic wave propagation problem rests in Newton's second law; namely, the vector sum of the forces acting on a body is equal to the product of mass times the resulting acceleration. In continuum mechanics this statement is incorporated into the equations of motion at a point (dynamic equilibrium) employing appropriate constitutive model representation for the transmitting medium. The simplest form of these equations describes dynamic equilibrium at a point on a one-dimensional rod subject to a longitudinal stress wave.

### One-Dimensional Wave Equation

11. If an element of the rod is examined in a free-body diagram, Figure 1, the equation of equilibrium is prescribed by Newton's second law:

$$\Sigma \bar{F}^* = \left( \frac{W}{g} \right) \bar{a} \quad (1)$$

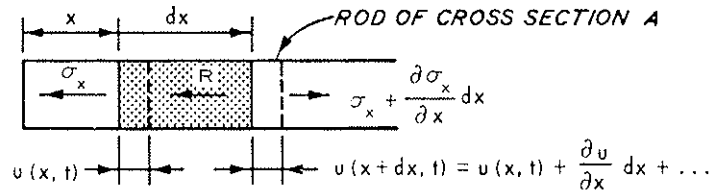
where

$\bar{F}$  = resultant force

$W$  = element weight

$g$  = gravity acceleration

$\bar{a}$  = particle acceleration



#### LEGEND

$u(x, t)$  = DISPLACEMENT AT A POINT ON THE ROD, L

$\sigma_x(x, t)$  = STRESS AT A POINT ON THE ROD, F/L<sup>2</sup>

$R(x, t)$  = RESISTANCE AT A POINT ON THE ROD, F/L

$A(x)$  = CROSS-SECTIONAL AREA AT A POINT ON THE ROD, L<sup>2</sup>

$\rho(x)$  = MASS DENSITY AT A POINT ON THE ROD, M/L<sup>3</sup>

Figure 1. Rod element free-body diagram

---

\* For convenience, symbols and unusual abbreviations are listed and defined in the Notation (Appendix B).

12. Regardless of the deformation properties of the rod, the sum of the forces applied to the element equates to the product of the elemental mass times the resultant acceleration in the form:

$$\left[ -\sigma_x + \left( \sigma_x + \frac{\partial \sigma_x}{\partial x} dx \right) \right] A - R dx = (\rho A dx) \frac{\partial^2 u}{\partial t^2} \quad (2)$$

where

$\sigma_x = \sigma_x(x, t)$ ; stress at a point on the rod,  $F/L^2$  where  $F$  = force and  $L$  = length

$x$  = coordinate location of a point along the rod

$A = A(x)$ ; cross-sectional area,  $L^2$

$R = R(x, t)$ ; element resistance force, lb\*,  $F/L$

$\rho = \rho(x)$ ; mass density,  $M/L^3$ , where  $M$  = mass

$u = u(x, t)$ ; element displacement,  $L$

$t$  = time

13. Rewriting Equation 2 after cancelling and factoring like terms gives the wave equation in terms of stresses

$$A \frac{\partial \sigma_x}{\partial x} - R = \rho A \frac{\partial^2 u}{\partial t^2} \quad (3)$$

If the material may be assumed to be a linearly elastic solid subject only to infinitesimal strains, a Hookean stress-strain law for small strain theory yields

$$\sigma_x = E \epsilon_x = E \frac{\partial u}{\partial x} \quad (4)$$

where

$E = E(x)$  = Young's modulus,  $F/L^2$

$\epsilon_x$  = strain at point along the rod

14. Imposing these assumptions on Equation 3 gives the general differential equation of motion as a function of the unknown displacement  $u(x, t)$  in the form:

---

\* A table of factors for converting U. S. customary units of measurement to metric (SI) units is presented on page 3.



$$A \frac{\partial}{\partial x} \left( E \frac{\partial u}{\partial x} \right) - R = \rho A \frac{\partial^2 u}{\partial t^2} \quad (5)$$

15. With a knowledge of the material properties as well as the resistance behavior along the rod, the differential equation can be solved. To determine a solution to a particular problem, sets of initial conditions and physical boundary conditions must also be known.

16. Initial conditions generally specify the displacement, velocity, and resistance distributions at a known instant of time,  $t_0$ . Boundary conditions establish the appropriate deformation response of the rod at each end. For example, the boundary at the free end must be stress-free such that the strain is zero. At a rigidly fixed boundary, the displacement remains constant.

17. Writing out the system of equations which completely define a problem gives the differential equation (wave equation):

$$A \frac{\partial}{\partial x} \left( E \frac{\partial u}{\partial x} \right) - R = \rho A \frac{\partial^2 u}{\partial t^2} \quad (6)$$

a. Initial conditions:

$$u(x, t) = u_0(x) \quad \text{at} \quad t = t_0$$

$$\frac{\partial u}{\partial t}(x, t) = V_R(x) \quad \text{at} \quad t = t_0$$

$$R(x, t) = R_0(x) \quad \text{at} \quad t = t_0$$

where

$o(\text{subscript})$  = initial value with respect to time

$V_R$  = ram impact velocity

b. Boundary conditions:

$$u(x, t) \text{ or } \frac{\partial u}{\partial x}(x, t) \text{ at } x = 0$$

$$u(x, t) \text{ or } \frac{\partial u}{\partial x}(x, t) \text{ at } x = L$$

18. Application of these initial and boundary conditions satisfies a necessary condition for the existence of a unique solution. An exact mathematical solution to such a system of equations is practicable only for certain special cases. For general problems, an engineering solution is usually found by approximate methods.

19. Some simplifications of the differential equation should be discussed. For an isotropic, homogeneous rod,  $E$  and  $\rho$  are constants, such that

$$\frac{E}{\rho} \frac{\partial^2 u}{\partial x^2} - \frac{R}{A\rho} = \frac{\partial^2 u}{\partial t^2} \quad (7a)$$

20. For a freely suspended rod, the resistance  $R$  vanishes such that the differential equation becomes

$$\frac{E}{\rho} \frac{\partial^2 u}{\partial x^2} = \frac{\partial^2 u}{\partial t^2} \quad (7b)$$

This is the most common form of the one-dimensional wave equation described in engineering mechanics texts.<sup>1,2</sup> The quantity  $E/\rho$  is usually given as a term  $c^2$ ;  $c$  is defined as the velocity of wave propagation, a measurable material property.

21. The influence of end conditions and the resulting stress wave reflection deserve consideration at this point. For a freely suspended uniform elastic rod, an impact compression stress wave travels with constant velocity  $c$  and no change in wave shape. As this compression stress wave reaches a free end (stress-free boundary), the boundary condition imposes a zero stress state at the end. As a result, an incident stress wave is reflected from a free end traveling in the opposite direction with the same wave shape but with the opposite stress sense; i.e., a compression stress wave is reflected as a tension stress wave. At a fixed end, on the other hand, the stress wave is reflected as an identical stress wave of the same stress sense traveling in the opposite direction. This causes the stress wave to "stack up" at a fixed boundary, and indeed double the stress wave magnitude at the boundary. Typical physical problems provide

intermediate boundary conditions to these two extremes (see Figure 2).

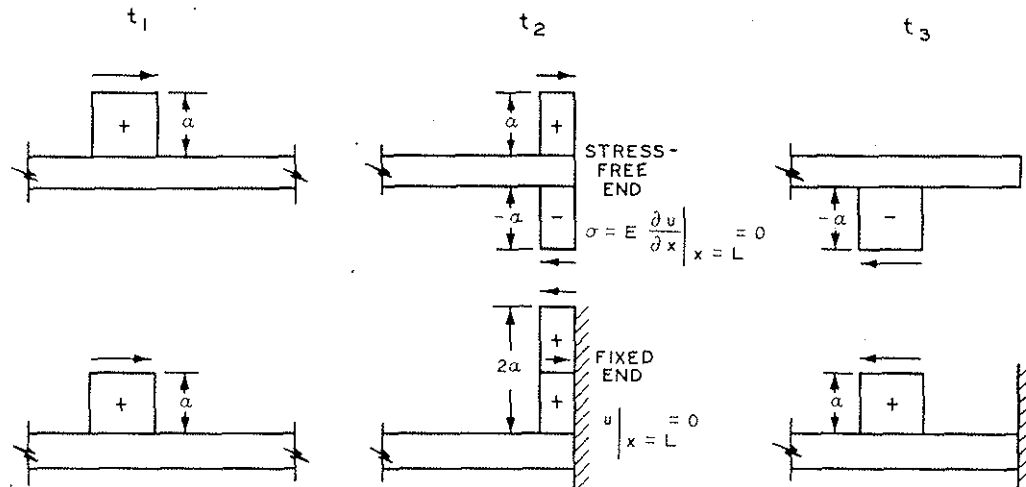


Figure 2. Boundary stress wave reflection

#### Assumptions

22. The limitations and discrepancies involved in the mathematical formulation of a problem are often unclear. It is therefore important to reiterate the assumptions involved in the problem derivation.

23. Equilibrium Equation 5 imposes small strain theory (infinitesimal displacements) for the rod. As long as the rod is stiff relative to the stress level, this assumption causes little inaccuracy. Were the rod relatively soft, the three-dimensional effects and geometric nonlinearity could cause considerable errors. In most physical problems, the rod is assumed to behave as a linear elastic solid, following the stress-strain relation given by Equation 4. Significant material nonlinearity may also require reevaluation of these assumptions.

24. The dynamic resistance to motion due to external forces may be a complex function of space- and time-dependent variables. For example, the resistance at a point along the rod may depend on the displacement and time derivatives of displacement at that location. Material damping and related dynamic phenomena may be included as "resistance" forces opposing the rod motion.

25. The problem of pile-soil interaction is the focus of the one-dimensional wave equation analysis described herein. Equation 5 permits variations in cross section, Young's modulus, mass density, and resistance along the axis of the rod. The determination of "known" material behavior parameters is no simple task. Knowledge of soil stress-deformation conditions in the vicinity of a laboratory model test pile is rather limited. For the field problem, the estimation of the pile-soil interaction properties is, at best, a crude exercise of engineering judgment.

26. The one-dimensional wave equation is the mathematical representation of an idealized, classical mechanics problem. In applying solutions to the wave equation, it is of utmost importance to recognize the gross simplification that is required to provide an engineering solution to an extremely complicated problem. As in all engineering problems, the solution may be only as reliable as the assumptions required by the method.

### PART III: MATHEMATICAL MODELS

27. The solution to an engineering problem generally requires a mathematical formulation which represents the problem and which may be solved economically with "reasonable" accuracy. The pile-driving problem is extremely complex in terms of physical variables which significantly influence pile behavior. Incorporating all these factors in a rational formulation of the problem is a mammoth undertaking. It is generally concluded that approximate solutions of considerably simplified (solvable) problems are the only reasonable engineering solutions available.

28. Finite difference numerical analogs to the physical problem have been employed with much success in the past decade. Numerical solutions to the idealized problem have been developed using both digital and analog computer programming techniques. Finite element techniques have developed sufficient sophistication to describe the possible material behavior and soil-pile interaction adequately. With finite element methods, a finite difference scheme is generally employed to include time-dependent behavior iteratively. To date, however, a dynamic finite element formulation of the pile-driving problem has not been presented in the literature.

29. This part will describe the basic mathematical formulation in some detail. The limitations and advantages of each procedure will be discussed for practical purposes.

#### Finite Difference Method

30. A finite difference approximation to a differential equation discretizes the physical problem into small segments. For the wave equation solution, the pile must be subdivided longitudinally into discrete masses interconnected by springs allowing equivalent deformation characteristics between mass centroids. Time also must be subdivided into small increments. The solution to a pile-driving problem may be approximated by integration with respect to time

progressing from prescribed initial displacement, stress, and velocity conditions for all elements in the hammer-pile-soil system. A brief derivation of a finite difference representation follows.

31. The first partial derivative of displacement with respect to location,  $\frac{\partial u}{\partial x}$ , may be written in finite difference form as

$$\frac{\partial u}{\partial x}_{m-1,m} \approx \frac{u(m, n) - u(m-1, n)}{\Delta x} \quad (8a)$$

for the change in  $u$  with respect to  $x$ , where  $\Delta x$  is the pile element length, between pile elements  $m$  and  $m-1$  during time interval  $n$ . The change in  $u$  with respect to  $x$  between elements  $m+1$  and  $m$  may also be written in this form replacing appropriate element displacements

$$\frac{\partial u}{\partial x}_{m,m+1} \approx \frac{u(m+1, n) - u(m, n)}{\Delta x} \quad (8b)$$

such that the change in  $u$  with respect to  $x$  is defined between elements  $m-1$  and  $m$  and between elements  $m$  and  $m+1$ . In a similar fashion, the second derivative with respect to  $x$  across element  $m$  may be approximated as the difference between equations (the changes in  $u$  with respect to  $x$ ) divided by  $\Delta x$ , or

$$\begin{aligned} \frac{\partial^2 u}{\partial x^2} &\approx \left[ \frac{u(m+1, n) - u(m, n)}{\Delta x} - \frac{u(m, n) - u(m-1, n)}{\Delta x} \right] \frac{1}{\Delta x} \\ \frac{\partial^2 u}{\partial x^2} &\approx \frac{u(m+1, n) - 2u(m, n) + u(m-1, n)}{(\Delta x)^2} \end{aligned} \quad (9)$$

32. An identical operation may be performed to obtain the second partial derivative of  $u$  with respect to time  $t$  such that one may write

$$\frac{\partial^2 u}{\partial t^2} \approx \frac{u(m, n+1) - 2u(m, n) + u(m, n-1)}{(\Delta t)^2} \quad (10)$$

where  $\Delta t$  is the time increment magnitude used for calculation.



33. In the one-dimensional wave equation (Equation 6) as described in Part II, these quantities may be substituted in difference form for the partial derivatives. For the solution to a general problem, these difference equations may require some modifications. Equations 9 and 10 assume that the change in length  $\Delta x$  and the change in time  $\Delta t$  are constants. The quantity  $\Delta t$  usually is a selected constant, but the quantities  $\Delta x$ ,  $A$ ,  $E$ , and  $\rho$  may vary (composite or tapered pile, for examples). These cause complications in generalizing this finite difference formulation since a change in stiffness (due to changes in  $A$ ,  $E$ ,  $\Delta x$ , or  $\rho$ ) between elements causes a change in the prescribed quantities between elements.

#### Smith's Numerical Model

34. To account for such possibilities, an alternate approach may be taken. Recalling that the differential wave equation represents dynamic equilibrium at a point along the pile, E. A. L. Smith formulated the difference equation describing the equilibrium of a discrete "point" mass in the discretized hammer-pile-soil system.<sup>3,4</sup> Smith's 1960 paper<sup>4</sup> provides the most thorough description of his numerical procedure, along with several excellent analogies for clarification.

35. Smith describes a subdivided hammer-pile-soil system as a one-dimensional problem, i.e., one degree of freedom per element. Each element in the hammer-pile-soil system is described as a combination of point masses, weightless springs, and dashpots. The system is interconnected as discrete elements, and these elemental properties are lumped parameters approximating the continuous system of components; namely, hammer-capblock-cushion assembly, discretized pile elements, and soil shaft and tip resistances. A typical representation of a hammer-pile-soil system is given in Figure 3.

36. The equilibrium equation for pile element  $m$  during time increment  $n$  may be written as Newton's second law, Equation 1. The pile spring forces are related as a function of relative element displacements. Soil resistance acting on an element is computed using

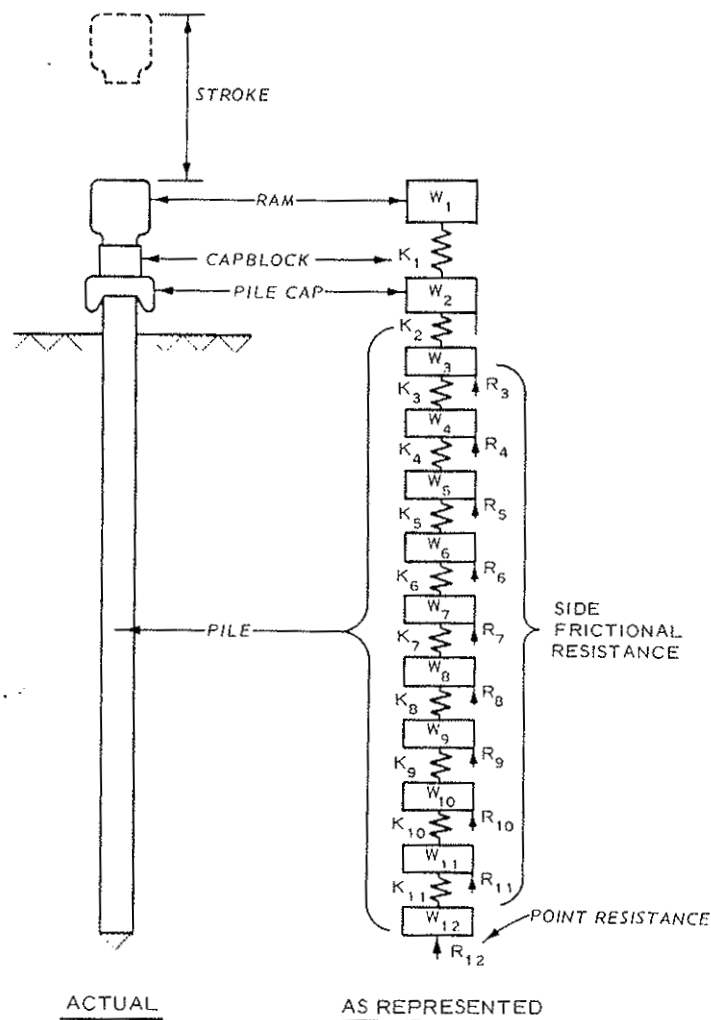


Figure 3. Smith's lumped parameter representation  
(from Reference 4)

element displacement and velocity values. The total displacement of element  $m$  after  $n$  time increments is generally computed by integration with time from specified initial conditions using the equilibrium equation of motion in difference form.

37. Smith's notation will be described and used in presenting his algorithm. The use of uppercase (capital) letters denotes quantities after the current time increment  $n$ ; lowercase letters represent values after the previous time increment,  $n - 1$ . The asterisk value of a

variable, for example  $d_m^*$ , is defined as the variable's value after two time intervals previous,  $n - 2$ . The variable subscript  $m$  denotes the element component.

$A$  = cross-sectional area, sq in.

$C$  = spring compression, in.

$D$  = displacement, in.

$D'$  = plastic displacement, in.

$e$  = coefficient of restitution

$E$  = modulus of elasticity, lb/sq in.

$F$  = spring force, lb

$g$  = gravity acceleration, 32.2 ft/sec/sec

$J$  = point resistance damping constant, sec/ft

$J'$  = shaft resistance damping constant, sec/ft

$K$  = pile spring constant, lb/in.

$K'$  = soil spring constant, lb/in.

$\ell$  = pile element length, in.

$(\text{subscript})^m$  = pile element

$(\text{subscript})^n$  = current time interval of computation

$p$  = value of  $m$  subscript at pile point

$Q$  = quake (maximum elastic soil deformation), in.

$R$  = resistance, lb

$RU$  = maximum static soil resistance, lb

$s$  = permanent pile set, in.

$T_m$  = critical time interval for spring  $m$ , sec

$u$  = element displacement, in.

$V$  = element velocity, ft/sec

$W$  = element weight, lb

$Z$  = resultant force, lb

$\rho$  = mass density,  $\frac{\text{lb-sec}^2}{\text{ft}^4}$

$\Delta t$  = time increment magnitude used for calculation, sec

38. Smith's algorithm in general form employs a nest of five

basic equations which he presented originally in 1955.<sup>3</sup> These equations are in the forms:

$$D_m = d_m + v_m (12 \Delta t) \quad (11a)$$

$$C_m = D_m - D_{m+1} \quad (11b)$$

$$F_m = C_m K_m \quad (11c)$$

$$Z_m = F_{m-1} - F_m - R_m \quad (11d)$$

$$V_m = v_m + Z_m \frac{\Delta t g}{W_m} \quad (11e)$$

39. Smith<sup>4</sup> showed that these five equations can be combined to solve for displacement  $D_m$  as follows:

$$D_m = 2d_m - d_m^* + \frac{12 g (\Delta t)^2}{W_m} \times \left[ \left( d_{m-1} - d_m \right) K_{m-1} - \left( d_m - d_{m+1} \right) K_m - R_m \right] \quad (12)$$

where  $d_m^*$  is the value of displacement after  $n - 2$  time intervals.

40. If Equations 9 and 10 are substituted into the differential equation, Equation 6, Smith's notation may be used to substitute for quantities as follows:

$$D_m = u(m, j + 1)$$

$$d_m = u(m, j)$$

$$d_m^* = u(m, j - 1)$$

$$R_m = \ell_m R$$

$$K_m = \frac{AE}{\ell_m}$$

$$\rho = \frac{W_m}{\ell_m A(12g)}$$

Rewriting Equation 6 in these terms gives

$$A \frac{\partial}{\partial x} \frac{K_m \ell_m}{A} \frac{(d_{m+1} - d_m)}{\ell_m} - \frac{R_m}{\ell_m} = \frac{W_m}{\ell_m (12g)} \frac{D_m - 2d_m + d_m^*}{(\Delta t)^2} \quad (13)$$

Performing the partial difference on the left-hand side gives

$$A \frac{K_{m-1} (d_m - d_{m-1}) - K_m (d_m - d_{m+1})}{A \ell_m} - \frac{R_m}{\ell_m} = \frac{W_m}{\ell_m (12g)} \frac{D_m - 2d_m + d_m^*}{(\Delta t)^2} \quad (14)$$

Solving Equation 14 for  $D_m$  gives a solution identical with Smith's formulation, Equation 12.

41. In order to apply this procedure for a pile-driving problem, several significant conditions need clarification. Most of these points are discussed in detail in Smith's paper.<sup>4</sup>

42. Time increment magnitude  $\Delta t$  used in the calculations is particularly important for assuring a convergent, stable solution. If too large a time increment is chosen, the stress wave may "bypass" an element, and the solution would become unstable. Should too small an interval be selected, the economy of the solution would be seriously reduced and possible numerical errors may be magnified.

43. The "critical" value of the time increment would be at least as small as the time required for the stress wave to traverse each element in one or more intervals. The stress wave velocity in a freely suspended elastic rod is given by the quantity  $E/\rho$ . The time required to transmit a stress wave a given distance along the rod is simply determined as the distance divided by the wave velocity.

44. For the discrete elements of the procedure, a finite time interval may also be defined. The value of  $\rho$  may be computed as

$$\rho = \frac{W}{A \ell g}$$

Likewise, the value of  $K$  is defined by

$$K = \frac{AE}{\ell}$$

45. For the critical time interval for spring,  $m$ , the stress wave may pass in either direction such that the "critical" value of time interval for this spring is the lesser of two values defined by the equation set:

$$\begin{aligned} T_m &= \frac{1}{1.9648} \sqrt{\frac{W_m + 1}{K_m}} \\ T_m &= \frac{1}{1.9648} \sqrt{\frac{W_m}{K_m}} \end{aligned} \quad (15)$$

46. In the case of a freely suspended rod with equally spaced, uniform segments, a time increment computed by Equation 15 would give the "exact" solution.<sup>4</sup> In pile-driving problems, the composition of the pile, the soil resistance, and the boundary conditions influence the wave transmission velocity at a given location. For that reason, the magnitude of time interval  $\Delta t$  generally is chosen as a fraction of the minimum  $T_m$  value of the pile-soil system (commonly  $0.5 T_m$ ).

47. Soil resistance behavior is usually specified in a simplified fashion due to the uncertainties involved in estimating in situ soil conditions. Pile driving introduces significant soil system disturbances, causing large shear deformations, soil volume change and/or excess pore fluid pressures, and serious changes in soil stress conditions from "at rest" conditions.

48. Smith proposed the use of a simple elastic-plastic soil deformation model for static soil response. As such, the entire element behavior can be defined by two parameters: the elastic quake  $Q$  and the peak elemental soil resistance  $RU_m$  (see Figure 4). The elastic stiffness of the soil spring is defined as

$$K'_m = \frac{RU_m}{Q} \quad (16)$$



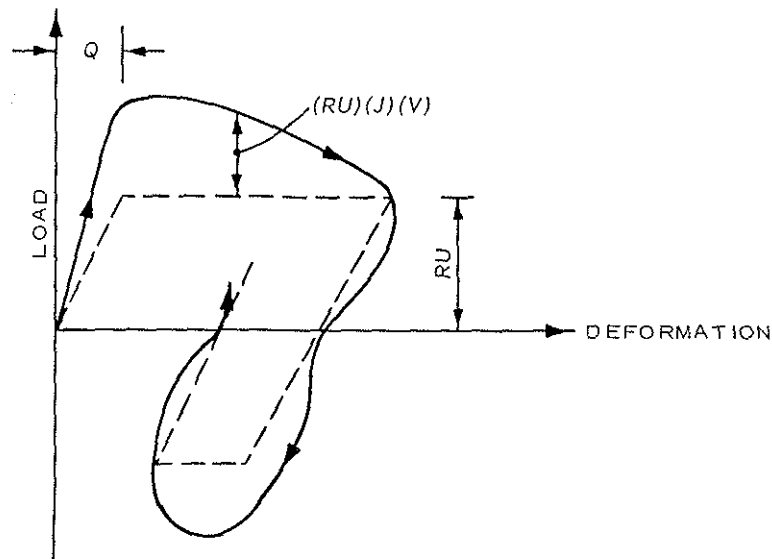
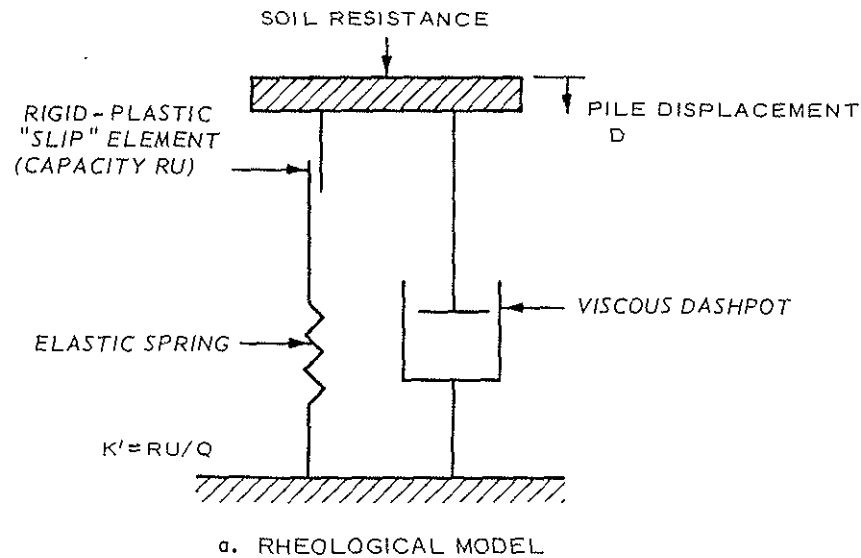


Figure 4. Soil behavior model (after Smith<sup>4</sup>)

and, therefore, the static resistance in the elastic range of displacements ( $-Q \leq D_m \leq Q$ ) is proportional to  $D_m$ . For values of  $D_m$  outside the elastic range ( $|D_m| > Q$ ), the static resistance remains a constant value ( $\pm RU_m$ ). To facilitate computations, Smith introduced a value of plastic displacement  $D'_m$  as the difference between  $D_m$  and the corresponding quake ( $\pm Q$ ). The static soil resistance may be

written as

$$R_m = (D_m - D'_m)K'_m \quad (17)$$

where  $R_m$  = shaft element resistance in which the value of  $D'_m$  must be set equal to zero whenever  $D_m$  is elastic.

49. Recognizing the occurrence of transient resistance forces during driving, Smith proposed that a viscous component of resistance be included. This assumes that the transient driving effects are separable from static resistance forces as dynamic components of resistance. Smith defines the dynamic resistance as the product of the instantaneous values of static resistance and velocity and an appropriate damping constant,  $J$  or  $J'$ , for the tip or shaft behavior, respectively. The damping constants are prescribed in seconds per foot. The general form of shaft element resistance,  $R_m$ , is given as

$$R_m = (D_m - D'_m)K'_m(1 + J'v_m) \quad (18)$$

and for the point resistance,  $R_{p+1}$ , the proper constants are substituted as

$$R_{p+1} = (D_p - D'_p)K'_{p+1}(1 + Jv_p) \quad (19)$$

50. It must be noted that the dynamic resistance curve shown in Figure 4b does not correspond to the damping effects represented in Equation 18. The damping component for negative resistance forces with negative element velocities in Equation 18 describes a dynamic resistance force that is less than the static (dashed curve) force level. For conventional analyses (single blow stopped at the start of tip rebound) this error is inconsequential. Further discussion of this is given elsewhere.<sup>5</sup>

51. Cushion inelasticity may have a profound effect on the energy transmitted by the hammer to the pile. Permanent deformation of cushion materials causes energy losses which reduce the efficiency of

the pile-driving system. Smith suggested that an equivalent bilinear cushion model could be applied in the numerical model with little loss in accuracy.

52. The coefficient of restitution  $e$  is readily computed from the ratio of energy output (during unloading) to the energy input (during loading), i.e.,

$$e^2 = \frac{\text{Energy Output}}{\text{Energy Input}}$$

53. For the case of a bilinear material, Figure 5, the ratio of the load modulus to the unload modulus is equivalent to  $e^2$ , such that the cushion deformation behavior may be defined by two parameters,  $K$  and  $e$ , where  $K$  is the loading stiffness of the cushion.

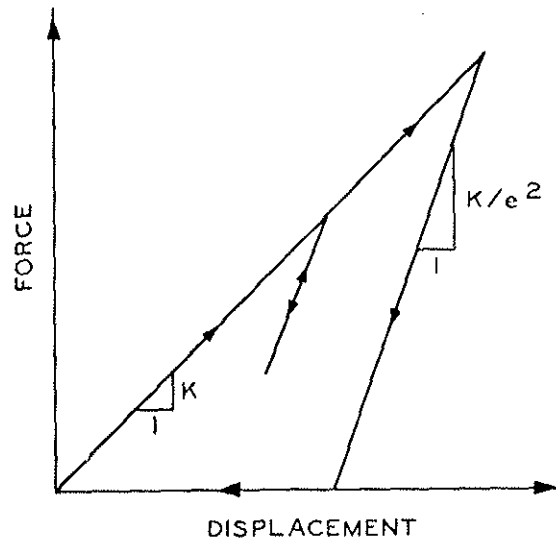


Figure 5. Bilinear elastic spring defined  
(from Smith<sup>4</sup>)

54. Using the bilinear representation, Smith<sup>4</sup> prescribed an alternate to Equation 11c for an inelastic spring in the form

$$F_m = \frac{K_m}{(e_m)^2} C_m - \left[ \frac{1}{(e_m)^2} - 1 \right] K_m C_{m \max} \quad (20)$$

whenever the spring compression  $C_m$  is less than the temporary maximum compression value previously computed,  $C_{m \max}$ . This formulation provides for an unload/reload modulus which models cushion inelasticity as in Figure 5.<sup>4</sup>

55. For real materials the load-displacement behavior is generally nonlinear. The normal recommendation is that secant modulus values be selected, and these are dependent upon the peak stress level. The details of the behavior of cushion materials are described in Part IV.

56. No tension conditions occur wherever interconnecting elements are incapable of transmitting tension stresses/strains across their boundaries. The ram impact does not involve any contact tension stresses. The helmet, pile cap, and cushions are usually loosely fitted to prevent the transmission of tension stresses across these elements. The soil tip resistance has no capability of generating tension stresses to resist motion. Finally, some joints may be included or required in a pile. These connections can permit unrestrained or limited tensile deformation at such a joint to reduce or eliminate tensile strains and stresses. Smith discusses procedures involved in establishing such element conditions in the numerical model.<sup>4</sup> Programmable computer logic can easily accommodate these conditions.

57. Smith generated a computer program incorporating these equations.<sup>4</sup> Subsequent investigations have refined this method to improve the computational accuracy based upon program usage and field observations. The most extensive efforts have pursued the determination of system material properties and correlations with field tests. The results of these studies are discussed in subsequent parts.

#### Electronic Analog Method

58. An alternative method for solving systems of differential equations involves the use of analog computers. Basic concepts and various applications of analog computation are beyond the scope of this report. Fundamental texts on this subject may be referred to for

specific techniques.<sup>6,7</sup> This discussion will be limited to one particular study of the pile-driving problem.

59. In his dissertation Parola developed an analog computer program to model the behavior of impact between a ram and a drivehead, transmitting driving energy to a continuous elastic rod.<sup>8</sup> He assumes that the rod is of infinite length to eliminate reflection boundary conditions. In the equilibrium equations of motion, he neglects the weight of the drivehead in order to simplify the system of equations, but does include the drivehead mass. With these points in mind, the equations of motion for the ram and drivehead may be written in the form

$$\frac{W_1}{g} \ddot{u}_1 + K_1 (u_1 - u_2) - W_1 = 0 \quad (21)$$

$$\frac{W_2}{g} \ddot{u}_2 + \rho c A \dot{u}_2 - K_1 (u_1 - u_2) = 0 \quad (22)$$

where

$W_1$  = ram weight, lb

$g$  = 386 in./sec/sec

$\ddot{u}_m = \frac{d^2 u_m}{dt^2}$ , in./sec/sec, where  $m$  = subscript denoting element number

$K_1$  = cushion stiffness or spring constant, lb/in.

$u_1$  = ram displacement, in.

$u_2$  = drivehead displacement, in.

$W_2$  = drivehead weight, lb

$\rho$  = pile mass density, lb-sec<sup>2</sup>/in.<sup>4</sup>

$c$  = wave propagation velocity, in./sec

$A$  = pile cross-sectional area, sq in.

$\dot{u}_m = \frac{du_m}{dt}$ , in./sec

60. In Equation 22, the term  $\rho c A$  represents the "pile impedance" to motion, a quantity dependent upon material properties and

ing capacities" by 23 percent, 32 percent, and 20 percent, respectively.

180. Analyses of pile tests conducted for Jonesville Lock and Dam, Jonesville, Louisiana,<sup>41</sup> indicated that significantly different soil parameters were in order. Example problems from these pile tests are also included in the next section.

181. Precast concrete piles, 18 by 18 in. square, were driven into an abandoned course deposit of medium dense to very dense fine sands, with a highly penetration-resistant lense between 35 ft and 40 ft below grade. Test pile 1 penetrated 38 ft so that the tip rested in this stiffer material. Test piles 2 and 3 penetrated through this stiffer layer with tips at elevations 45 ft and 54 ft, respectively, well within a very dense sand deposit.

182. The use of a higher quake value (0.15 in.) underestimated the pile capacities considerably. The standard value (0.10 in.) did not sufficiently correct the estimates. Reducing the tip damping parameter to zero provided the best "prediction" for test pile 1. Recognition of higher tip capacity in the stiff layer was also necessary. Test piles 2 and 3 still had somewhat lower "predicted" capacities, nonetheless. The data for these problems are presented graphically in the results of these example problems.

183. A study examining the driveability of large-diameter steel pipes with a fixed soil plug introduced some interesting facts that were borne out by field observations. Wave equation analyses of the 6-ft-diam, 1.5-in.-thick walled pipe with a 19-ft soil plug at the bottom revealed that the added mass of the soil in the tip caused serious stress reflection and "stacking" at the diaphragm because of the discontinuity. It was recommended that these piles were unsuitable for driving with such a plug. Piles which had been driven previously exhibited buckling behavior at the diaphragm.<sup>42</sup>

184. The results of the various investigations indicate that accurate pile capacity predictions require a prior knowledge of soil parameters that vary as much as site conditions. This is not surprising since the behavior of every single pile is a unique engineering problem.



prediction. TAMU investigators have held that the tip quake should be relatively independent of any scale effects. For the case of large-diameter piling, particularly in softer soils, it might be expected that the "elastic" displacement (quake) is somewhat larger in magnitude.

176. The consideration that tip quake might in some manner be proportional to the tip diameter was discussed at the Second CWRU Pile-Driving Seminar, August 1972. A tip quake value of 0.10 in. per foot of tip diameter was suggested.

177. Use of larger tip quake values profoundly reduces the apparent pile driveability or the attainable pile capacity for a particular impact hammer. An increase in tip quake value reduces the computed set and therefore increases the blowcount. It is of interest to note that the computed total pile tip displacement is little affected by the tip quake value assumed. The significant factor rests with the assumption of full elastic tip rebound commonly used in the computations.

178. The details of analyses performed on test piles 1, 2, and 3 of the Arkansas River Lock and Dam No. 4 pile test project<sup>40</sup> are included in the example problems. Briefly, steel pipe piles were embedded approximately 53 ft into a medium dense deposit of primarily fine sands and silty sands. Smith's standard soil parameters were assumed except for the tip quake values. These piles were 12.75-in., 16-in., and 20-in. OD pipe piles driven closed-end. The tip quake was assumed proportional to the tip diameter for these analyses.

179. By using the adjustment to tip quake values, better  $RU_{TOTAL}$  values were "predicted" than when 0.10-in. tip quake was assumed. Note that  $RU_{TOTAL}$  is the maximum resistance that must be overcome to cause penetration. Pile capacities based upon bearing capacity criteria often are significantly less than the maximum load the pile would sustain during the load test, especially for piles in cohesionless soils. Any correlations must take this into consideration. The wave equation predictions underestimate  $RU_{TOTAL}$  (measured) by 13 percent, 9 percent, and 9 percent for test piles 1, 2, and 3, respectively. In these cases, however,  $RU_{TOTAL}$  (measured) was greater than the "bear-

employ procedures for inputting force pulse data in lieu of hammer impact simulation. The TAMU report includes pile-driving force and acceleration measurements in the analyses.<sup>25</sup>

172. In addition to the wave equation procedure, CWRU has developed a simplified method which has been adapted to a specialized field computer. The procedure involves integration circuitry to determine the velocity at the pile top from acceleration input. The pile is assumed to behave as a rigid mass, but the scheme uses the average of the force measured at the time of zero velocity  $t_0$  and at one full wave length later  $t_0 + 2L/C$ , less the average inertia resistance over the time interval  $(t_0, t_0 + 2L/C)$ . The field computer instantaneously performs this function calculation and displays the computed resistance for every blow or every  $n$ th blow as required.<sup>33,36</sup>

173. The field computer operation and measurement methods have been demonstrated at two seminars held at CWRU and at the Specialty Conference held at Purdue University in June 1972.<sup>39</sup> The field instrumentation may include a pipe pile section designed as a force transducer, or "clip-on" strain transducers, and piezoelectric accelerometers. These are arranged and connected such that bending effects can be cancelled out. The most significant advances have come in the development of four-channel magnetic tape recordings of the instrumentation data and in the development of an analog-to-digital conversion process that have streamlined the operation immeasurably.

174. The modified, time-sharing version of the TAMU computer program, TAMFOR, has been used at WES to analyze several pile-driving problems. Pile tests conducted at Arkansas River Lock and Dam No. 4 and at Jonesville Lock and Dam, Jonesville, Louisiana, were analyzed in detail. The example problems at the end of the part include these piles. Analyses of an off-shore pile and a large-diameter, partially plugged pile were also studied. The wave equation program has also been used to evaluate the performance of the WES soil compaction hammer.

175. One consideration which was investigated involved the influence of tip quake magnitude in the eventual pile capacity

this research has also been published.

167. The method prescribed by the CWRU group utilizes the mathematical redundancy of having measurements for both force and acceleration. With acceleration data, the force can be computed as an output from a one-dimensional wave equation (lumped mass) solution. The CWRU procedure adjusts element soil resistance parameters (linear elastic-plastic springs and linear viscous dashpots) numerically to match the measured force-versus-time data using the acceleration-versus-time data as the input boundary condition at the pile top. In this fashion, both the pile capacity and the resistance distribution along the pile may be predicted.

168. The dynamic measurements used in the prediction scheme are made upon re-driving of the pile after all transient effects (setup, pore pressure dissipation, etc.) are assumed to have passed. The numerical procedure used to generate the solution employs a predictor-corrector method (Newmark method) which the CWRU group recommends as more efficient and more accurate than current techniques being applied to pile-driving analyses.<sup>33</sup>

169. The results obtained by the CWRU studies indicate reasonably accurate predictions of both pile capacities and load distributions for piles in cohesionless soils. Differentiation between static and dynamic resistance forces was remarkably consistent for piles in cohesionless deposits.

170. Predictions determined for piles in cohesive soils were far less accurate. The CWRU group attributed the inaccuracies to inadequacy of the soil resistance model for predicting the response of cohesive soils.

171. The primary advantage of obtaining force and acceleration measurements is obviously that these quantities are measured directly at the pile top. Inaccuracies in assumptions and simulations of hammer assembly behavior can be avoided since the acceleration- and/or force-versus-time records can be used as input to the pile top in the wave equation analysis. The research version of the TAMU computer program<sup>15</sup> and the finite difference program used by Parola in his dissertation<sup>8</sup>

tions may be subject to considerable scatter. In a TAMU study, pile load tests in sands, in clays, and in layered sands and clays revealed appreciable scatter in the prediction accuracy.<sup>31</sup> Soil resistance distributions, soil quake, and soil damping parameters were varied to determine a "best fit" of the field data; nonetheless, the scatter was significant. For piles in sands only, the average error was computed as  $\pm 25$  percent with some errors as great as  $\pm 40$  percent. For piles in clays only, the average error approached  $\pm 55$  percent while in two cases, capacities estimated by the wave equation were more than twice the pile capacities at driving. The error in terms of load magnitude was comparable to that noted for piles in sands since the piles in clay generally had lower capacity.

164. Similar correlation studies have been performed in an effort to improve predictions by the wave equation. A new soil resistance model was developed from laboratory soil testing and model pile tests.<sup>21,23</sup> The revised model has proven unacceptable in applications to full-scale pile tests, such that TAMU researchers have returned to Smith's basic model, Equation 18, with appropriate adjustments to the parameter values to correct the computation predictions.<sup>24,25,32</sup>

165. Foye et al.<sup>25</sup> adjusted pile capacities to values estimated at the time of driving. For the case of piles load-tested long after driving, he corrected for pile "setup." In some cases, redriving data after pile load tests were used to determine wave equation predictions. With these modifications to the application of wave equation results, Foye's data provided superior "predictions" of pile capacity. Once again, the new values for soil parameters, listed in Table 5, were used in Smith's rheological model.<sup>25</sup>

166. Investigators at Case Western Reserve University (CWRU) have developed a sophisticated instrumentation scheme to record continuous impact force and acceleration data at the pile top during driving. Detailed information on the CWRU research is provided in the August 1970 project report.<sup>33</sup> Papers published in various technical journals and presented at technical sessions of conferences describe the on-going research at CWRU.<sup>34-37</sup> A dissertation by Rausche<sup>38</sup> concerning

formulae for timber, precast concrete, and steel piles. Other investigators have performed similar exercises rendering "corrected" formulae using analyses of their own data.

159. The general dissatisfaction with the use of pile-driving formulae to predict pile bearing capacity accurately is well documented in the literature. The vast number of formulae available testifies to the futility of such formulations. Nonetheless, dynamic formulae are still used in foundation design and are also written in many building codes in lieu of a reasonable alternative. Dynamic formulae have been used quite successfully in analyses of "standard piles" in local projects where considerable field data have been correlated.

160. Wave equation analyses provide a rational method of incorporating almost every conceivable variable in a mathematical model of the physical problem. As such, the wave equation solution is the most versatile and most complete procedure for analyzing pile-driving problems. Since a host of variable combinations are possible, the wave equation solution does not condense into a single formula.

161. With regard to pile capacity predictions, the wave equation computer program calculates pile penetration under a single hammer blow. The pile-soil resistance properties are input parameters for the particular problem. The computation progresses from the initial ram impact, employing numerical integration with respect to finite time increments. Pile element displacements are accumulated until the pile tip element begins to rebound. The pile set per blow (for the prescribed  $RU_{TOTAL}$  capacity) is determined as the maximum tip displacement minus the elastic quake,  $Q_p$ .

162. A series of problems can be solved for a given hammer assembly-pile system using a range of  $RU_{TOTAL}$  values anticipated in the design. The results may be presented graphically as a curve of pile capacity (during driving) versus blow count (1/set). Pile capacities can be predicted directly from the curve by comparison with routine blow count field data.

163. Comparisons between wave equation calculations and pile load tests indicate that the predictive performance of wave equation solu-

as precast concrete piles.

155. Piles of low impedance may prevent achievement of designed foundation performance. High impedance piling may be inefficient and, therefore, less economical under some circumstances. The selection of an efficient pile-hammer-soil system should include a parametric evaluation of the equipment under consideration at the design phase. This is subject to the foundation design, the contractor equipment availability, and the effective selection of accessories consistent with engineering decisions necessary. The optimum design of pile foundations requires a delicate balance of equipment and foundation conditions.<sup>8</sup>

#### Bearing Capacity Prediction

156. The determination of pile bearing capacity from measurements made during pile driving has been the subject of hundreds of engineering studies. The results from most of these investigations have been limited in value at best and generally inadequate for practical purposes.

157. Several hundred pile-driving formulae proliferate in the literature.<sup>29</sup> These formulae usually assume rigid mass impact between the hammer and pile. The interaction of the hammer assembly-pile-soil system is crudely approximated, if at all, in every case. Behavior variables in stress wave transmission are impossible to include in these formulations.

158. Many of the pile-driving formulae are generated using empirical correlations, and published formulae often are subsequently modified after correlation studies of other investigators. A typical study of the performance of several formulae in predicting pile capacities in sands<sup>30</sup> indicated that the type of pile significantly influenced the accuracy of a given formula. For the 93 pile tests examined by Olson and Flaate,<sup>30</sup> the Engineering News formula and the Pacific Coast Uniform Building Code formula exhibited considerably more scatter than some others they studied. Based upon correlations, these investigators modified the Gates formula and recommended new

stresses may be calculated for preliminary analyses are also included in Reference 8. It should be noted that these curves do not include the effects of resistance magnitude and distribution which can cause an increase in peak stresses under hard driving.

151. Piles stiffer (having higher impedance values) than prescribed by Equation 36 cause the ram to rebound and thus retain energy. Piles having too low an impedance obtain only a part of the energy as the ram will follow the pile after impact, causing less efficient driving and possible pile damage. Either extreme reduces the efficiency of energy transmission significantly.<sup>8</sup>

152. The most efficient combination of components for driving piling involves not only the efficient transfer of energy to the pile, but also includes the shape of the transmitted force pulse. As described previously, more efficient driving under particular resistance conditions may require a longer impact duration (easy driving), or a short duration and higher driving stresses (hard driving). An impedance match using Equation 36 is only a guide.

153. A softer cushion and/or a heavier drivehead cause an increase in stress wave length (impact duration) and reduction in peak driving stress.<sup>8,14</sup> A larger coefficient of restitution causes higher efficiency of energy transmission to the pile. Cushion material and accessory selection can be evaluated for a particular problem using the wave equation computer program to assist in an efficient and damage-free pile design.

154. Parola suggests guidelines for pile design based upon the results of his research.<sup>8</sup> With the knowledge that impact duration is roughly inversely proportional to pile impedance, two general extremes in pile-driving systems are discernable. Long-duration impact and low pile stresses are recommended for low pile impedance conditions. These conditions are more efficient for low pile capacities (easy driving conditions). Short-duration impact and high driving stresses are compatible with high pile impedance values, yielding more efficient driving for high pile capacities (hard driving conditions). Caution against pile damage must be emphasized for high impedance piling such

detail that is often overlooked in engineering practice, though it may significantly influence both the efficiency (cost) of the construction and the quality of the final product. Wave equation analyses provide an economical method for assisting the foundation engineer in designing a compatible pile-driving system. Some applications of wave equation solutions to the selection of proper driving equipment are discussed in a subsequent section.

### Equipment Selection

148. The wave equation solution provides a particularly useful tool for selecting compatible hammer-pile-soil systems. Preliminary design studies may best employ curves and formulations based upon wave equation analyses without need for computer calculations. Detailed computer computations based upon alternative designs will thereafter provide a more accurate assessment of a proper selection, as well as delineate potential problems that may be encountered.

149. Parola<sup>8</sup> studied the hammer-cushion-pile system compatibility problem using analog computer methods. He proposes a method of equipment selection based upon the maximization of pile-driving energy transmitted to the pile. In an impact problem, transmitted energy is maximized by transferring the ram mass energy to the pile head as efficiently as possible. Based upon his analyses, Parola determined a range of values for hammer-cushion-pile parameters for which the energy transfer exceeds 90 percent efficiency. For pile drivers commonly used in practice, the match of hammer and pile impedance is accomplished if the parameters are within a range given by the relationship:

$$\rho cA = [0.6 \text{ to } 1.10] \sqrt{\frac{W_1}{g}} K \quad (36)$$

150. The quantity  $\rho cA$  denotes pile impedance while the term  $\sqrt{(W_1/g)K}$  represents a hammer system impedance (see Part III). Pile impedance values and equivalent pile section data are included in Table 1 (after Parola<sup>8</sup>). Design curves for parameters from which pile



transmitted to the pile is greatly dependent on the coefficient of restitution of the cushion materials. The cushion properties directly affect the shape of the impact force pulse imparted to the pile.<sup>8,14</sup> Thus, cushions play a dominant role in preventing hammer/pile damage and improving pile driveability. Because of the influence of peak stresses and impact duration on pile driveability and pile damage conditions, the selection of compatible and efficient cushion(s) may profoundly affect the overall design of the pile-driving system.

144. Problems of pile damage during driving can be very expensive. Several possible causes of damage may be cited. Eccentricity of ram impact can create bending and torsion stresses and stress concentrations which may damage the pile butt. The striking of an obstruction or excessively hard driving may cause compression failure near the pile tip. Bending in the pile due to obstructions or misalignment can cause pile buckling.

145. Precast, reinforced concrete piles may exhibit damage due to excessive tensile stresses/strains. Depending upon pile length and driving conditions, breakage may occur at specific points along driven piles. A TAMU research report<sup>28</sup> provides specific recommendations for driving precast concrete piles based upon wave equation analyses and field observations.

146. Parola<sup>8</sup> studied the effect of pile length upon driveability. He found that for relatively stiff piles, the impact duration is short, such that pile length and reflected stress waves have minor influence. Piles having low impedance values exhibit longer impact duration, and consequently, longer stress wave length. This is an advantage for short piles of low impedance since the addition of a reflected stress wave at the tip can perform useful work as the stress wave interacts at the tip. Parola found that for piles of low impedance, shorter piles drive more efficiently; for piles of high impedance, the pile length made little difference.

147. Proper cushion selection, based upon hammer-pile-soil conditions of a given project, is an integral part of the foundation design. The proper choice of cushion materials and dimensions is a

impact than the "equivalent" single-acting hammer under otherwise identical conditions.

139. The influence of force pulse shape has been examined analytically to evaluate pile driveability under various driving conditions. For easy driving conditions, the penetration per blow was found to be primarily dependent upon the impact duration. The longer the impact duration (stress wave), the greater the penetration. Peak force level had little effect on the penetration obtained for easy driving.<sup>8</sup>

140. For hard driving conditions (high blow counts), pile penetration was relatively independent of impact duration.

141. The peak driving stress transmitted to the pile tip has the dominant influence on the attainable pile set. The driving conditions may, therefore, cause one type of hammer to be more economical than another type for a given pile-soil system, though each hammer may have the same rate of energy.

142. Pile stiffness has a comparable influence on peak driving stresses. The use of a higher impedance (stiffer and heavier) pile causes an increase in peak pile stresses and a decrease in impact duration. This has a profound influence on driveability that might not be readily apparent. The selection of a heavier pile section under otherwise identical conditions improves the driveability of a pile under hard driving conditions. A heavier, stiffer pile might drive to a desired penetration when a lighter pile cannot. Under easy driving conditions the lighter pile will exhibit more penetration per blow.<sup>8,27</sup> This comparison is not directly applicable for a stiffer pile with a greater effective tip area and greater shaft area. These changes generally would produce a greater penetration resistance as well.

143. The choice of pile-driving accessories often has a pronounced effect on the stress wave. The primary purpose of capblock and cushion materials is to reduce driving stresses in the hammer and pile to tolerable levels. A stiffer cushion transmits higher peak stresses with shorter impact durations. The magnitude of energy

advantage in a user package described as the MAX SYSTEM. Within the remote terminal control, MAX can be called upon to list any user file, including data files, externally at the computer system printer. This availability reduces on-line terminal usage (expense) and may permit more rapid printing of the computational results. Indeed, the detailed output could be processed in this fashion since the normal remote terminal carriage character limitations would not interfere with the computer output.

134. A listing of TAMFOR, the time-sharing version of the TAMU computer program, is included in Appendix A. Details of input file usage paralleling the usage guidelines prescribed by TAMU<sup>26</sup> are also included. Example problems offered in this part were solved using TAMFOR.

#### Basic Concepts

135. The wave equation analyses have clarified several fundamental concepts of impact pile-driving behavior that, heretofore, could be interpreted only from experience. A brief discussion of these concepts should facilitate understanding of pile-driving observations.

136. Pile-driving stresses are often a critical concern to the designer. Driving conditions, hammer and accessory selection, and pile driveability are all related to driving stresses.

137. For a given driving system, the peak impact stresses are proportional to the ram impact velocity. This is obvious in the case where the ram stroke is increased, since the energy is proportionally increased. For two different hammers delivering the same energy to the pile, a lighter ram impacting at higher velocity will cause higher peak driving stresses. The higher peak stress will be accompanied by a shorter impact duration and, therefore, shorter stress wave length.

138. Diesel hammers and double-acting or differential-acting hammers generally have lighter rams and higher impact velocities than single-acting hammers at the same rate of energy. The force pulse for these hammers will show higher peak force and shorter duration of

128. For most practical problems, a simpler version of the wave equation program normally will suffice. A design-oriented computer program, adapted from Smith's basic model, is well documented in the TTI Research Report 33-11, "Piling Analysis Wave Equation Computer Program Utilization Manual."<sup>26</sup> Program listing, usage guidelines, and sample problems are included. A batch computer deck reproduced from the program list is operational on the computer system at WES.

129. A condensed version of the design-oriented computer program has been adapted for use on the WES time-sharing facilities. The major modifications concern the reduction of output to essential information in a form suitable for printout on a remote time-sharing terminal. The detailed output option on the TAMU program is deleted from the time-sharing version. For detailed output the batch mode is far more economical.

130. Program documentation and utilization guidelines for the batch version of the TAMU program are identical with those given in TTI Research Report 33-11.<sup>26</sup> The time-sharing version employs the same input sequence of parameters as the batch version. For convenience and economy, both the input and the output to the time-sharing program are accomplished using stored data files in the computer.

131. The input data file, PILES 2, uses free-form input of parameters. On the WES system, this involves the use of fixed-point and floating-point values for the parameters for which either a comma or a space specifies the end of a data item. Line numbers are used to sequence the data input in the same fashion as properly sequenced data cards are used for batch programs.

132. The data files, OUTPUT and PLOTIT, permit the storage of the computer program output. This may serve multiple purposes. The time-sharing output during program execution is usually more expensive than external listing of data files. The output data files may be renamed and saved for later listing to permit the reuse of program output files for a new problem. Several separate problems may be run in turn before the listing of the output data files by renaming these.

133. The time-sharing facilities at WES provide an additional

## PART V: WAVE EQUATION APPLICATIONS

123. Since Smith presented the first viable solution to pile-driving problems using a one-dimensional wave equation formulation, much progress has been made in application of such methods.

124. A brief description of the finite difference computer program developed at TAMU is given in this part. Some practical applications of the wave equation by various researchers are discussed in some detail. Example problems are solved using a version of the TAMU computer program adapted for use on time-sharing computer facilities. A listing of the time-sharing version of the wave equation program is included in Appendix A.

### Finite Difference Wave Equation Computer Program

125. The lumped mass discrete element model described in Part II is the basic representation of the hammer-pile-soil system used in the finite difference solution (see Figure 3). The various components which may be included in the physical system include the ram, capblock, pile cap (drivehead), cushion, pile, and soil resistance. The hammer assembly may include additional items such as an anvil. Certain elements of this configuration may be absent, such as the cushion between the drivehead and the pile. Any combination of elements is easily accommodated in the mathematical model.

126. The original program developed by Smith has been modified by several research engineers to facilitate program usage. Flexibility of input/output procedures, detailed computations of additional useful information, and minor technical changes are the main modifications that have been made to Smith's original program.

127. TAMU has published two wave equation computer programs in Texas Transportation Institute (TTI) reports.<sup>14,15</sup> A highly versatile, research-oriented program has been developed to examine the effect of virtually any variable on pile-driving behavior. A listing of this program with input parameter guidelines is given elsewhere.<sup>15</sup>

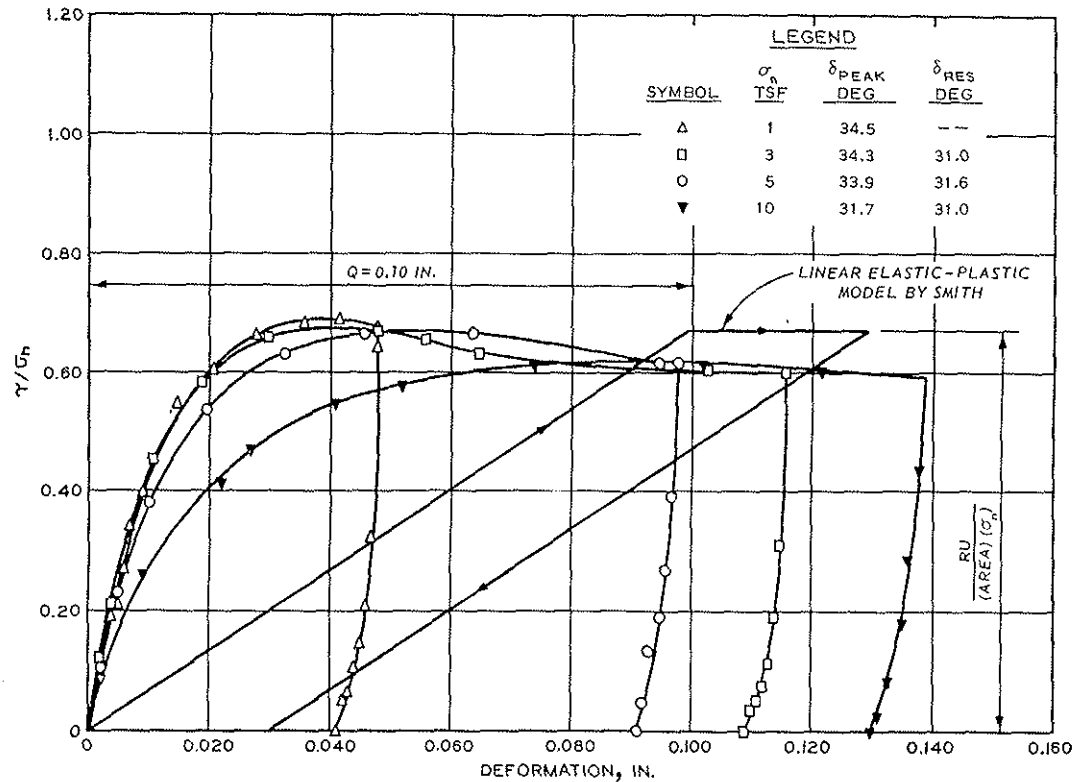


Figure 11. Typical interface shear test results for sand on mortar

final predicted blow count with the measured static pile capacity at final penetration. Having these soil parameters from one load test with a particular hammer-pile-soil system may not be sufficient for a major change in hammer, pile, or soil conditions.

122. Smith's rheological model is also prescribed for tip penetration resistance. A commonly assumed quake of 0.10 in. is usually taken to be independent of pile cross section (scale effects). For nominal pile sections in everyday practice, this assumption is reasonable. For larger diameter displacement piles, experimental evidence suggests that the "elastic" tip displacement at bearing increases with increasing diameter. The theory will be discussed in Part V.

represent correlations for which the  $RU_{TOTAL}$  versus blow count curve most closely approximated the driving resistance-blow count point corresponding to final penetration.

117. The vulnerability of the correlation procedure should be emphasized at this stage. These tabulated values are reasonable estimates on which to base preliminary calculations. Should the magnitude of the project warrant pile load tests, an effort to derive appropriate soil parameters should be included in the foundation analysis. Even with pile load test correlations, such values for soil parameters represent a one-point correlation through which a multitude of curves could conceivably pass. The generalization of such parameters for a foundation design change must be done with great care, especially if the pile bearing capacity correlation is under consideration.

118. The frictional resistance model deserves comparison with laboratory measurements of pile-soil interface shear behavior. A direct shear box may be used to simulate interface behavior. The lower section of soil is replaced by a block of pile material and the shear deformation is imposed at the material interface.

119. A plot of laboratory interface shear tests in the form of the ratio of shear stress to (constant) normal stress ( $\tau/\sigma_n$ ) versus relative displacement is shown in Figure 11 for a medium dense sand on mortar. The peak shear resistance is developed prior to the elastic quake value commonly assumed ( $Q = 0.10$  in.), and there is significant nonlinearity in the interface shear behavior. The load modulus and the unload modulus values deviate significantly from the stiffness generated by Smith's assumed quake.

120. The area between the laboratory test curve and the linear elastic-plastic model represents a substantial amount of energy which, for this material at least, is not accounted for by the static resistance model. For given hammer-pile-soil conditions, it is conceivable that the dynamic component can be adjusted to compensate for such an error in assumed static behavior.

121. It would be expected that, within bounds, a compatible quake and damping combination may be determined that correlated the

sensitive clays, the remolded strength is substantially less than the undisturbed strength such that driven piles may, indeed, reduce the soil resistance capacity. There is often a strength regain in these materials due to consolidation (pore pressure dissipation) of the material after driving. This behavior is commonly described as "setup." A strength regain in some sensitive clays may continue for many years due to consolidation and thixotropy. Piles driven in loose cohesionless deposits may also exhibit an increase in capacity after driving due to pore pressure dissipation. The actual soil resistance during driving may be considerably less than that observed after setup in these materials.

112. For granular materials in dense deposits, pile driving may induce negative pore pressures which increase the soil resistance and the related pile capacity during driving. A pile test (or subsequent re-driving) after these pore pressures have dissipated may reveal considerably less resistance to penetration. This phenomenon is referred to as "relaxation."

113. In order to correlate wave equation results with pile load test data, an estimate of the amount of soil setup or relaxation must be incorporated in the analysis. An alternate method of achieving an accurate account of such behavior would include a re-driving of the pile and recording of the penetration due to the first few hammer blows. This re-driving should be performed after sufficient time has elapsed to ensure pore pressure dissipation.

114. For piles driven in dense cohesionless deposits, the re-driving procedure should be an essential check of the foundation behavior since relaxation is an unconservative change in predicted pile capacity.

115. The most recent correlation study performed by TAMU researchers returns the deformation model to the form of Smith's original model. The values of soil damping parameters for use in Equations 18 and 19 are given in Table 5 after Foye et al.<sup>25</sup>

116. These values provided the best correlation with driving resistances corrected for soil setup and relaxation estimates. These



upon Smith's experience with wave equation analyses. He suggested that these values would suffice until more accurate quantities could be obtained, either by correlation or testing procedure.

108. Static and dynamic triaxial tests have been performed in order to determine appropriate deformation parameters. Reeves et al.<sup>20</sup> employed a triaxial testing apparatus to measure relevant parameters for saturated sands in the laboratory; Gibson and Coyle<sup>21</sup> investigated the behavior of clay soils. The testing device in each study employed impact loading conditions under various sample confining pressures. The data suggested that the dashpot parameter  $J$  as applied in Smith's model is velocity-dependent. These investigators modified Smith's model to account for this discrepancy by raising the velocity  $V$  to an exponent,  $N$ , in order to determine a constant  $J$  value, as follows:

$$R_{\text{dynamic}} = R_{\text{static}} (1 + JV^N), \quad 0 < N \leq 1.0 \quad (35)$$

109. The  $J$  value is assumed to represent the tip damping parameter over the range of velocities encountered at a driven pile tip. Model piles were driven in clays to examine the side friction damping parameter  $J'$ .<sup>22,23</sup> The results of these studies indicate that the tip quake and tip damping parameters for clay soils are best represented as the values assumed by Smith (i.e.,  $N = 1$  in Equation 35):

$$Q = 0.10 \text{ in.} \quad \text{and} \quad J = 0.15 \text{ sec/ft}$$

110. The side friction values for clay were determined parametrically to include

$$Q = 0.03 \text{ in.}, \quad J' = 1.25 \text{ sec/ft}, \quad \text{and} \quad N = 0.35$$

to be used in Equation 35.<sup>24</sup>

111. The influence of soil disturbance on driving resistance and subsequent static load test capacity may be quite pronounced. For

roughly 3 pile diameters wide and extends one pile diameter beneath the tip.<sup>17</sup>

103. Soil disturbance due to driving includes high effective stresses, shear deformations, volume change, and pore pressure development. These conditions severely affect the deformation behavior of the foundation materials during pile penetration. An adequate means of evaluating the soil response due to pile driving remains to be found.

104. The pile-driving problem involves high-amplitude impact stresses which are designed to "fail" the soil and cause pile penetration. The material beneath the tip is highly compressed, and the volume of the pile penetrating the soil must be displaced and/or compressed into the adjacent soil. The volumetric compression of the material beneath the tip causes a tendency for the soil immediately adjacent to the tip to stretch. This behavior has been observed experimentally,<sup>18,19</sup> as well as predicted numerically.<sup>11,13</sup>

105. Obviously, the stress-strain state which exists at any point in the pile-soil system depends on a multitude of factors. Nonetheless, reasonable approximations to the shaft friction resistance and point-bearing resistance are needed and can be made to model the problem numerically.

106. The most common assumption, in lieu of more accurate data, employs the proposed model of Smith<sup>4</sup> or some variation of this model. This rheologic behavior is described in Figure 4a, and the equations for computation of resistance forces are included in Part III. Basically it includes a modified Kelvin model with an elastic-plastic spring and a nonlinear viscous dashpot linked in parallel. The spring represents the static soil resistance response while the dashpot superimposes the rate dependency of the resistance force. This implicitly assumes that the static and dynamic components of resistance are separable, though the dynamic component is proportional to the static resistance, Equations 18 and 19.

107. Smith proposed that the value of soil quake be set as  $Q = 0.10$  in., while the  $J$  value be equated to  $0.15$  sec/ft. The side damping parameter,  $J'$ , was estimated as  $J/3$ . These values were based

with length. Smith<sup>4</sup> provides excellent analogies to represent these considerations in simple terms.

98. The choice of dynamic pile spring stiffness should be based upon appropriate "elastic" moduli values. For most soil conditions, the development of a soil plug (in an open-end pile, for instance) should have minor influence on the element stiffness value, but the mass of a "fixed" plug should be included in the calculations as equivalent pile weight.

99. A change in pile spring stiffness along the pile length (due to change in cross section or material) can cause some numerical instability in the calculation. It would be advantageous to employ pile segment lengths which minimize the difference between values of critical time interval,  $T_m$ , for pile elements, Equation 15. For a uniform pile, the use of equal pile segments is advisable.

100. Some typical values for Young's modulus and mass density of three basic materials are given in Table 1. For different materials an appropriate material property handbook should be consulted. An alternative method might involve material testing and/or wave velocity and density determinations for a suspended pile. For many wave equation analyses, the values in Table 1 should be adequate.

101. The assumption of a linear elastic equivalent pile spring constant is justifiable, providing that the peak stress is well below a yield stress level. The effect of pile damage may be described as a reduced stiffness for the affected element, such as for pile breakage. The influence of material damping (hysteresis) in the pile has been found to be negligible for most problems.<sup>14</sup>

#### Pile-Soil Interaction

102. The behavior of soil in the vicinity of a driven pile is a very complicated phenomenon. It has been observed that the zone of soil disturbance for piles driven into sands is on the order of 7 to 12 pile diameters wide and extends to a depth of 3 to 5 pile diameters beneath the pile tip. For piles driven into clayey soils, this zone is

consideration in a design, these modulus values may be compared with details of TAMU laboratory results.<sup>16</sup> Computed peak cushion stresses from the preliminary calculations should be used. A substantial difference from the selected modulus (greater than  $\pm 25\%$ ) may influence the peak pile stresses computed and may cause a significant change in the blow count, particularly for higher resistances. A sample calculation of stress magnitude and cushion modulus selection is given in Part V.

### Piling

95. There are numerous ways to classify foundation piles. They may be grouped, for example, according to shape, material, purpose, method of manufacture, or method of installation. Several significant considerations may be involved in determining the most effective and most economical design for driven foundation piles. Wave equation analyses provide an excellent method for examining the alternatives available in terms of driveability, damage prevention, and comparative economy.

96. Several guidelines are recommended in applying the finite difference method to a given problem. A subdivision of the pile into 10 or more segments generally permits the stress wave propagation to generate a smooth function with length. For longer pile lengths (greater than 100 ft) it may be necessary to increase the number of segments. Smith recommends segment lengths on the order of 5 to 10 ft.<sup>4</sup> The total number of elements must be less than the array dimension for pile properties prescribed in the computer program.

97. This dimension may be increased to accommodate very long piles. A normal rule of thumb for discretizing a pile might be: a minimum of 10 pile segments; a maximum pile segment length of 10 ft. These limits provide for a smooth stress distribution of the traveling stress wave with reasonable accuracy. The use of a greater number of pile segments than necessary increases computational effort with little improvement in accuracy. The use of segments longer than 10 ft does not permit a smooth mathematical representation of the stress wave

upon peak driving stress condition in the cushion. Moreover, the secant modulus and coefficient of restitution may vary, depending on the applied load cycle number. It is recommended that for analyses of piles near bearing that "well-consolidated" cushion properties be selected. The only material which did not exhibit appreciable change in stress-strain behavior with repeated load cycles was the Micarta plastic.<sup>16</sup>

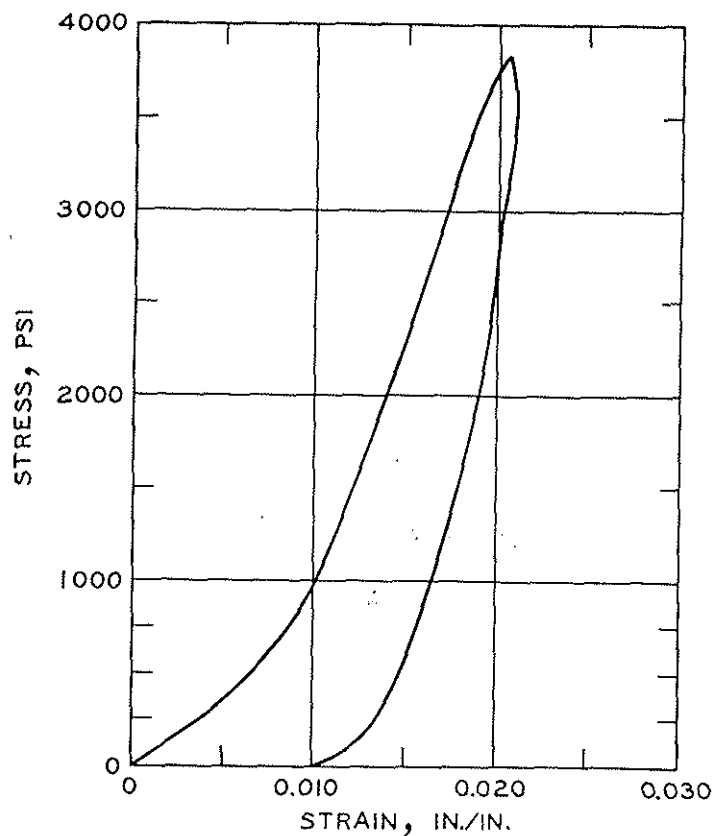


Figure 10. Typical stress-strain curve for a Micarta cushion block (from Lowery<sup>14</sup>)

94. Table 4 gives typical secant moduli and coefficients of restitution for various cushion materials based upon TAMU measurements.<sup>14</sup> Should ram stresses or pile stresses become a critical

### Driving Accessories

89. Numerous combinations of accessory elements may be included in the hammer assembly. There are four fundamental purposes in selecting necessary driving accessories: to prevent hammer damage during impact; to prevent pile damage during driving; to adapt the connection between the hammer and the pile; and to obtain the most efficient combination of these elements to drive the pile economically.

90. All four of these purposes are usually interdependent for a particular pile-driving problem. This section discusses the mechanical properties of these elements. The proper assemblage of these components will be discussed in Part V.

91. The basic means of reducing hammer and/or pile damage is the use of cushioning material to "soften" the impact. A vast assortment of materials and a multitude of combinations and dimensions have been used for pile-driving cushions. Cushions may be used between the hammer striking parts and a drivehead, and between the drivehead and the pile. Indeed, either or both cushions and even the drivehead may be absent in the contractor's setup.

92. Two types of cushions may be distinguished in general practice: a hard (stiff) cushion component of Micarta, asbestos, aluminum, or hardwood, which gives a high modulus of elasticity and a reasonably high coefficient of restitution; and a soft cushion composed of softwoods having a low modulus of elasticity and a low coefficient of restitution.

93. Laboratory tests on cushion blocks performed at TAMU have shown that the dynamic and static stress-strain behaviors of most cushion materials are very similar.<sup>16</sup> Analyses using the wave equation have shown that the use of a bilinear cushion representation is the most suitable approximation available. The nonlinear characteristics of the stress-strain data require the selection of an appropriate secant modulus for the linear load modulus. A typical stress-strain curve for a Micarta cushion block is shown in Figure 10.<sup>14</sup> It should be emphasized that the value selected for secant modulus is dependent

$$E_R = W_R h \quad (31c)$$

while the impact velocity of the ram is determined by the equation

$$V_R = \sqrt{2g(h - \bar{d})} \quad (32)$$

87. A modification to this system to increase the driving rate and driving energy employs air pressure at the top of the ram during the impact stroke. These hammers are described as closed-end diesel pile drivers. The equations for hammer energy output and velocity are given as follows:

$$E_R = W_R h_e \eta \quad (33)$$

$$V_R = \sqrt{2g(h_e - \bar{d})\eta} \quad (34)$$

$h_e$  depends upon the bounce chamber pressure. Manufacturer's charts provide evaluation of this quantity based upon bounce chamber pressure gage readings during the driving operation.<sup>14</sup>

88. A schematic diagram for each of these types of impact pile hammers is given in Figure 9. Typical quantities for properties of commercially available hammers are given in Tables 2 and 3.

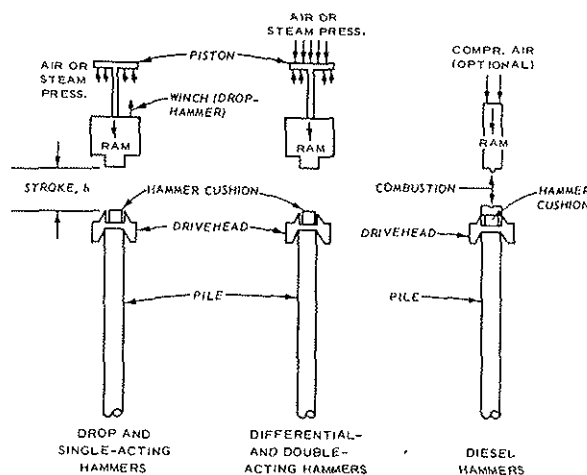


Figure 9. Schematic diagrams of impact pile drivers

80. Using this procedure of energy computation, the mechanical efficiency of the double-acting hammer is approximately 85 percent.<sup>14</sup>

81. For single-acting and drophammers, the hammer efficiency is normally estimated in the range of 75 percent to 85 percent.<sup>14</sup> The higher efficiency values are generally associated with heavier rams.

82. Diesel hammers provide the most recent innovation in impact pile drivers. For these hammers, the combustion of diesel fuel during ram-anvil impact in an enclosed chamber provides the energy necessary to return the ram to the peak stroke. The explosive force of the diesel hammer also outputs energy that performs useful work during pile penetration.

83. The rated kinetic impact energy for an open-end diesel hammer is given as

$$E_K = W_R (h - \bar{d}) \quad (31a)$$

where

$E_K$  = rated kinetic impact energy, FL

$\bar{d}$  = distance from exhaust ports to anvil, L

84. This equation assumes that the ram velocity remains constant after the ram passes the exhaust ports on the impact stroke. Thereafter the air-fuel mixture is compressed in the combustion chamber.

85. The rated explosive energy is the useful work done by the explosive force after ram impact. It is generally on the same order as the quantity<sup>14</sup>

$$E_E \approx W_R \bar{d} \quad (31b)$$

where  $E_E$  = explosive energy of the system which performs useful work, FL.

86. Thus, the total rated energy is given as the sum of these quantities. The normal efficiency of these hammers based upon the energy calculation shown is considered to be 100 percent, such that the output energy of the open-end diesel hammer is given as<sup>14</sup>



economical will be the pile-driving operation. The next stage in hammer development involves the use of steam or air pressure to raise the ram to the required stroke prior to free fall of the ram. This hammer is described as a single-acting pile driver, and its output energy,  $E_R$ , and impact velocity,  $V_R$ , are also computed from Equations 28 and 29, respectively. The obvious advantage to this hammer is the opportunity to increase drive rate to a limit of about 60 blows per minute.

78. A second innovation in steam or air hammers employs pressure to raise the ram to the height of stroke  $h$  at which time downward pressure on the piston is developed to increase the accelerating force, adding energy by increasing impact velocity. Such hammers are termed double-acting or differential-acting pile drivers, depending on the ratio of piston areas for upward and downward strokes of the ram. The addition of useful work force on the downstroke increases the frequency appreciably to rates in excess of 120 blows per minute in some instances.

79. Evaluation of the output energy of double-acting and differential-acting hammers requires consideration of the additional driving force. It is commonly assumed that

$$E_R = W_R h_e \eta \quad (30)$$

where  $h_e$  = "equivalent" hammer stroke, L, and

$$V_R = \sqrt{2gh_e \eta}$$

The value of  $h_e$  may be determined for a double-acting pile driver as

$$h_e = h \left[ 1 + \frac{P}{P_{\text{rated}}} \times \frac{W_H}{W_R} \right]$$

where

$P$  = operating air or steam pressure,  $F/L^2$

$P_{\text{rated}}$  = manufacturer's rated pressure,  $F/L^2$

$W_H$  = weight of hammer housing, F

#### PART IV: MATERIAL BEHAVIOR REPRESENTATIONS

74. A significant portion of the engineering research into pile-driving behavior has been in search of appropriate material behavior parameters. The weight of striking parts, stroke, and efficiency of the hammer, the deformation properties of the cushions and piling, and the soil response parameters are integral parts of any analysis. A summary of available information on these various components is given below.

##### Hammers

75. The impact pile driver may include a vast assortment of driving accessories necessary to adapt a particular hammer to the pile and to the driving conditions. The behavior of vibratory pile-driving equipment is beyond the scope of current wave equation applications. For this reason, impact hammers will be examined exclusively herein.

76. The simplest hammer available is the drophammer. The ram mass is raised mechanically to a desired stroke and released. The free-fall force of gravity imparts energy to the mass which strikes the pile-driving assembly and transmits driving energy to the pile. The energy output by the hammer is given as the product:

$$E_R = W_R h \eta \quad (28)$$

where

$E_R$  = ram output energy, FL

$W_R$  = ram weight, F

$h$  = hammer stroke (height of fall), L

$\eta$  = hammer mechanical efficiency

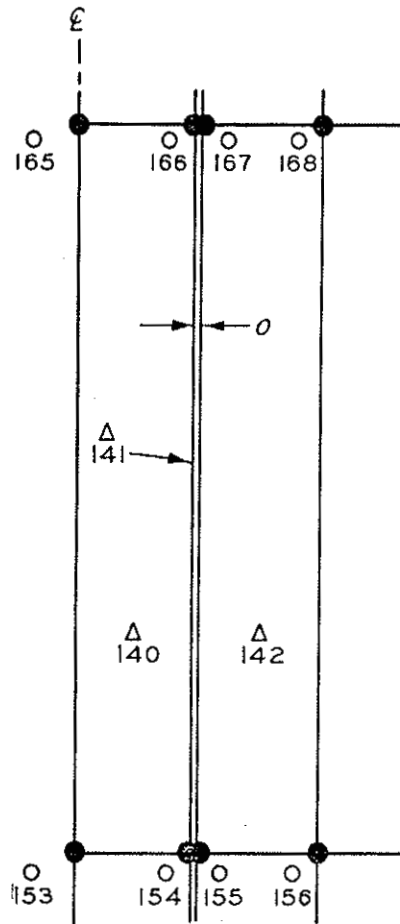
The velocity of the ram at impact is given as

$$V_R = \sqrt{2gh\eta} \quad (29)$$

77. The greater the driving rate (blows per minute), the more

and constitutive relations for these elements are major tasks. Proper discretization of the model in both space and time variables in such a nonhomogeneous system in order to propagate accurately both shear and compression stress waves is perhaps the most severe difficulty.

7. The use of finite element techniques in a pile-driving analysis will remain in the research domain for quite some time. The complexity of the pile-soil system interaction, site nonhomogeneity, soil behavior representation, and, most obviously, economic considerations require that improvements and refinements of the one-dimensional analysis should take precedence in research activities.



(NOT TO SCALE)

Figure 8. Detail of interface element  
(from Desai and Holloway<sup>11</sup>)

71. These studies involved pile load test analysis; therefore, only static behavior was investigated. The system of equilibrium equations could readily be modified to account for dynamic behavior with greater mathematical complexity, of course. The computational effort is much greater than that applied to the one-dimensional analysis after Smith, but the modeling of the problem is clearly more suitable to the purist.

72. The major obstacle to the development of a finite element procedure for analysis of pile-driving behavior rests with the proper representation of the dynamic pile-soil interaction in the soil and interface elements. Determination of in situ stress/strain conditions

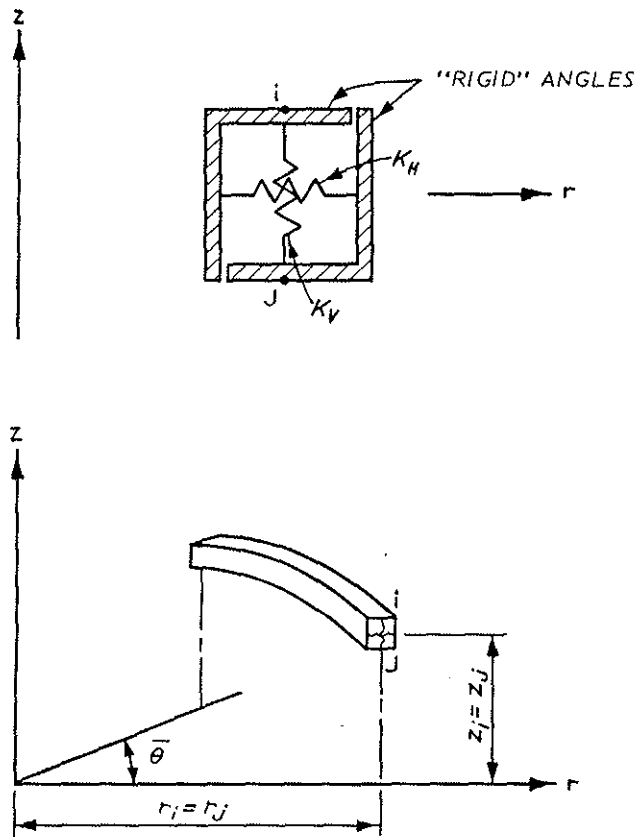


Figure 7. Details of axisymmetric point spring element (from Ellison<sup>12</sup>)

70. In another study of pile load test behavior, Desai and Holloway<sup>11</sup> found comparable accuracy in predicting load-deformation behavior using finite element techniques. In this work, a stress-dependent, nonlinear (hyperbolic), elastic constitutive model for deformation behavior was used for the soil and pile-soil interface. Instead of employing nondimensional node springs, "one-dimensional" axisymmetric joint elements modeled the interface behavior. These elements permit interelement slip with deformations prior to failure (see Figure 8). The constitutive parameters were generated from laboratory interface shear tests.<sup>11</sup> The results of both these finite element analyses show great promise in the potential applications to piling problems.

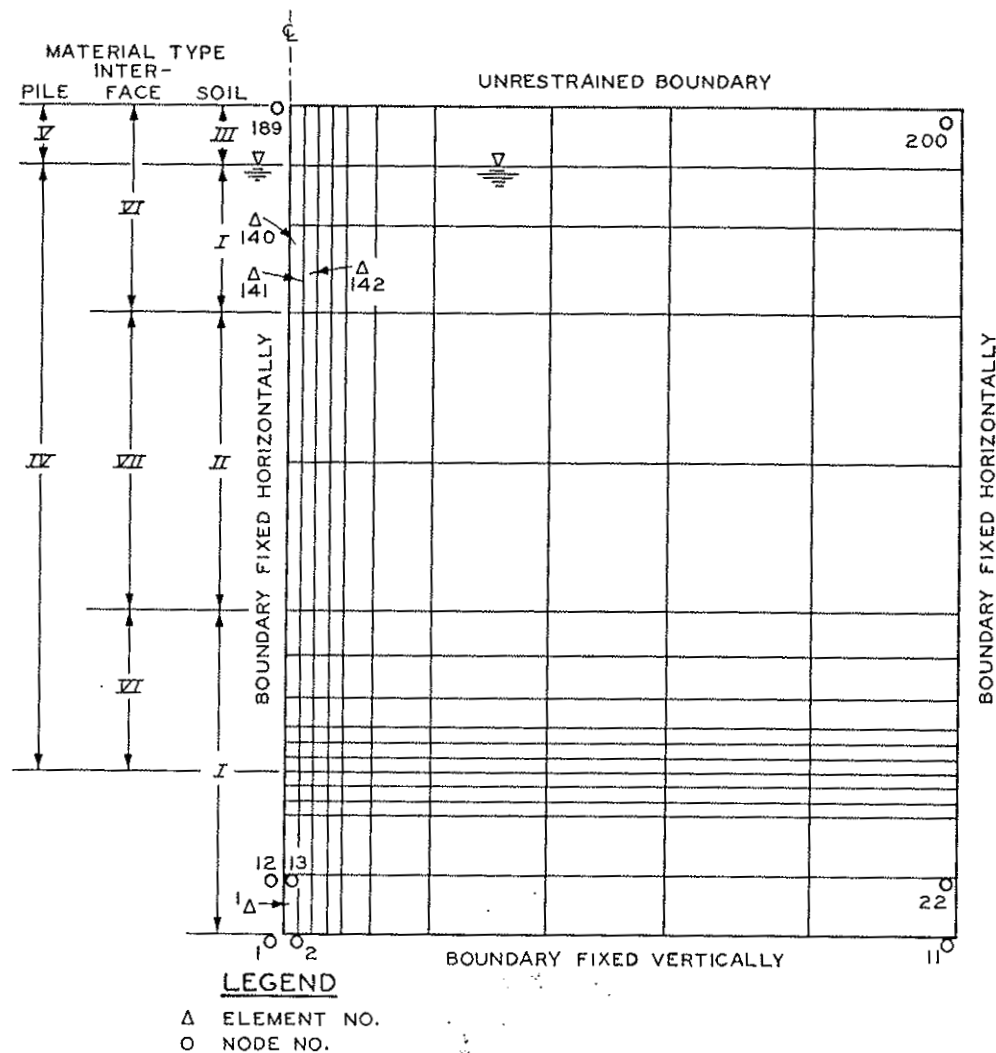


Figure 6. Finite element mesh  
(from Desai and Holloway<sup>11</sup>)

A later journal article presents a portion of that research.<sup>13</sup> The constitutive model for soils involves a trilinear approximation to the stress-strain curves employing an incremental procedure. The stress-deformation behavior of the pile-soil interface is prescribed by the application of nondimensional (point) spring elements (see Figure 7). The deformation between corresponding pile and soil is concentrated at these nodes. When the stress exceeds the Mohr-Coulomb strength at the interface, the spring is allowed to "slip" with no further stress-retaining capacity permitted.

The value of  $V_R$  depends upon the ram weight, the output energy, and mechanical efficiency of the hammer. The hammers studied by Parola did not include the direct interaction of diesel hammers. The representation of equivalent force pulse replacing the hammer was applied in the case of one diesel hammer by inputting measured pile head stresses to the analysis.<sup>8</sup>

66. This procedure allows the parametric evaluation of several driving components in a unified fashion. The results of Parola's study are presented in terms of generalized parameters described in design-oriented curves. For the purpose of selecting compatible hammer-pile systems to maximize energy transmission without excessive pile head stresses, the procedure devised by Parola should provide invaluable assistance to the designer and pile contractor. Additional analyses by Parola clarified several points that are of direct interest in pile-driving analysis and design. These findings will be discussed in subsequent parts.

#### Finite Element Method

67. Applications of the finite element method to engineering problems have propagated as rapidly as the development of electronic digital computers. Details of finite element techniques may be found in texts dealing exclusively with the method.<sup>9,10</sup> The subsequent discussion will focus on finite element applications to pile foundation problems which have appeared in the literature.

68. The single pile analysis may be represented as an axis-symmetric idealization of the three-dimensional problem. The problem is defined in a vertical plane which includes the axis of the vertical pile. The use of an axisymmetric stress-strain formulation is required. A typical finite element mesh for a pile-soil system is given in Figure 6. Note that these elements project as wedge segments in the horizontal plane.

69. The first analyses of pile-soil interaction problems using the finite element method are described in a dissertation by Ellison.<sup>12</sup>

$$\ddot{u} = \frac{d^2 u}{d\zeta^2}$$

$$\bar{A} = \frac{\rho c A}{\sqrt{\frac{W_1}{g}} K_1} \bar{B}$$

$$\bar{B} = \frac{W_1}{W_2}$$

The analogous initial conditions are given as

$$u_1 = u_2 = \dot{u}_2 = 0 \quad (27a)$$

$$\dot{u}_1 = V_R \bar{T} \quad (27b)$$

The schematic of the analog computer system necessary to solve these equations is included in the appendixes of the dissertation.<sup>8</sup> Parola advises that only linear elastic and bilinear (inelastic) cushion behavior can be analyzed using these nondimensional parameters.

63. The quantity  $\bar{B}$  gives the ratio of ram weight to drivehead weight, while the  $\bar{A}$  term relates the "hammer impedance"  $\sqrt{(W_1/g)K_1}$  to the pile impedance. For his analyses, Parola employed  $\bar{B}$  values of 1, 3, 5, 10, and 20 whereas most typical operating ranges involve  $\bar{B}$  values between 3 and 10. Low pile impedance values corresponded to thin-walled pipe and timber piling, while high pile impedance values represented heavy-walled pipe and mandrel-driven, concrete, and steel H-piles.

64. Pile impedance forces represent dynamic resistance to the motion of the rod, and are proportional to the instantaneous velocity at the pile head. The theoretical derivation of the mechanical impedance concept is given elsewhere.<sup>1,2</sup> Pile impedance values with equivalent pile sections are given in Table 1 (after Parola<sup>8</sup>).

65. The input variables to the analog computer program include the ram and drivehead weights, the load-deformation parameters of the cushion, the pile impedance, and the initial ram velocity at impact  $V_R$ .



geometry of the pile.

61. The initial conditions for these equations are given by

$$\begin{aligned} u_1 &= u_2 = \dot{u}_2 = 0 \\ \dot{u}_1 &= V_R \end{aligned} \quad (23)$$

where  $V_R$  is the initial ram velocity at impact. In addition, it is generally specified that the quantity

$$K_1(u_1 - u_2) \geq 0 \quad (24)$$

to eliminate any tension forces in the capblock cushion.

62. In order to facilitate computations, these quantities are replaced by proper substitutions of terms

$$\bar{T} = \sqrt{\frac{W_1/g}{K_1}} \quad (25a)$$

and

$$\zeta = t/\bar{T} \quad (25b)$$

where

$\bar{T}$  = pseudoperiod of the ram cushion, sec

$\zeta$  = dimensionless time variable

Rewriting the equation of motion gives

$$\dot{u}_1 + (u_1 - u_2) - g\bar{T}^2 = 0 \quad (26a)$$

$$\ddot{u}_2 + \bar{A}\dot{u}_2 - \bar{B}(u_1 - u_2) = 0 \quad (26b)$$

where

$\bar{A}$  = ratio of ram weight to drivehead weight

$\bar{B}$  = ratio of hammer impedance to pile impedance

and

$$\dot{u} = \frac{du}{d\zeta}$$

185. The prediction of pile capacities by any procedure involves a number of system variables that cannot readily be included in any mathematical representation. Predictions based upon dynamic pile-driving behavior are subject to even greater uncertainties.

186. Dynamic hammer, cushion, and pile properties are easily determined. Interaction behavior among these elements is often subject to question. Dynamic laboratory tests of soils have shown that loading (strain) rate effects are manifest in deformation and failure behavior of the samples.

187. In the vicinity of a driven pile, very large deformations, pore pressure changes, and stress level changes certainly occur. The effects of these changes are particularly significant for cohesive soil deposits. The soil remolded due to driving in the vicinity of a pile may exhibit very little resemblance to the material surrounding the pile weeks or months after the pile was driven. Even the first few blows of redriving of the pile may cause deformation behavior that in no way reflects the "static" resistance to pile penetration.

188. It is easily noted that soil "constants" may vary from pile test to pile test on the same site, even more for piles at separate sites and in different soils. The gross simplification of Smith's rheological model lumps a multitude of causative factors into a fundamental model that may deviate considerably from measured soil properties.

189. In view of these uncertainties, the scatter in predicted versus measured pile capacities is not surprising. To predict the pile capacity and pile-driving behavior accurately is beyond the current state of the art. Nonetheless, the wave equation is still the most versatile engineering tool available to the foundation engineer. Indeed, it is the only rational method that even attempts to quantify the vast number of variables included in the physical problem. Great care must be exercised to assure that experience and engineering judgment are included in any pile-driving analysis.

#### Example Problems

190. Pile tests at two different sites under different driving

conditions were analyzed to determine the capability of the wave equation solutions for predicting pile capacities. The time-sharing version of the TAMU program, TAMFOR, was used in these tests. The results of the computer calculations will be presented graphically.

191. The first set of problems was selected from pile tests at Lock and Dam No. 4 on the Arkansas River.<sup>40</sup> Test piles 1, 2, and 3 were driven closed-end. Pertinent hammer assembly information is given in Table 6.

192. The three test piles included steel channels throughout their lengths to protect the instrumentation. The steel in these was included in the net cross section for equivalent spring constant computations. The total pile length for each pile was 55 ft. A pile segment length of 5 ft was selected, giving 11 equal pile segments in the wave equation analysis. Pile section properties for the three test piles are described in Table 7.

193. As described in the previous section, pile tip quake values were assumed proportional to the pile tip diameter. The percentage of pile capacity at the tip was computed from pile instrumentation data given near the "failure" load. Field measurements indicated that the pile tip capacities generated percentages of 24 percent, 30 percent, and 36 percent of the total capacities for test piles 1, 2, and 3, respectively. For the medium dense, fine to silty sands of the foundation, a triangular skin friction distribution was assumed.

194. It is advantageous at this point to examine the input data file PILES 2 directly to discuss the problem input parameters for TAMFOR. Within the time-sharing computer system, the data files for these three test piles were stored under the names LD4TP1, LD4TP2, and LD4TP3. File LD4TP1 will be described in detail below. These three data files are listed in Table 8.

195. For test pile 1, data file LD4TP1 was established as a new file. The program input data for the test pile was stored in this data file in the same sequence required in the TAMU utilization manual,<sup>26</sup> and described for the TAMFOR program in Appendix A of this report. For line 10 the entries are as follows:

Case number (enclosed in quotations): "LD4/1"  
The number of problems contained in the data file: 6  
1/DELTAT: 0  
The number of problem elements, P: 13  
The first three SLACK values: 1000, 1000, 0  
Four input options: 2, 1, 1, 2  
The detailed output interval, IPRINT: 20  
The mass number of the first pile segment, NSEG1: 3

196. Several of these items deserve further description. The entry 1/DELTAT = 0 permits the computer program to calculate the time increment. The first two large SLACK values specify that the first two spring elements cannot transmit tension forces between the ram and cap-block and between the pile cap and the pile. OPTION 1 = 2 indicates that element areas will be read in separately. OPTION 2 = 1 specifies that the soil resistance distribution will not be listed, but rather generated by a subsequent option. OPTION 3 = 1 defines the SLACK values for elements 4 through P such that tension stresses will be transmitted, i.e., given zero SLACK values. OPTION 4 = 2 provides that a TAMU computational routine be employed. Any value for IPRINT will be sufficient since the detailed output option is omitted from the TAMFOR options.

197. Line 20 of LD4TP1 lists the weights of elements  $W(1), \dots, W(P)$  in pounds. The actual value of  $W(1)$  is specified in a subsequent input line; line 30 (continued on line 40) inputs the element spring constants  $K(1), \dots, K(P-1)$ , inclusive. The value of  $K(P)$  represents the soil tip spring to be determined elsewhere in the program. Line 50 (continued on line 60) lists the values of element areas to be assigned, as specified by OPTION 1 = 2.

198. For this test pile and the others in these example problems, the choice of problem format involved single calculations at specific  $RU_{TOTAL}$  values based upon expected pile capacities. This procedure provides  $RU_{TOTAL}$  versus blowcount data in a range of anticipated values. This procedure is recommended instead of the multiple calculations based upon program-generated  $RU_{TOTAL}$  values.

199. Line 100 (continued on line 110) lists the problem number,

1; the ram weight,  $W(1) = 14,000$  lb; the spring element to be varied for the problem,  $NC = 15$ ; the spring constant,  $K(NC) = 1.0$ ; the hammer efficiency,  $n = 0.85$ ; the rated hammer energy, 36,000 foot-pounds; the coefficient of restitution of the first three spring elements, 0.80, 1.0, 1.0; the  $RU_{TOTAL}$  value for the problem calculation, 100,000 lb; the pile tip capacity as a percentage of  $RU_{TOTAL}$ , 24 percent; the mass number of the first pile element upon which soil resistance acts,  $MO = 3$ ; the tip quake, side quake, tip damping, and side damping parameters,  $Q_p = 0.11$  in.,  $Q_s = 0.10$  in.,  $J_p = 0.15$  sec/ft, and  $J_s = 0.05$  sec/ft; the hammer explosive force = 0; and finally, the problem options to be required,  $OPTION\ 11 = 2$ ,  $OPTION\ 12 = 2$ ,  $OPTION\ 13 = 0$ ,  $OPTION\ 14 = 1$ , and  $OPTION\ 15 = 1$ .

200. The tip quake reflects the tip diameter scale effect discussed previously. The remaining soil parameters are those recommended by Smith.<sup>4</sup> The program options selected were as follows:  $OPTION\ 11 = 2$  specifies a single calculation problem;  $OPTION\ 12 = 2$  requests that a triangular skin friction distribution be generated by the program;  $OPTION\ 13 = 0$  indicates that no plot routine option is requested;  $OPTION\ 14 = 1$  includes the effects of gravity in the calculation before impact; and finally,  $OPTION\ 15 = 1$  denotes that a normal data printout is in order. As discussed previously, the detailed output option ( $OPTION\ 15 = 2$ ) is deleted in TAMFOR computer code.

201. Subsequent lines in the input file list single calculation problems at higher  $RU_{TOTAL}$  values. The final line in the file establishes the end of the data file. In order to perform the program calculations, the file LD4TP1 was renamed and saved in the file named PILES 2. PILES 2 is the data file used by the program TAMFOR.

202. To store the output of calculations for case "LD4/1," the file OUTPUT must be renamed and saved. In order to perform analyses on test piles 2 and 3, files LD4TP2 and LD4TP3 were renamed and saved as PILES 2 for the program runs. The OUTPUT file for each case was renamed and saved to be listed after all calculations were performed.

203. The results of these calculations were plotted for comparison with the field measurements in Figures 12, 13, and 14.  $RU_{TOTAL}$

versus blows per foot data are plotted in these figures, along with peak driving stress versus blows per foot. An interesting point to note in the data plotted concerns the change in peak driving stress with changes in blow count, discussed as follows:

- a. Under easy driving conditions (low blow counts), the maximum stress is that caused by the impact of the ram, and occurs near the drivehead. As driving resistance increases, however, maximum compression stresses can exceed this value due to reflected compression stresses along the shaft, especially from the pile tip.
- b. Variations in soil parameters can have a significant influence on stress magnitude for a given blow count. A reduced quake value causes a stiffer spring response and, therefore, a higher reflected stress. Higher damping parameters cause more energy to be absorbed and increase the blow count while the peak stress remains about the same for the same static resistance value,  $RU_{TOTAL}$ .

The bearing capacity predictions were discussed previously. As "pre-dictions," these values are quite satisfactory for engineering purposes.

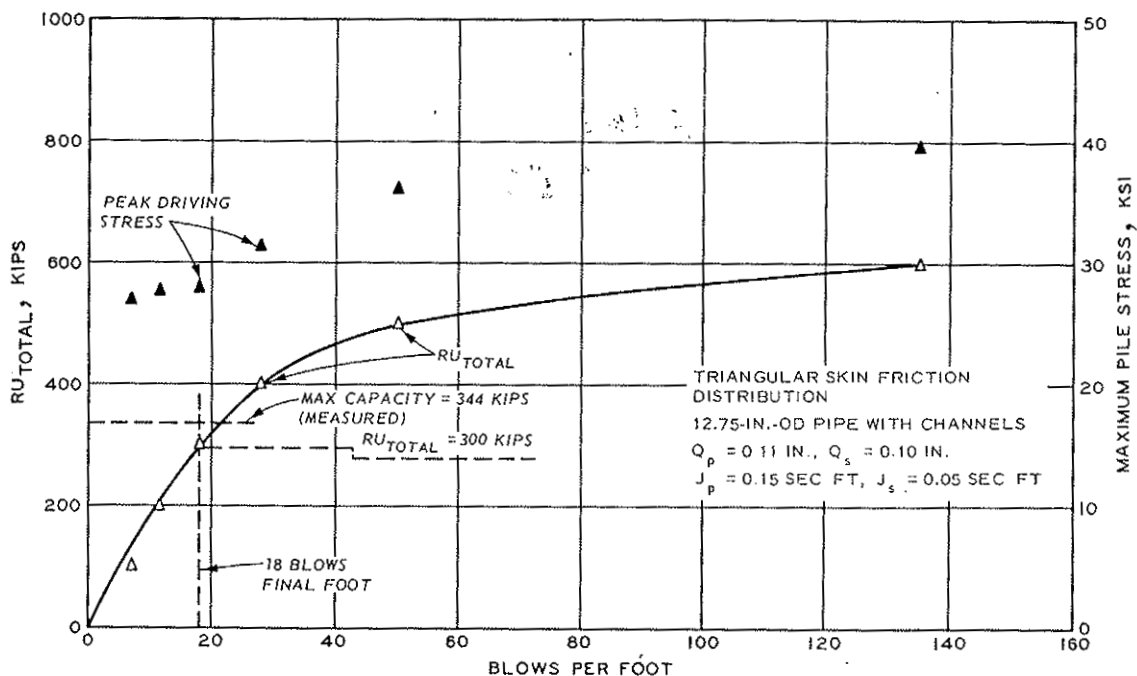


Figure 12. Test pile 1, Lock and Dam No. 4

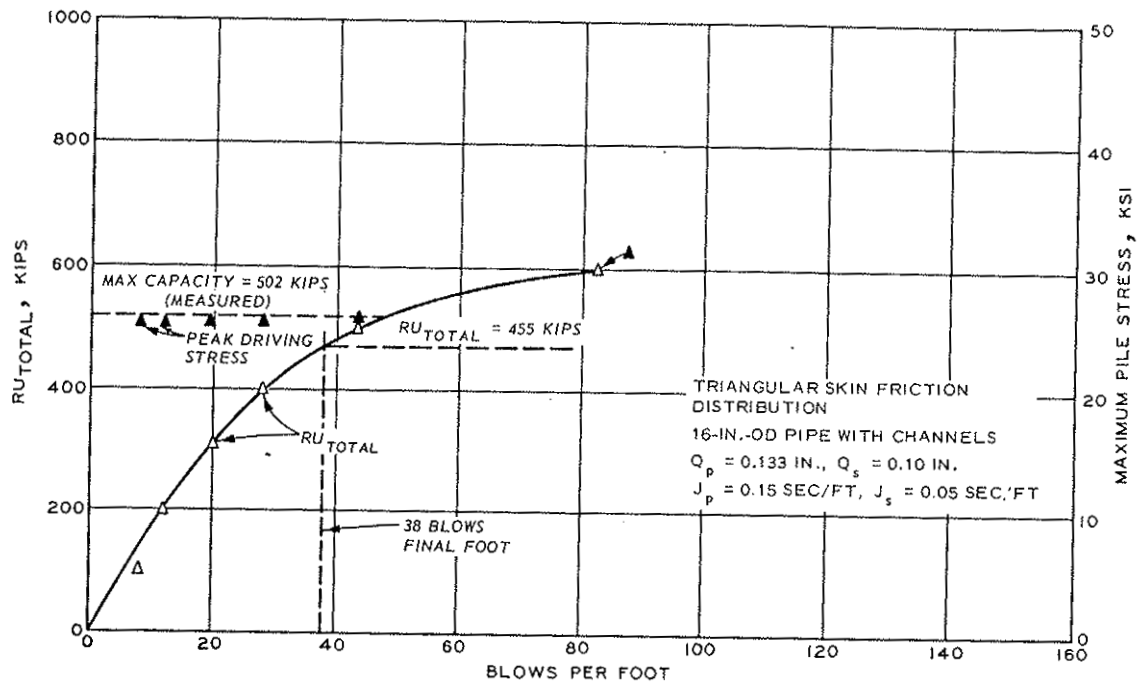


Figure 13. Test pile 2, Lock and Dam No. 4

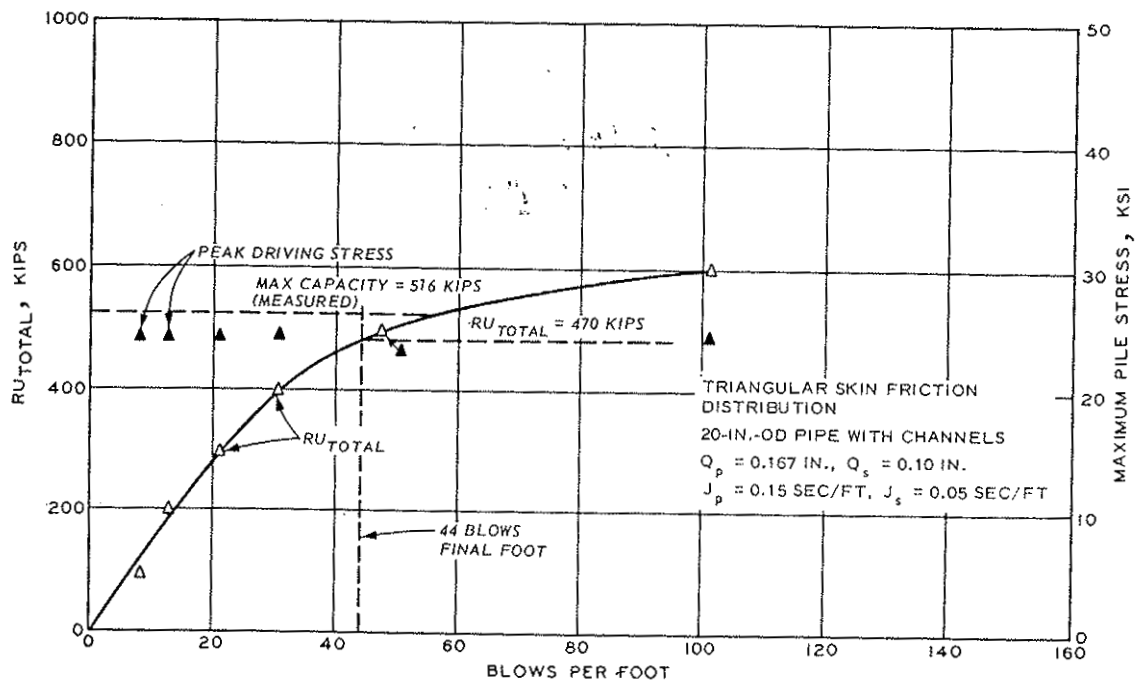


Figure 14. Test pile 3, Lock and Dam No. 4

204. The second set of example problems involves pile tests performed at the site of Jonesville Lock and Dam near Jonesville, Louisiana.<sup>41</sup> These piles were 18-in.-square, precast concrete driven into a dense deposit of fine sand. Test pile 1 was driven to a depth of 38 ft into a very stiff layer between depths of 35 ft and 40 ft. Test Pile 2 penetrated the stiff layer into the very dense sand stratum to a depth of 45 ft. Test pile 3 was driven to a final penetration of 54 ft into the same very dense stratum.

205. Information regarding the pile-driving assembly is listed in Table 9. For the case of precast concrete piles, the common assembly includes a capblock, pile cap, and pile cushion beneath the hammer. The precast concrete piles were assumed to have a modulus of roughly  $3.0 \times 10^6$  psi. The material was also assumed to have a density of 150 lb/ft<sup>3</sup>. Since these piles were driven with oak cushion blocks, the stress level in the cushion block has a significant influence upon the secant modulus value that should be assigned to the cushion.

206. A value of 39,300 psi (corresponding to a stress level of 2,000 psi) was assumed as a first estimate to the cushion modulus. Equations presented in a TAMU report<sup>16</sup> permit the estimation of peak pile stress. Using the appropriate equations, the peak stress predicted was approximately 2,500 psi. Based upon this value, it was assumed that the secant modulus for the oak cushion of 39,300 psi would be acceptable. Moreover, this 2,500-psi stress level indicated that the asbestos capblock should be assigned a secant modulus of 41,400 psi.<sup>16</sup> The calculations from the program indicated peak stresses in these elements for all cases between 2,000 and 2,500 psi. For all three piles, the segment length was established as 3 ft.

207. The results of the analyses of Jonesville test piles introduced several additional considerations. A triangular skin friction distribution was assumed. For test piles 1, 2, and 3, the assumption of a larger tip quake, as before, was clearly underestimating capacity. Even using Smith's recommended parameters,<sup>4</sup> the estimated pile capacities were still low. A final try for these piles involved reduc-



ing the tip damping parameter  $J_p$  to zero. The results for test piles 2 and 3 still underestimated the pile capacities by 24 percent and 20 percent, respectively. Test pile 1 indicated that the error was on the order of 12 percent.

208. Preliminary calculations of the pile tip bearing capacities were based upon static formulae after Vesic.<sup>18</sup> A stiffer deposit was clearly observed in the layer in which the tip of test pile 1 rested. Using the static resistance estimates, triangular skin friction distribution parameters were computed for test piles 2 and 3. Assuming the same skin friction distribution for test pile 1, a revised tip capacity was calculated. Employing this revision, the "prediction" of test pile 1 capacity was significantly improved. The results of these problems are given in Figures 15, 16, and 17.

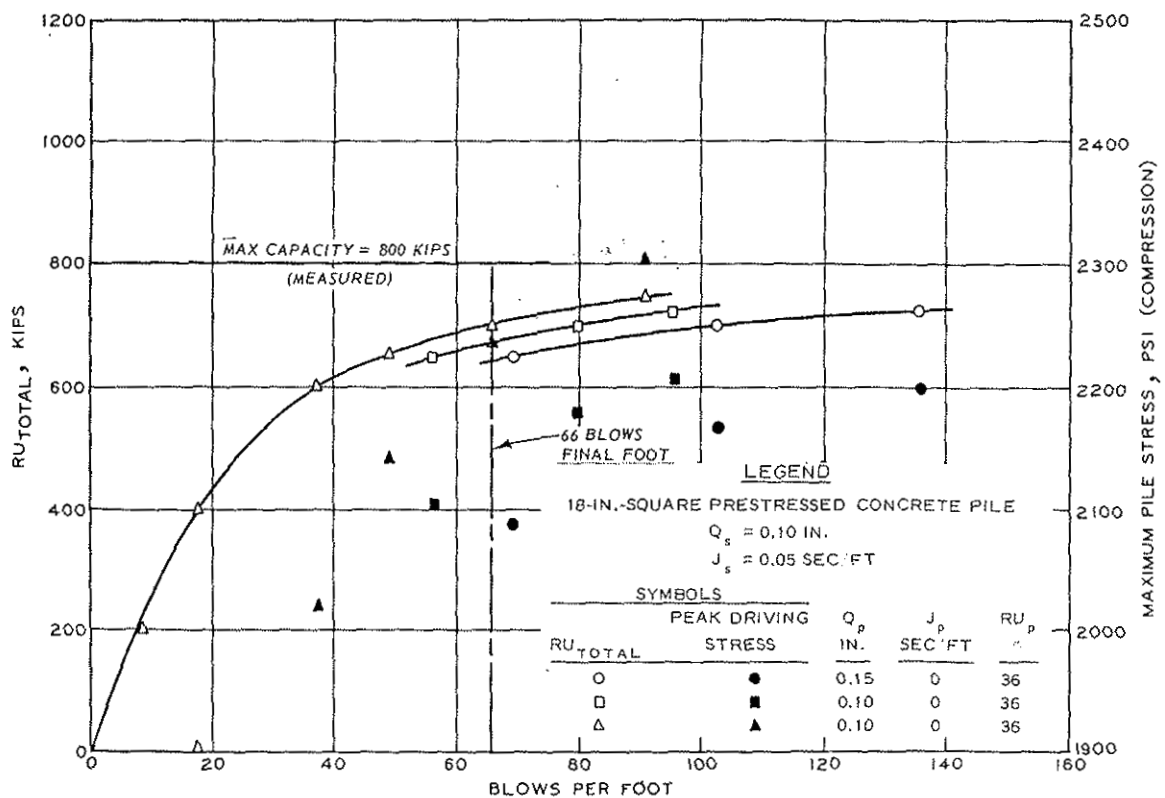


Figure 15. Test pile 1, Jonesville Lock and Dam

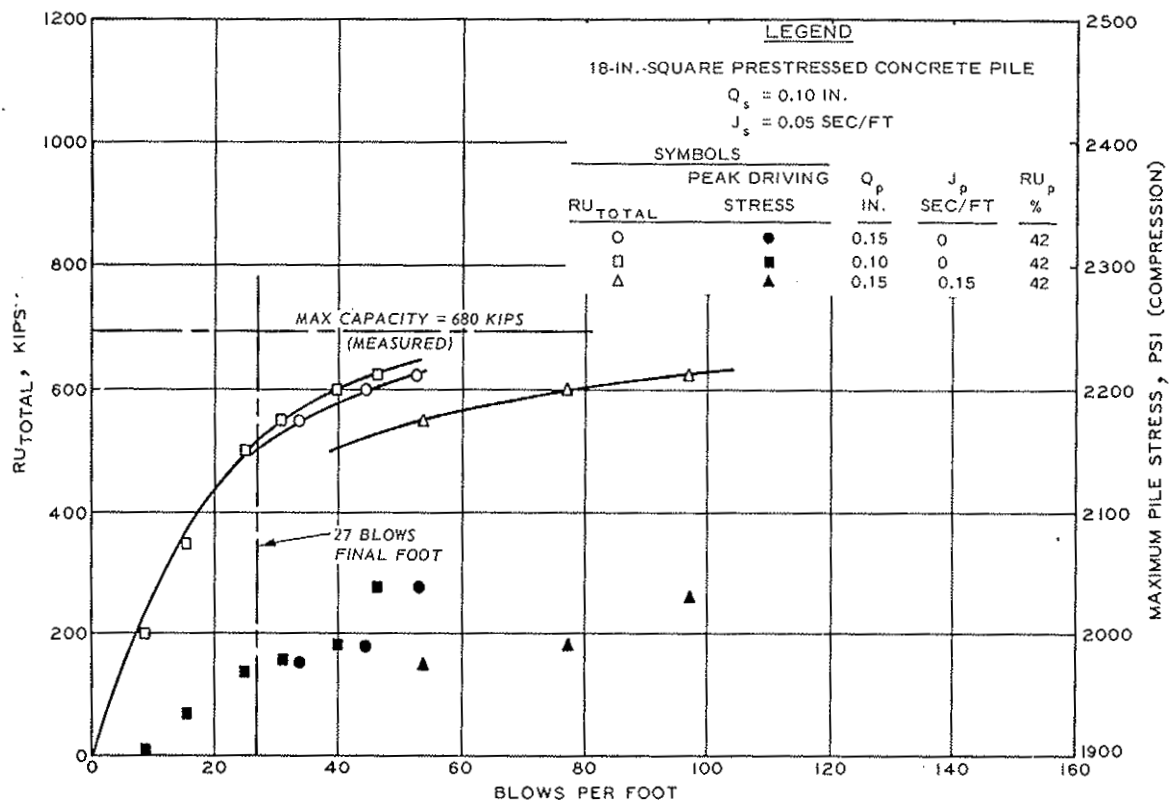


Figure 16. Test pile 2, Jonesville Lock and Dam

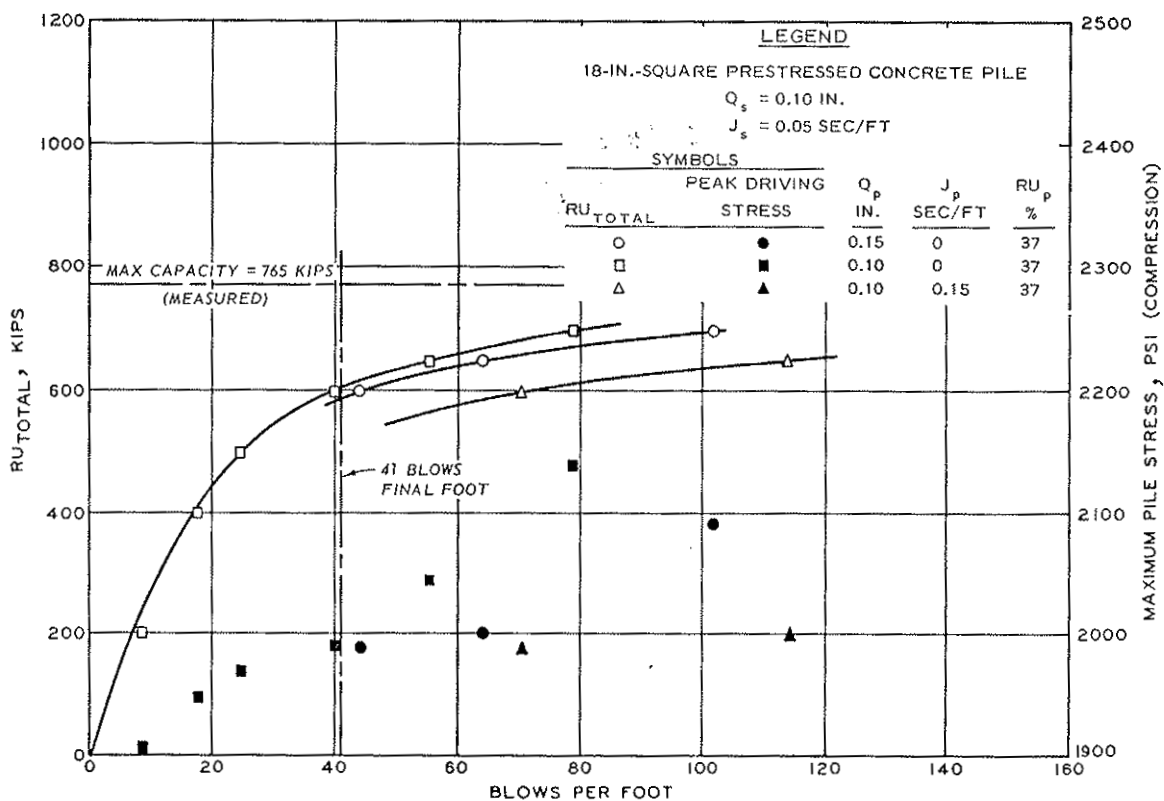


Figure 17. Test pile 3, Jonesville Lock and Dam

209. The Jonesville Lock and Dam test piles indicate that a significantly different set of soil parameters is necessary to correlate blow count data. The values of quake and damping parameters could, no doubt, be adjusted to give "accurate predictions." These problems demonstrate that the pile capacity predictions may be particularly sensitive to soil properties prescribed to the system. These values are obviously not constant. Moreover, "best" values may give considerably different predictions from measured field behavior for other cases. The fact that  $RU_{TOTAL}$  values should correlate with maximum applied loads rather than pile bearing capacities is often overlooked.

## PART VI: CONCLUSIONS AND RECOMMENDATIONS

210. Wave equation analysis of pile-driving behavior is the most versatile procedure available for incorporating problem variables in a mathematically consistent formulation. The results of typical analyses include predictions of peak pile stresses and pile penetration under a single blow of an impact pile driver. Detailed information about pile stresses, displacements, and velocities at specific time intervals after impact can be generated if desired.

211. Important contributions to the state of the art of pile-driving have been made by others using wave equation methods. The selection of effective pile-hammer-soil combinations for economical foundations, pile driveability, pile-driving stress determinations, and prediction of bearing capacity at time of driving can be accomplished using wave equation analyses. The most successful applications of wave equation solutions have involved the selection of compatible driving equipment and determination of pile driveability. Evaluation of peak driving stresses can be used to reduce the incidence of pile breakage.

212. The successful prediction of pile bearing capacity from pile-driving measurements has been limited. Inaccurate predictions of capacity usually reflect the inability of the soil models to describe the pile-soil interaction behavior, especially in cohesive soils.

213. An alternative scheme to the direct wave equation solution approach (set calculated for an assumed resistance distribution) developed at CWRU has been reasonably accurate for piles in cohesionless soils. Scatter for piles in cohesive deposits has led CWRU investigators to conclude that their soil deformation model is incorrect for cohesive soils.

214. The most satisfactory correlations of pile bearing capacities with pile load tests have been found for piles that were redriven after all transient behavior could be assumed complete. For piles driven into soils where relaxation or setup may be expected, the redriving procedure will better account for changes in the pile-soil system that transpire between installation and loading. Experience

with similar hammer-pile combinations in the vicinity may be used to correct pile capacity predictions based upon installation data.

215. Improved soil deformation representations should be a primary research goal. "Best fit" values for the present soil deformation models are necessarily dependent upon numerous system variables. To include pile tests from various sites in a statistical exercise directly incorporates scatter in the predictions. Results of numerous investigations indicate that pile test correlations produce different soil parameters to fit into the particular soil behavior representation. The particular rheological model generally is a gross simplification of measurable behavior in laboratory tests. Nonetheless, these are the best approximations available at this time.

216. The wave equation analysis of pile-driving behavior is an indispensable aid to the foundation engineer. It should be involved in the earliest stages of pile foundation design. Contractor equipment availability, pile-driving experience in the vicinity, current driving practice, and building codes will provide considerable guidance for a given project, in selection of compatible equipment to satisfy the foundation design. Wave equation analyses can be performed to determine the most economical hammer-pile system for the prevailing site conditions. Finally, the pile(s) selected in the design can be analyzed to provide an estimate of predicted capacity versus blow count curve(s) as a reference.

217. The analysis of pile load test data can provide an "improved" set of soil parameters for adjusting the static capacity versus blow count curve. A great deal of care should be exercised in using "improved" soil parameters to predict pile capacities where considerably different driving resistance is encountered on the site. These improved values generated from a one-point correlation are in no way a unique fit. If a significant redesign of the foundation is deemed necessary after load testing, the soil parameters generated under different driving conditions are subject to change.

## REFERENCES

1. Timoshenko, S. and Goodier, J. M., Theory of Elasticity, McGraw-Hill, New York, 1951.
2. Kolsky, H., Stress Waves in Solids, Dover Publications, New York, 1963.
3. Smith, E. A. L., "Impact and Longitudinal Wave Transmission," Transactions, American Society of Mechanical Engineers, Paper No. 54, Aug 1955.
4. \_\_\_\_\_, "Pile Driving Analysis by the Wave Equation," Journal, Soil Mechanics and Foundations Division, American Society of Civil Engineers, Vol 86, No. SM4, Proceedings Paper 2574, Aug 1960, pp 35-61.
5. Holloway, D. M. "Analysis of Pile-Soil Interaction in Cohesionless Soils," Contract Report (in preparation), U. S. Army Engineer Waterways Experiment Station, CE, Vicksburg, Miss.
6. Johnson, C. L., Analog Computer Techniques, 2d ed., McGraw-Hill, New York, 1963.
7. Korn, G. A. and Korn, T. M., Electronic Analog Computers, 2d ed., McGraw-Hill, New York, 1956.
8. Parola, J. F., Mechanics of Impact Pile Driving, Ph.D. Dissertation, University of Illinois, Urbana, Ill., 1970.
9. Zienkiewicz, O. C., The Finite Element Method in Engineering Science, McGraw-Hill, New York, 1971.
10. Desai, C. W. and Abel, J. F., Introduction to the Finite Element Method, Van Nostrand, New York, 1972.
11. Desai, C. S. and Holloway, D. M., "Load-Deformation Analysis of Deep Pile Foundations," Proceedings, Symposium on Applications of the Finite Element Method to Problems in Geotechnical Engineering, U. S. Army Engineer Waterways Experiment Station, CE, Vicksburg, Miss., Sep 1972, pp 629-656.
12. Ellison, R. D., An Analytical Study of the Mechanics of Single Pile Foundations, Ph.D. Dissertation, Carnegie-Mellon University Pittsburgh, Pa., 1969.
13. Ellison, R. D., D'Appolonia, E., and Thiers, G. R., "Load-Deformation Mechanism for Bored Piles," Journal, Soil Mechanics and Foundations Division, American Society of Civil Engineers, Vol 97, No. SM4, Proceedings Paper 8052, Apr 1971, pp 661-678.
14. Lowery, L. L., Jr., et al., "Pile Driving Analysis - State of the Art," Research Report No. 33-13 (Final), Jan 1969, Texas Transportation Institute, Texas A&M University, College Station, Tex.

15. Lowery, L. L., Jr., Hirsch, T. J., and Samson, C. H., Jr., "Pile Driving Analysis - Simulation of Hammers, Cushions, Piles, and Soils," Research Report No. 33-9, Aug 1967, Texas Transportation Institute, Texas A&M University, College Station, Tex.
16. Hirsch, T. J. and Edwards, T. C., "Impact Load-Deformation Properties of Pile Cushioning Materials," Research Report No. 33-4, May 1966, Texas Transportation Institute, Texas A&M University, College Station, Tex.
17. Broms, B. B., "Method of Calculating the Ultimate Bearing Capacity of Piles; A Summary," Sols (Soils), Vol V, No. 18/19, 1966, pp 21-32.
18. Vesic, A. S., "Bearing Capacity of Deep Foundations in Sand," Stresses in Soils and Layered Systems, Highway Research Record No. 39, 1963, National Academy of Sciences, National Research Council, Washington, D. C., pp 112-153.
19. Robinsky, E. I. and Morrison, C. F., "Sand Displacement and Compaction Around Model Friction Piles," Canadian Geotechnical Journal, Vol I, No. 2, Mar 1964, pp 81-93.
20. Reeves, G. N., Coyle, H. M., and Hirsch, T. J., "Investigation of Sands Subjected to Dynamic Loadings," Research Report No. 33-7A, Dec 1967, Texas Transportation Institute, Texas A&M University, College Station, Tex.
21. Gibson, G. C. and Coyle, H. M., "Soil Damping Constants Related to Common Soil Properties in Sands and Clays," Research Report No. 125-1, Sep 1968, Texas Transportation Institute, Texas A&M University, College Station, Tex.
22. Raba, C. F. and Coyle, H. M., "The Static and Dynamic Response of a Miniature Friction Pile in Remolded Clay," Paper presented at Meeting of Texas Section American Society of Civil Engineers, 1968, San Antonio, Tex.
23. Korb, K. W. and Coyle, H. M., "Dynamic and Static Field Tests on a Small Instrumented Pile," Research Report No. 125-2, Feb 1969, Texas Transportation Institute, Texas A&M University, College Station, Tex.
24. Bartoskewitz, R. E. and Coyle, H. M., "Wave Equation Prediction of Pile Bearing Capacity Compared with Field Test Results," Research Report No. 125-5, Dec 1970, Texas Transportation Institute, Texas A&M University, College Station, Tex.
25. Foye, R., Jr., et al., "Wave Equation Analysis of Full Scale Test Piles Using Measured Field Data," Research Report No. 125-7, 1972, Texas Transportation Institute, Texas A&M University, College Station, Tex.
26. Texas Transportation Institute, "Piling Analysis Wave Equation Computer Program Utilization Manual," Research Report No. 33-11, 1969, Texas A&M University, College Station, Tex.

27. Bender, C. H., Jr., Lyons, C. G., and Lowery, L. L., Jr., "Applications of Wave-Equation Analysis to Offshore Pile Foundations," Preprints, Offshore Technology Conference, Vol I, Paper No. OTC 1055, 1969, pp 575-586.
28. Hirsch, T. J. and Samson, C. H., Jr., "Driving Practices for Prestressed Concrete Pile," Research Report No. 33-3, Apr 1965, Texas Transportation Institute, Texas A&M University, College Station, Tex.
29. Chellis, R. D., Pile Foundations, 2d ed., McGraw-Hill, New York, 1961.
30. Olson, R. E. and Flaate, K. S., "Pile-Driving Formulas for Friction Piles in Sand," Journal, Soil Mechanics and Foundations Division, American Society of Civil Engineers, Vol 93, No. SM6, Proceedings Paper 5604, Nov 1967, pp 279-296.
31. Lowery, L. L., Jr., Edwards, T. C., Hirsch, T. J., "Use of the Wave Equation to Predict Soil Resistance on a Pile During Driving," Research Report No. 33-10, Aug 1968, Texas Transportation Institute, Texas A&M University, College Station, Tex.
32. Van Reenen, D. A., Coyle, H. M., and Bartoskewitz, R. E., "Investigation of Soil Damping on Full-Scale Test Piles," Research Report No. 125-6, 1971, Texas Transportation Institute, Texas A&M University, College Station, Tex.
33. Goble, G. G., Rausche, F., and Moses, F., "Dynamic Studies on the Bearing Capacity of Piles, Phase III," Final Report to Ohio Department of Highways, Aug 1970, Case Western Reserve University, Cleveland, Ohio.
34. Goble, G. G., Moses, F., and Rausche, F., "Prediction of Pile Behavior from Dynamic Measurements," Proceedings, Conference on the Design and Installation of Pile Foundations and Cellular Structures, Apr 1970, Lehigh University, Bethlehem, Pa., pp 281-296.
35. Goble, G. G. and Rausche, F., "Pile Load Test by Impact Driving," Pile Foundations, Highway Research Board Record No. 333, 1970, National Academy of Sciences, National Research Council, Washington, D. C.
36. Rausche, F., Goble, G. G., and Moses, F., "A New Testing Procedure for Axial Pile Strength," Preprints, Offshore Technology Conference, Vol II, Paper no. OTC 1481, 1971, pp 633-641.
37. Rausche, F., Moses, F., and Goble, G. G., "Soil Resistance Predictions from Pile Dynamics," Journal, Soil Mechanics and Foundations Division, American Society of Civil Engineers, Vol 98, No. SN9, Proceedings Paper 9220, Sep 1972, pp 917-937.
38. Rausche, F., Soil Response from Dynamic Analysis and Measurements on Piles, Ph.D. Dissertation, 1970, Case Western Reserve University, Cleveland, Ohio.



39. Goble, G. G., Walker, F. K., and Rausche, F., "Pile Bearing Capacity - Prediction vs. Performance," Proceedings, Specialty Conference on Performance of Earth and Earth-Supported Structures, 11-14 Jun 1972, Purdue University, Lafayette, Ind., Vol 1, Part 2, pp 1243-1258.
40. Fruco and Associates, "Pile Driving and Loading Tests, Lock and Dam No. 4, Arkansas River and Tributaries, Arkansas and Oklahoma," Report prepared for U. S. Army Engineer District, Little Rock, CE, Sep 1964, St. Louis, Mo.
41. Furlow, C. R., "Pile Tests, Jonesville Lock and Dam, Ouachita and Black Rivers, Arkansas and Louisiana," Technical Report S-68-10, Dec 1968, U. S. Army Engineer Waterways Experiment Station, CE, Vicksburg, Miss.
42. Clarke, A. A., et al., "Port Construction in the Theater of Operations," Technical Report H-73-9, Jun 1973, U. S. Army Engineer Waterways Experiment Station, CE, Vicksburg, Miss.

Table 1  
Tabulation of Pile Impedances and Pile Types (after Parola<sup>8</sup>)

Pile Impedance pca lb-sec/in.	Pile Material					
	Steel*	Concrete*			Wood*	
		Area in. <sup>2</sup>	Diameter in.	Width in.	Area in. <sup>2</sup>	Diameter in.
725	5 (Thin-Wall Pipe)	23.5	5.5	4.8	82	10.2
1450	10	47	7.8	6.9	164	14.5
2900	20	94	11.0	9.7	328	20.4
5800	40 (Mandrel)	188	15.5	13.7	656	29.0
8700	60	282	18.0	16.8	984	--

\* The following material properties were used to determine pile dimensions from impedances. Subscripts denoting the material (s = steel, c = concrete, w = wood) are used.

$$\text{Steel: } E_s = 29 \times 10^6 \text{ psi} \quad \rho_s = 15.2 \frac{\text{lb-sec}^2}{\text{ft}^4}$$

$$c_s = \sqrt{E_s / \rho_s} = 16,600 \text{ ft/sec} \quad (\rho c)_s = 145 \frac{\text{lb-sec}}{\text{in.}}$$

$$\text{Concrete: } E_c = 4.25 \times 10^6 \text{ psi} \quad \rho_c = 4.65 \frac{\text{lb-sec}^2}{\text{ft}^4}$$

$$c_c = \sqrt{E_c / \rho_c} = 11,500 \text{ ft/sec} \quad (\rho c)_c = 30.9 \frac{\text{lb-sec}}{\text{in.}}$$

$$\text{Wood: } E_w = 1.3 \times 10^6 \text{ psi} \quad \rho_w = 1.24 \frac{\text{lb-sec}^2}{\text{ft}^4}$$

$$c_w = \sqrt{E_w / \rho_w} = 12,300 \text{ ft/sec} \quad (\rho c)_w = 8.84 \frac{\text{lb-sec}}{\text{in.}}$$

Table 2  
Impact Pile-Driver Data (from Parola <sup>8</sup>)

Rated Energy ft-lb	Make of Hammer	Size	Type	Blows per min	Stroke at Rated Energy in.	Weight Striking Parts, lb	Total Weight lb	Length of Hammer	Air cfm	A.S.M.E. Boiler H.P.	Steam or Air psi	Size of Hose in.	$\sqrt{E_p \times W_1}$ Rating (ft-lb <sup>2</sup> ) <sup>1/2</sup>
Energy over 100,000 ft-lb													
180,000	Vulcan	060	Single-act.	62	36	60,000	121,000	18' 6"	4626	740	130	(2)4	103,900
130,000	McKiernan-Terry	S-40	Single-act.	55	39	40,000	96,000	16' 0"	---	375	150	4	72,100
120,000	Vulcan	040	Single-act.	60	36	40,000	87,500	17' 11"	3400	535	120	(2)3	69,300
113,478	Super-Vulcan	400C	Differential	100	16 1/2	40,000	83,000	16' 9"	4659	700	150	5	67,400
Energy 50,000 to 100,000 ft-lb													
97,500	McKiernan-Terry	S-30	Single-act.	60	39	30,000	86,000	16' 0"	---	280	113	4	54,000
79,600	Kobe	K42	Diesel	45-60	98	9,200	22,000	14' 6"	---	---	---	---	27,100
60,000	Vulcan	020	Single-act.	60	36	20,000	39,000	15' 0"	1756	278	120	3	34,600
60,000	McKiernan-Terry	S20	Single-act.	60	36	20,000	38,650	18' 5"	1720	280	150	3	34,600
56,500	Kobe	K32	Diesel	45-60	98	7,060	15,400	13' 7"	---	---	---	---	20,000
50,200	Super-Vulcan	200C	Differential	98	15 1/2	20,000	39,050	13' 2"	1746	260	142	3	31,700
Energy 30,000 to 50,000 ft-lb													
48,750	Vulcan	016	Single-act.	60	36	16,250	30,250	14' 6"	1290	210	110	3	28,100
48,750	Raymond	0000	Single-act.	46	39	15,000	23,000	---	---	85	140	2 1/2	27,000
44,500	Kobe	K22	Diesel	45-60	98	4,850	10,600	13' 4"	---	---	---	---	14,700
42,000	Vulcan	014	Single-act.	60	36	14,000	27,500	14' 6"	1282	200	110	3	24,200
40,600	Raymond	000	Single-act.	50	39	12,500	21,000	15' 7"	---	70	135	2 1/2	22,500
39,800	Delmag	D-22	Diesel	42-60	n/a	4,850	10,054	12' 10 1/2"	---	---	---	---	13,900
37,500	McKiernan-Terry	S14	Single-act.	60	32	14,000	31,600	14' 10"	1260	190	100	3	23,000
36,000	Super-Vulcan	140C	Differential	103	15 1/2	14,000	27,984	12' 3"	1425	211	140	3	22,000
32,500	McKiernan-Terry	S10	Single-act.	55	39	10,000	22,200	14' 1"	1000	140	80	2 1/2	18,000
32,500	Vulcan	010	Single-act.	50	39	10,000	18,750	15' 0"	1002	157	105	2 1/2	18,000
32,500	Raymond	00	Single-act.	48	96	4,000	11,275	15' 0"	---	55	125	2	18,000
32,000	McKiernan-Terry	DE-40	Diesel	50	39	10,000	18,500	15' 0"	---	---	---	---	11,300
30,225	Vulcan	OR	Single-act.	50	39	9,300	16,765	15' 0"	1020	---	100	2 1/2	16,800
Energy 20,000 to 30,000 ft-lb													
26,300	Link-Belt	520	Diesel	80-84	43 1/6	5,070	12,545	16' 6"	---	---	---	---	11,500
26,000	McKiernan-Terry	C-8	Double-act.	77-85	20	8,000	18,750	9' 9"	875	110	100	2 1/2	14,400
26,000	Vulcan	08	Single-act.	50	39	8,000	16,750	15' 0"	880	127	80	2 1/2	14,000
26,000	McKiernan-Terry	S8	Single-act.	55	39	8,000	18,100	14' 4"	850	119	80	2 1/2	14,400
24,450	Super-Vulcan	80C	Differential	111	16 1/2	8,000	17,885	11' 4"	1245	180	120	2 1/2	14,000
24,500	Vulcan	8M	Differential	111	n/a	8,000	18,400	10' 6"	1245	180	120	2 1/2	14,000
24,370	Vulcan	0	Single-act.	50	39	7,500	16,250	15' 0"	841	---	80	2 1/2	13,500
24,000	McKiernan-Terry	C-826	Double-act.	85-95	18	8,000	17,750	12' 2"	875	120	125	2 1/2	13,900
22,600	Delmag	D-12	Diesel	42-60	n/a	2,750	5,440	12' 7 3/4"	---	---	---	---	7,900
22,400	McKiernan-Terry	DE-30	Diesel	48	96	2,800	9,075	15' 0"	---	---	---	---	7,900
24,400	Kobe	K13	Diesel	45-60	98	2,870	6,400	12' 8"	---	---	---	---	8,400
Energy 10,000 to 20,000 ft-lb													
19,875	Union	0	Double-act.	110	24	3,000	14,500	10' 1"	800	---	125	2	6,360
19,850	McKiernan-Terry	11R3	Double-act.	95	19	5,000	14,500	11' 1"	900	126	100	2 1/2	9,700
19,500	Vulcan	06	Single-act.	60	36	6,500	11,200	13' 0"	625	94	100	2	11,200
19,200	Super-Vulcan	65C	Differential	117	15 1/2	6,500	14,886	12' 1"	991	152	150	2	11,200
18,250	Link-Belt	440	Diesel	86-90	36 7/8	4,000	10,300	14' 6 1/4"	---	---	---	---	8,540
16,250	McKiernan-Terry	S5	Single-act.	60	39	5,000	12,375	13' 3"	600	84	80	2	9,000
16,000	McKiernan-Terry	C5	Compound	48	96	2,000	6,325	13' 3"	---	---	---	---	5,650
15,100	Super-Vulcan	50C	Differential	110	18	5,000	11,880	8' 9"	585	56	100	2 1/2	8,940
15,100	Vulcan	5M	Differential	120	15 1/2	5,000	11,782	10' 2"	880	125	120	2	8,690
15,000	Vulcan	1	Single-act.	120	15 1/2	5,000	12,900	9' 4"	880	125	120	2	8,690
15,000	Link-Belt	312	Diesel	60	36	5,000	10,100	13' 0"	565	81	80	2	8,660
13,100	McKiernan-Terry	10R3	Double-act.	100-105	30 7/8	3,857	10,375	10' 0"	---	---	---	---	7,610
12,725	Union	1	Double-act.	105	19	3,000	10,850	9' 4"	750	104	100	2 1/2	6,270
				125	121	1,600	10,000	8' 2"	600	---	100	1 1/2	4,530
Energy 5,000 to 10,000 ft-lb													
9,040	Delmag	D5	Diesel	42-60	n/a	1,100	2,401	11' 2 1/2"	---	---	---	---	3,150
9,000	McKiernan-Terry	C-3	Double-act.	130-140	16	3,000	8,500	7' 9 1/2"	450	60	100	2	5,200
9,000	McKiernan-Terry	S3	Single-act.	65	36	3,000	8,800	12' 4"	400	57	80	1 1/2	5,200
8,800	McKiernan-Terry	DE-10	Diesel	48	96	11,000	3,518	12' 2"	---	---	---	---	3,110
8,750	McKiernan-Terry	983	Double-act.	145	17	1,600	7,000	8' 2"	600	85	100	2	3,740
8,280	Union	1 1/2A	Double-act.	135	18	1,500	9,200	8' 4"	450	---	---	---	3,520
8,100	Link-Belt	180	Diesel	90-95	37 5/8	1,725	4,550	11' 3"	---	---	---	---	3,740
7,260	Vulcan	2	Single-act.	70	29 3/4	3,000	7,100	12' 0"	336	49	80	1 1/2	4,670
7,260	Super-Vulcan	30C	Differential	133	12 1/2	3,000	7,036	8' 11"	488	70	120	1 1/2	4,670
7,260	Vulcan	3M	Differential	133	n/a	3,000	8,490	7' 11"	488	70	120	1 1/2	4,670
6,500	Link-Belt	105	Diesel	90-96	35 1/4	1,445	3,885	10' 3"	---	---	---	---	3,070
Energy Under 5,000 ft-lb													
4,900	Vulcan	DGH900	Differential	238	10	900	5,000	6' 9"	580	75	78	1 1/2	1,900
3,600	Union	3	Double-act.	160	14	700	4,700	6' 4"	300	---	100	1 1/4	1,600
3,600	McKiernan-Terry	7	Double-act.	225	9 1/2	800	5,000	6' 1"	450	63	100	1 1/2	1,700
445	Union	6	Double-act.	340	7	100	910	3' 10"	75	---	100	3/4	210
386	Vulcan	DGH100A	Differential	303	6	100	786	4' 2"	74	8	60	1	200
356	McKiernan-Terry	3	Double-act.	400	5 3/4	68	675	4' 10"	110	---	100	1	150
320	Union	7A	Double-act.	400	6	80	540	3' 7"	70	---	100	3/4	160

$E_p$  = rated striking energy in foot-pounds;  $W_1$  = weight of striking parts in pounds.

Note: Ram weights of drop hammers vary from 500 to 10,000 lb with variable strokes therefore variable energy.

Table 3  
Summary of Diesel Hammer Properties and  
Operating Characteristics (After Lowery<sup>14,15</sup>)

Hammer Manufacturer	Hammer Type	Maximum Rated Energy (ft-lb)	Ram Weight (lb)	Anvil Weight (lb)	Maximum Equiv- alent Stroke (ft)	d* (ft)	Explosive Force (lb)	Cap Block (Normally Specified)
Link Belt	312	18,000	3857	1188	4.66	0.50	98,000	5 Micarta disks 1" x 10 7/8" dia.
	520	30,000	5070	1179	5.93	0.83	98,000	
MKT Corp	DE20	16,000	2000	640	8.00	0.92	46,300	nylon disk 2" x 9" dia.
	DE30	22,400	2800	775	8.00	1.04	98,000	nylon disk 2" x 19" dia.
	DE40	32,000	4000	1350	8.00	1.17	138,000	nylon disk 2" x 24" dia.
Delmag	D-12	22,500	2750	754	8.19	1.25	93,700	15" x 15" x 5"
	D-22	39,700	4850	1147	8.19	1.48	158,700	German Oak 15" x 15" x 5" German Oak

\* Distance from anvil to exhaust ports

Table 4  
Typical Secant Moduli of Elasticity (E)  
and Coefficients of Restitution (e) of Various  
Pile Cushioning Materials (from Lowery<sup>14</sup>)

	E psi	e
Micarta Plastic	450,000	0.80
Oak (Green)	45,000*	0.50
Asbestos Discs	45,000	0.50
Fir Plywood	35,000*	0.40
Pine Plywood	25,000*	0.30
Gum	30,000*	0.25

\* Properties of wood with load applied perpendicular to wood grain.

Table 5  
Soil Damping Parameters (from Foye<sup>25</sup>)

Soil Type	J' sec/ft	J sec/ft
Clay (CL, CH, Hardpan)	0.20	0
Partially saturated sands and silts	0.05	0
Saturated sands and silts	0.50	0
Soft peat	0.00	0

Table 6  
Hammer Assembly Data, Lock and Dam No. 4

Hammer

Vulcan 140 C double-acting hammer

Rated energy

36,000 ft-lb

Ram weight, W(1)

14,000 lb

Efficiency (assumed)

85%

Capblock

Top plate: steel

4 in. thick by 17.75 in. in diameter with 3.5-in.  
bored center hole; assumed rigid

Bottom plate: steel

4.5 in. thick by 17.75 in. in diameter with 3.5-in.  
bored center hole; assumed rigid

Cushion: Micarta

Ten 1.0-in.-thick disks 17.5 in. in diameter  
with 4.5-in. bored center hole

Young's modulus

$4.5 \times 10^5$  psi

Spring stiffness

$$K_1 = \frac{AE}{\Delta x} = \frac{\pi/4[17.5)^2 - (4.5)^2]}{10} (4.5 \times 10^5)$$

$$K_1 = 1.01 \times 10^7 \text{ lb/in.}$$

Coefficient of restitution (assumed)

0.80

Pile Cap

Assumed rigid weight

1,710 lb

Table 7  
Pile Element Properties, Lock and Dam No. 4

Property	Test Pile 1	Test Pile 2	Test Pile 3
Outer diameter	12.75 in.	16.0 in.	20.0 in.
Net cross section	17.12 in. <sup>2</sup>	23.86 in. <sup>2</sup>	27.36 in. <sup>2</sup>
Element weight	293 lb	408 lb	468 lb
Spring stiffness, $\frac{AE}{\Delta x}$	$8.56 \times 10^6$ lb/in.	$1.19 \times 10^7$ lb/in.	$1.37 \times 10^7$ lb/in.

Table 8  
Input Data Files,  
Lock and Dam No. 4

\*OLD LD4TP1  
READY  
\*LIST

[illegible]

\*OLD LD4TP2  
READY  
\*LIST

[illegible]

\*OLD LE4TP3  
READY  
\*LIST

[illegible]

Table 9

Hammer Assembly Data, Jonesville Lock and DamHammer

Vulcan 016 single-acting air hammer

Ram weight, W(1)	16,250 lb
Stroke	3 ft
Energy	48,750 ft-lb
Efficiency (assumed)	85%

Capblock

Asbestos

Cross section (assumed)	255 in. <sup>2</sup>
Thickness, L	6 in
Coefficient of restitution (assumed)	0.60
Secant modulus (dependent upon peak stress level)	$4.14 \times 10^4$

Helmet

Weight, W(2)	3,000 lb
--------------	----------

Cushion Block - Oak

18 by 18-in. cross section	324 in. <sup>2</sup>
Thickness, L	6 in.
Coefficient of restitution (assumed)	0.47
Secant modulus (dependent upon peak stress level)	39,399 psi



## APPENDIX A

### WAVE EQUATION COMPUTER PROGRAM TAMFOR (TIME-SHARING VERSION)

1. As described in the main text, a time-sharing version, TAMFOR, of the Texas A&M University (TAMU) design-oriented computer program has been adapted for use on the U.S. Army Engineer Waterways Experiment Station (WES) computer facilities. A batch listing of the original program and a usage guide to the program are given in the TAMU publication, "Piling Analysis Wave Equation Computer Program Utilization Manual."<sup>26\*</sup> Because utilization guidelines are basically the same for using TAMFOR, the TAMU guidelines will be briefly described, with emphasis on the particular differences between the time-sharing program and the TAMU program. A sample printout of the time-sharing program is shown in Figure A1.

2. The primary difference between the batch program and the time-sharing program involves the use of data files for both input and output in the time-sharing mode. Data storage files permit continuous execution of the FORTRAN program without change of control between the remote terminal and the computer during the run.

3. An input data file, PILES 2, is filled with the free-form input information that would be punched on cards for a batch program processing. The input data items are listed on statement lines in PILES 2, and each piece of information is separated from the next by a comma or a blank space. For decimal numbers the input may be in fixed-point or floating-point notation. The end of a data card in the batch mode corresponds to the end of a statement line in the time-sharing. The input of alphanumeric data in free form is accomplished by enclosing the name in quotation marks.

4. Output data from TAMFOR are listed in the data file OUTPUT. The format of OUTPUT has been condensed to permit printing on an 80-

---

\* Raised numbers refer to similarly numbered items in the References at the end of the main text.

character remote terminal. The normal output option and the summary output options from the TAMU program are included in TAMFOR, but the detailed output option, IOPT15 = 2, is not permitted (it gives only normal data printout). The normal printout includes listing of input data (including  $RU_{TOTAL}$ ) and system parameters used in the calculation. The calculated peak pile stresses and corresponding time intervals of occurrence, the final velocity of all elements, and the final element displacements are tabulated; and finally, the computed pile set and blow count values are printed out with the total number of time intervals used in the calculation.

#### Basic Parameters

5. The input data file, PILES 2, controls the computations and the form of the output. The sequence of input data is identical with that used in the TAMU report.<sup>26</sup> The format is somewhat more flexible. A detailed example is given in Part V for using TAMFOR. An explanation of the various input parameters follows.<sup>26</sup>

Case Number = Any combination of six or less numeric characters inclosed in quotation marks. This information will be listed with every set of output for the particular run.

Number of Problems = Total number of problem sets in the file for the particular run.

1/DELTAT = An entry of zero will permit the program calculation of a critical value for the computation. A number larger than the critical value may be entered here. The program will select the larger value between that entered and the critical value to prevent inadvertent use of too small a value.

P = The total number of element weights in the problem.

SLACK(1) = This prescribes a specified looseness between  $W(1)$  and  $W(2)$ .

SLACK(1) = This permits an amount of movement in spring K(1) before it will take tension. A zero value permits tension between elements. A very large value, such as 1000, allows no interelement tension.

(Cont.)

SLACK(2) = As above

SLACK(3) = As above

OPTION 1 = Permits manual entry of element areas.

- a. Enter 1 and all areas will be set equal to 1.00. In this case no values will be listed in the input file.
- b. Enter 2 if the cross-sectional area of every element is to be entered below, AREA(1) to AREA(P).

OPTION 2 = Permits manual entry of element soil resistance percentages.

- a. Enter 1 if soil resistance values are to be specified by OPTION 12. No values of RU will be listed in PILES 2.
- b. Enter 2 if soil resistance percentage values are to be listed below. RU(1) through RU(p + 1) are to be listed in order. Note that RU(p + 1) is the pile tip resistance. The sum of the RU values must total 100 percent.

OPTION 3 = This option permits manual entry of the SLACK values.

- a. Enter 1 if all values SLACK(4), ..., SLACK(p - 1) are to be set to zero. This specifies that springs K(4), ..., K(p - 1) can take tension. No SLACK values will be listed below.
- b. Enter 2 if SLACK values are to be entered manually. Repeat SLACK(1) through SLACK(3) as before in the listing below.

OPTION 4 = This is an option to select a routine to simulate the behavior

OPTION 4 = of springs K(1) , K(2) , and  
(Cont.) K(3) .

- a. Enter 1 for use of Smith's Routine 3 and 4.
- b. Enter 2 for use of TAMU Routine. It is recommended by TAMU that 4 be taken as OPTION 2.

IPRINT = This is an option for use with the detailed output format. Any value may be entered for IPRINT since it is not used in TAMFOR in present form. A number must be entered to maintain input variable sequence.

NSEG1 = Mass number of the first pile segment.

6. This completes the first READ statement and generally completes the first data file line. A comma should follow the last item on every line in the file.

7. The total weight of each segment in pounds begins the next data line. The values W(1),...,W(p) are listed in order. The values of W(1) on a subsequent input line will supersede whatever value is listed for this series.

8. A new line is used to begin the listing of element spring constants in pounds per inch for springs K(1),...,K(p - 1) , inclusive. K(p) is the tip soil spring and is calculated by the program.

9. If OPTION 1 = 2, the next data line begins the list of average element areas, A(1),...,A(p) , inclusive. Units for these areas are subject to the needs of the output. If OPTION 1 = 1 , these data are omitted from the file PILES 2, and the program will specify values of 1.00.

10. If OPTION 2 = 2, the soil resistance of each element, expressed as a percentage of  $RU_{TOTAL}$  , is listed on the next data line, RU(1),...,RU(p + 1). RU(p + 1) represents the percentage of total resistance developed at the tip. If OPTION 2 = 1, no entry is made in PILES 2.

11. If OPTION 3 = 2, the physical slack or looseness in inches is entered on a new data line. If there can be no tension at a joint,

1000.0 is entered. SLACK(1),...,SLACK(p - 1) are listed because SLACK(p) = 1.000.0 is specified by the program since the tip cannot transmit tension. If OPTION 3 = 1, no entries are made for SLACK values at this time.

12. Note that the program currently has parameter arrays permitting 24 locations, such that p should be less than 23. The TAMU program will accommodate much larger arrays depending on the storage limitations, perhaps. Because TAMFOR requires a large time-sharing storage, exceeding the array size in the time-sharing mode may be more limited by computer capacity than in the batch version.

#### Problem Parameters

13. Problem sets, using the input data discussed previously as a basis, are input sequentially. All of the data for each problem set is read by a single loop of a READ statement. The program executes the calculation for that problem set and returns to read the parameters of the next set, and so on. For the particular problem, the input data are as follows:

PROBLEM NUMBER = An integer  
W(1) = Ram weight, pounds  
NC = Number of the spring for which  
K(NC) may be varied.  
K(NC) = The spring constant of the spring  
to be varied in pounds per inch.  
The original value is stored and  
reset after the problem is completed.  
EFF = Hammer efficiency, as a decimal.  
ENERGY = Kinetic energy of the falling ram.  
ERES(L) = Coefficient of restitution of  
spring, K(1).  
ERES(2) = Coefficient of restitution of  
spring, K(2).  
ERES(3) = Coefficient of restitution of  
spring, K(3).

- RU(TOTAL) = This value is used for single calculations, OPTION 11 = 2. It is the ultimate pile capacity in pounds. If OPTION 11 = 1, enter a zero.
- RU(P) = Percentage of RU(TOTAL) developed at the pile tip.
- MO = Enter the number of the first pile segment acted upon by soil resistance.
- QPOINT = Soil quake at the pile point in inches.
- QSIDE = Soil quake at the side of the pile in inches.
- JPOINT = Point damping constant in seconds per foot.
- JSIDE = Side damping constant in seconds per foot.
- FEXP = Diesel explosive force in pounds which acts on the ram and anvil of a diesel hammer. If there is no explosive force, enter a value of zero.
- OPTION 11 = This option provides for single or multiple (computer-generated) calculations.
- a. Enter 1 if multiple calculations of RU(TOTAL) values versus Blows per inch are required. The program will compute suitable RU(TOTAL) values for this case.
  - b. Enter 2 if a single calculation using the RU(TOTAL) value prescribed is desired.
- OPTION 12 = This option designates the skin friction distribution.
- a. Enter 1 for a uniform side friction distribution between segments MO and P.
  - b. Enter 2 for a triangular skin friction distribution.
  - c. Enter 3 when OPTION 2 = 2, signifying manual entry of RU values previously.

- OPTION 13 = This option provides for listing of RU(TOTAL) versus blows per inch data in a separate file, PLOTIT, which can be used to generate computer plots of data.
- a. Enter zero if no plot data are required.
  - b. Enter 1 to list RU(TOTAL) and blows per inch data in data file PLOTIT for external computer plotting purposes.
- OPTION 14 = This is used to include or exclude the effects of gravity (pile-hammer weight) on the calculations.
- a. Enter 1 if the forces of gravity are to be included in the calculations.
  - b. Enter 2 if the forces of gravity are to be excluded from consideration. This would be applied for piles driven horizontally or at an extreme batter, or perhaps for cases where the buoyancy forces approach the total pile weight.
- OPTION 15 = Output format option.
- a. Enter 1 to specify normal data printout.
  - b. Enter 3 to receive a summary printout of RU(TOTAL) versus blows per inch in conjunction with OPTION 11 = 1.

```

100C      WATERWAYS EXPERIMENT STATION
105C
110C      PILE DRIVING ANALYSIS BY THE WAVE EQUATION
120C      LUMPED PARAMETER FINITE DIFFERENCE METHOD
125C
130C      TEXAS A&M PROGRAM FROM TEXAS TRANSPORTATION INSTITUTE
140C      RESEARCH REPORT 33-11,"PILING ANALYSIS WAVE EQUATION
150C      COMPUTER PROGRAM UTILIZATION MANUAL"
160C
170C      PROGRAM HAS BEEN ADAPTED FOR TIMESHARING SYSTEM*
171C      INPUT:EXTERNAL DATA FILE,PILES2
172C      INPUT ORDER SAME AS IN 33-11 BUT FREE FORMAT SUCH THAT
173C      SPACE OR COMMA SEPARATES EACH PIECE OF DATA.
175C      OUTPUT:EXTERNAL DATA FILES,OUTPUT,PLOTIT
176C      OUTPUT:FORMAT CONDENSED FOR T/S PRINTER;DETAILED OUTPUT
177C      NOT AVAILABLE IN T/S VERSION(USE BATCH)
178C      PILE SET,BLOW COUNT,PEAK STRESSES & DISPLACEMENTS ARE
179C      LISTED IN DATA FILE OUTPUT.
180C      PLOTIT: DATA FILE STORING DX AND DY SCALE FACTORS AND
181C      X,Y VALUES OF BLOW COUNT,RUTOTL TO SCALE FOR PLOTTING.
182C      (FOR USE WITH OPTION11=1,OPTION13=1)
183C      NOTATION:SUFFIX X DENOTES PRECEDING VALUE;N DENOTES TIME
184C      INTERVAL;EXAMPLE, NFMAT= NUMBER OF TIME INTERVAL FOR
185C      WHICH THE MAXIMUM TENSION FORCE WAS RECORDED IN AN
186C      ELEMENT SPRING.
230 DIMENSIONAREA(24),C(24),CX(24),CMAX(24),D(24),DX(24)
240&,DMAX(24),DPRIME(24),ERES(24),F(24),FX(24),FMAXC(24),
250&FMAXT(24),K(24),KPRIME(24),LAM(24),NDMAX(24),
260&NFMAT(24),NFMAT(24),R(24),RU(24),SLACK(24),
270&UBLOWS(24),UFMAXC(24),URUTTL(24),V(24),
280&W(24),RULIST(24),RUHIL(30),RWENR(30),RWMICH(30),
290&XPLOT(50),YPLT(50),STRESS(24),KHOLD(24),
300&FCMAX(50),NCMAX(50),FTMAX(50),NTMAX(50)
310 REALJPOINT,JSIDE,K,KPRIME,NPASS,NP1,KHOLD
320 INTEGERP,PPLUS1,PLESS1,PROB,PROBS
330C      24 OF EACH OF ABOVE SUFFICIENT FOR USUAL PROBLEMS
340C ---- INPUT -- GENERAL
350 CALLOPENF(4,"PILES2")
360 CALLOPENF(1,"OUTPUT")
365 CALL OPENF(3,"PLOTIT")
370 5010READ(4,)(CASE,PROBS,TTDELTA,P,(SLACK(I),I=1,3),IOPT1,
380&IOPT2,IOPT3,IOPT4,IPRINT,NSEG1
390 WRITE(1:5003)
400 5003FORMAT(/32X,8H*****/)
410 IF(TTDELTA.LE.0.)TTDELTA=1.0
420 IF(IOPT4.LE.0)IOPT4=2
430 IF(IPRINT.LE.0)IPRINT=1
440 IF(NSEG1.LE.0)NSEG1=2
450 TDELTA=TTDELTA
460 5020DELTA=1./TDELTA
470 5021PPLUS1=P+1
480 5022PLESS1=P-1
490 5030READ(4,)(W(M),M=1,P)
500 5031W(PPLUS1)=-0.0
510C ----CALCULATE PILE WEIGHT
520 WPILE=0.
530 DO6JT=NSEG1,P
540 6WPILE=WPILE+W(JT)
550 5040READ(4,)(K(M),M=1,PLESS1)
560C      K(P) IS DETERMINED AT 5184
570 5041K(PPLUS1)=-0.0

```

Figure A1. Sample printout of TAMFOR (sheet 1 of 10)



```

580 5083D05084M=1,P
590 KHOLD(M)=K(M)
600 5084AREA(M)=1.0
610 5086AREA(PPLUS1)=-0.0
620 5087IF(IOPT1-2)5090,5088,5088
630 5088READ(4,)(AREA(M),M=1,P)
640 IF(AREA(1).LE.0.)AREA(1)=1.0
650 IF(AREA(P).LE.0.)AREA(P)=1.0
660 5090IF(IOPT2-2)5100,5092,5092
670 5092READ(4,)(RULIST(M),M=1,PPLUS1)
680 5100IF(IOPT3-2)5101,5104,5104
690 5101D05102M=4,PLESS1
700 5102SLACK(M)=0.0
710 5103GOTO5105
720 5104READ(4,5114)(SLACK(M),M=1,PLESS1)
730 5105SLACK(P)=1000.0
740 5106SLACK(PPLUS1)=-0.0
750 5110D05111M=4,P
760 5111ERES(M)=1.0
770 5112ERES(PPLUS1)=-0.0
780 5113FORMAT(A6,I3,F10.4,I3,3F7.3,4I1,1X13,I2)
790 5114FORMAT(8F10.3)
800 5115FORMAT(8F10.0)
810 5116FORMAT(8F10.7)
820 5117FORMAT(I2,F8.2,I1,F9.0,F3.2,F6.0,3F3.2,F9.1,F4.1,I3,4F3.2,F9.0
830&,5I1)
840 5118FORMAT(/5H CASE,A6,5H PROB,I6/
850&55H RU PERCENTAGES ON DATA SHEET PAGE 1 SHOULD TOTAL 100.0,
860&/18HBUT ACTUALLY TOTAL,F15.7)
870C ---- DO 5570 SOLVES PROBLEMS ONE AFTER ANOTHER
880 NC=1
890 KOPT15=0
900 5120D05570I=1,PROBS
910 K(NC)=KHOLD(NC)
920 5121READ(4,)(PROB,W(1),NC,K(NC),EFF,ENERGY,ERES(1),ERES(2),ERES(3)
930&,RUSUM,PERCNT,MO,QPOINT,QSIDE,JPOINT,JSIDE,FEXP,IOPT11,
940&IOPT12,IOPT13,IOPT14,IOPT15
950 IF(IOPT12.LE.0)IOPT12=3
960 VSTART=SQRT(64.4*EFF*(ENERGY/W(1)))
970 D09009M=1,50
980 FTMAX(M)=0.
990 9009FCMAX(M)=0.
1000 NKONT=0
1010 5140RUTTLX=0.0
1020 5141BLOWSX=0.
1030 5150V(1)=VSTART
1040 5152LT=0
1050C ---- FIRST DETERMINE VALUE OF RUTOTL
1060 5154IF(IOPT11-2)5151,5160,5151
1070C ---- FOR RUTOTL DATA GENERATED BY THE PROGRAM
1080 5151RUTOTL=W(1)*V(1)**2/12.0
1090 5153GOTO5170
1100C FOR SINGLE PROBLEM
1110 5160RUTOTL=RUSUM
1120 GOTO5170
1130C COMPUTER CYCLES FROM 707 NEAR END OF PROGRAM
1140 701SLOPE=(RUTOTL-RUTTLX)/(BLOWS-BLOWSX)
1150 SLOPE=AMAX1(10000.,SLOPE)
1160 IF(BLOWS-7.0)5164,702,702
1170 5164IF(IOPT4-2)5165,703,703
1180 702IF(BLOWS-20.0)704,704,705

```

Figure A1 (sheet 2 of 10)

```

1190 S165DB=1.00
1200 GOTO706
1210 703DB=1.25
1220 GOTO706
1230 704DB=2.5
1240 GOTO706
1250 705DB=5.0
1260 GOTO706
1270 706RUTTLX=RUTOTL
1280 RUTOTL=RUTTLX+(DB*SLOPE)
1290 BLOWSX=BLOWS
1300C ---- SECOND DETERMINE ALL VALUES OF RU(M)
1310 5170D013M=1,M0
1320 13RU(M)=0.0
1330 5171RUPINT=(PERCNT/100.0)*RUTOTL
1340 5172IF(IOPT12-2)143,146,5176.
1350C      FOR UNIFORM DISTRIBUTION
1360 143D0144M=M0,P
1370 144RU(M)=(RUTOTL-RUPINT)/FLOAT(P-M0+1)
1380 5173RU(PPLUS1)=RUPINT
1390 GOTO713
1400C      FOR TRIANGULAR DISTRIBUTION
1410 146D0145M=M0,P
1420 145RU(M)=(2.0*(RUTOTL-RUPINT)*(FLOAT(M-M0)+0.5))/(FLOAT(P-M0+1))*2
1430 5175RU(PPLUS1)=RUPINT
1440 GOTO713
1450C      FOR DISTRIBUTION PER RU LIST ON DATA SHEET
1460 5176TOTAL=0.0
1470 D05177M=1,PPLUS1
1480 5177TOTAL=TOTAL+RULIST(M)
1490 5178IF((ABS(TOTAL-100.0))-2.0)5180,5180,5179
1500 5179WRITE(1;5118)
1510 GOTO5570
1520 5180D05181M=1,PPLUS1
1530 5181RU(M)=(RULIST(M)/100.0)*RUTOTL
1540 GOTO713
1550C ---- THIRD DETERMINE STARTING VALUES OF V(M)
1560 713V(1)=VSTART
1570 D0180M=2,P
1580 180V(M)=0.0
1590 5183V(PPLUS1)=-0.0
1600C ---- FOURTH DETERMINE VALUE FOR K(P)
1610 5184K(P)=RU(PPLUS1)/QPOINT
1620C      FIFTH CHANGE CYCLE COUNT
1630 5186LT=LT+1
1640C ---- CHECK ON DELTAT
1650 CALLDELTC(NPASS,TTDELT,P,W,K,TDELTA,DELTAT,N2)
1660C ---- END DELTAT CHECK
1670C ---- ASSIGN OTHER VALUES REQUIRED (TEXAS A AND M REP1)
1680 D05218M=1,P
1690 32KPRIME(M)=RU(M)/QSIDE
1700 C(M)=0.0
1710 F(M)=0.0
1720 CMAX(M)=0.0
1730 LAM(M)=1
1740 D(M)=0.0
1750 NFMAXC(M)=0
1760 NFMAXT(M)=0
1770 DMAX(M)=0.0
1780 NDMAX(M)=0
1790 FMAXC(M)=0.0

```

Figure A1 (sheet 3 of 10)

```

1800 FMAXT(M)=0.0
1810 R(M)=0.0
1820 S218DPRIME(M)=0.0
1830 KPRIME(PPLUS1)=0.
1840 DPRIMP=0.0
1850 LAMP=1
1860C ---- SIXTH PRINT INPUT FOR ONE PROBLEM
1870 IF(KOPT15.GT.0.AND.10PT15.EQ.3)GOTO5258
1880 KOPT15=KOPT15+1
1890 5190WRITE(1;5200)CASE,PROB,PROBS
1900 5191WRITE(1;5201)
1910 5192WRITE(1;5202)TDELTA,P,10PT1,10PT2,10PT3,10PT4,10PT11,10PT12,
1920 10PT13,10PT14,10PT15,FEXP
1930 5193WRITE(1;5203)
1940 5194WRITE(1;5204)ENERGY,EFF,RUTOTL,PERCNT,MO,QPOINT,QSIDE,
1950 QJPOINT,JSIDE,N2
1960 5195WRITE(1;5205)
1970 5196WRITE(1;5206)(M,W(M),K(M),AREA(M),RU(M),SLACK(M),ERES(M),
1980 V(M),KPRIME(M),M=1,PPLUS1)
1990 5200FORMAT(///27HTexas A * M UNIVERSITY ,3X,
2000 &22H PILE DRIVING ANALYSIS/4X,9H CASE NO.,A6,4X,
2010 &12H PROBLEM NO.,I4,3H OF,I4)
2020 5201FORMAT(/4X,"1/DT P OPTIONS 1 2 3 4 11 12 13",
2030 &" 14 15 EXP F")
2040 5202FORMAT(/2X,F8.0,I3,8X,9I4,F14.0/)
2050 5203FORMAT(2X,"ENERGY HAMMER EFF RUTOTAL PT PERCENT MO QP"
2060 &" QS JP JS N2")
2070 5204FORMAT(/2F10.2,F10.0,F10.2,I6,4F5.2,I5/)
2080 5206FORMAT(14,F7.0,1X,E10.4,F8.2,F10.1,F8.2,F7.2,F7.2,1X,E9.3)
2090 5205FORMAT(3X,"M W(M) K(M) AREA(M) RU(M) SLACK(M)"
2100 &" ERES(M) USTART KPRIME"/)
2110C ---- EFFECT OF GRAVITY BEFORE RAM STRIKES--TEXAS A AND M SMITHSGRAVITY
2120 5258IF(10PT14-2)5220,5221,5221
2130 5220WTOTAL=0.0
2140 RTOTAL=0.0
2150 D05JT=2,PPLUS1
2160 WTOTAL=WTOTAL+W(JT)
2170 5RTOTAL=RTOTAL+RU(JT)
2180 D08JT=2,PLESS1
2190 R(JT)=(RU(JT)*WTOTAL)/RTOTAL
2200 8F(JT)=F(JT-1)+W(JT)-R(JT)
2210 IF(K(P))67,66,67
2220 66IF(KPRIME(P))67,63,67
2230 67D(P)=(F(PLESS1)+W(P))/(KPRIME(P)+K(P))
2240 IF(QSIDE-D(P))64,65,65
2250 64R(P)=RU(P)
2260 F(P)=F(PLESS1)+W(P)-R(P)
2270 D(P)=F(P)/K(P)
2280 GOTO63
2290 65R(P)=D(P)*KPRIME(P)
2300 F(P)=D(P)*K(P)
2310 63CONTINUE
2320 D0111JT=1,PLESS1
2330 JTM=P-JT
2340 C(JTM)=F(JTM)/K(JTM)
2350 D(JTM)=D(JTM+1)+C(JTM)
2360 DPRIME(JTM)=D(JTM)-WTOTAL*QSIDE/RTOTAL
2370 111CONTINUE
2380 D0800M=1,P
2390 8000STRESS(M)=F(M)/AREA(M)
2400 5221N=0

```

Figure A1 (sheet 4 of 10)

```

2410 LAY=1
2420C ---- DYNAMIC COMPUTATION BASED ON SMITHS PAPER MODIFIED (TEXAS REPN)
2430 5240LACK=1
2440 5241D068M=1,P
2450C      68 IS BETWEEN 5439 AND 5440
2460 D(M)=D(M)+V(M)*12.0*DELTAT
2470 IF(DMAX(M)-D(M))20,21,21
2480 20DMAX(M)=D(M)
2490 NDMAX(M)=N+1
2500 21CX(M)=C(M)
2510 IF(M-P)34,5400,34
2520 34C(M)=D(M)-D(M+1)-V(M+1)*12.0*DELTAT
2530C      STATEMENT 34 MUST USE A COMPUTED VALUE FOR THE ACTUAL D(M+1)
2540 5242IF(C(M))5243,30,30
2550 5243IF(ABS(C(M))-SLACK(M))5244,5244,5246
2560 5244C(M)=0.0
2570 5245GOTO30
2580 5246C(M)=C(M)+SLACK(M)
2590C      NOTE THAT ONLY A NEGATIVE VALUE OF C(M) RESULTS FROM 5246
2600 30FX(M)=F(M)
2610C      A TEXAS ROUTINE FOR B(M) IS OMITTED HERE
2620 5250IF(IOPT4-2)5300,36,5300
2630C ---- 36 TO 35 IS A TEXAS ROUTINE REPLACING SMITH ROUTINE 3 OR 4
2640 36IF(ABS(ERES(M)-1.0)-.00001)38,38,14
2650 38F(M)=C(M)*K(M)
2660 GOTO5400
2670 14IF(C(M)-CX(M))12,35,15
2680 15F(M)=FX(M)+((C(M)-CX(M))*K(M))
2690 GOTO35
2700 12F(M)=FX(M)+((C(M)-CX(M))*K(M)/ERES(M)**2)
2710 35F(M)=AMAX1(0.0,F(M))
2720 GOTO5400
2730C      A TEXAS ROUTINE FOR GAMMA IS OMITTED HERE
2740C ---- SMITH ROUTINE 3 OR 4
2750 5300IF(ERES(M)-1.00)5302,5301,5301
2760 5301F(M)=C(M)*K(M)
2770 GOTO5400
2780 5302IF(C(M))5303,5303,5304
2790 5303F(M)=0.0
2800 GOTO5400
2810 5304IF(C(M)-CMAX(M))5306,5305,5305
2820 5305CMAX(M)=C(M)
2830 F(M)=C(M)*K(M)
2840 GOTO5400
2850 5306F(M)=(K(M)/ERES(M)**2)*C(M)-(1./ERES(M)**2-1.)*K(M)*CMAX(M)
2860 F(M)=AMAX1(F(M),0.0)
2870 GOTO5400
2880 5400IF(M.GT.1)GOTO48
2890 IF(FEXP.LE.0.)GOTO48
2900 NP1=N+1
2910 IF(NP1.GT.(0.0125/DELTAT))GOTO48
2920 IF(NP1-0.01/DELTAT)46,46,90
2930 46IF(F(1)-FX(1))47,48,48
2940 47F(1)=AMAX1(F(1),FEXP,0.)
2950 GOTO48
2960 90F(1)=AMAX1(0.0,FEXP*(1.0-(DELTAT*(NP1-0.01/DELTAT)/0.0025)))
2970 48IF(KPRIME(M))50,55,50
2980 50IF(DPRIME(M)-D(M)+QSIDE)51,52,52
2990 51DPRIME(M)=D(M)-QSIDE
3000 52CONTINUE
3010 IF(DPRIME(M)-D(M)-QSIDE)53,53,54

```

Figure A1 (sheet 5 of 10)

```

3020 54DPRIME(M)=D(M)+QSIDE
3030 53CONTINUE
3040 5410LAP=LAM(M)
3050 GOTO(10,57),LAP
3060 10IF(D(M)-DPRIME(M)-QSIDE)56,57,57
3070 56R(M)=(D(M)-DPRIME(M))*KPRIME(M)*(1.0+JSIDE*V(M))
3080 GOTO55
3090 57R(M)=(D(M)-DPRIME(M)+JSIDE*QSIDE*V(M))*KPRIME(M)
3100 LAM(M)=2
3110 55CONTINUE
3120 73IF(M-P)71,74,71
3130 74IF(DPRIMP-D(P)+QPOINT)75,76,76
3140 75DPRIMP=D(P)-QPOINT
3150 76CONTINUE
3160 LAMP=LAMP
3170 GOTO(77,78),LAMP
3180 77IF(D(P)-DPRIMP-QPOINT)79,78,78
3190 79F(P)=(D(P)-DPRIMP)*K(P)*(1.0+JPOINT*V(P))
3200 GOTO171
3210 78F(P)=(D(P)-DPRIMP+JPOINT*QPOINT*V(P))*K(P)
3220 LAMP=2
3230 171F(P)=AMAX1(0.0,F(P))
3240 71CONTINUE
3250C GRAVITY OPTION
3260 5420IF(IOPT14-2)5421,5423,5423
3270 5421IF(LACK-2)58,72,72
3280 58V(1)=V(1)-(F(1)+R(1)-W(1))*32.17*DELTAT/W(1)
3290 LACK=2
3300 GOTO5429
3310 72V(M)=V(M)+(F(M-1)-F(M)-R(M)+W(M))*32.17*DELTAT/W(M)
3320 5422GOTO5429
3330 5423IF(LACK-2)5424,5427,5427
3340 5424V(1)=V(1)-(F(1)+R(1))*32.17*DELTAT/W(1)
3350 5425LACK=2
3360 GOTO5429
3370 5427V(M)=V(M)+(F(M-1)-F(M)-R(M))*32.17*DELTAT/W(M)
3380 5429CONTINUE
3390 IF(M.GT.1)GOTO5430
3400 IF(F(1).LE.0..AND.V(1).LE.-0.1)V(1)=-VSTART
3410 5430FMAXC(M)=AMAX1(FMAXC(M),F(M))
3420 FMAXT(M)=AMIN1(FMAXT(M),F(M))
3430 5439IF(FMAXC(M)-F(M))166,167,166
3440 167NFMAXC(M)=N+1
3450 166IF(FMAXT(M)-F(M))68,69,68
3460 69NFMAXT(M)=N+1
3470 68STRESS(M)=F(M)/AREA(M)
3480 N=N+1
3490C THIS IS END OF DO 68 STARTING AT 5241
3491C ---- DETAILED OUTPUT(OPT15=2) OMITTED HERE-TAMU#5440TO 5444
3500 5444GOTO(5443,192),LAY
3510 5443IF((V(P)+0.1).GT.0.)GOTO192
3520 WV=0.0
3530 DO193JA=NSEG1,P
3540 193WV=WV+W(JA)*V(JA)
3550 IF(V(1).LT.0..AND.WV.LT.0..AND.DMAX(P).GT.D(P))GOTO190
3560 GOTO192
3570 190LAY=2
3580 192IF(V(2)/VSTART-3.1)61,60,60
3590 60WRITE(1;105)
3600 105FORMAT(51H THE RATIO OF THE VELOCITY OF W(2) TO THE VELOCITY,

```

Figure A1 (sheet 6 of 10)

```

3610&22HOF THE RAM EXCEEDS 3.1)
3620 GOT05570
3630 61IF(V(P)/VSTART-3.1)163,62,62
3640 62WRITE(1;106)
3650 GOT05570
3660 106FORMAT(42H THE RATIO OF THE VELOCITY OF W(P) TO THE/
3670&30HVELOCITY OF THE RAM EXCEEDS 3.1)
3680C ---END OF TEXAS REPN
3690 163CONTINUE
3700 IF(LAY.EQ.2)GOT05447
3710 IF(N-N2)5240,5447,5447
3720C ---- 5240 CYCLES FOR NEXT TIME INTERVAL
3730 5447D05449M=1,P
3740 5448FMAXC(M)=FMAXC(M)/AREA(M)
3750 5449FMAXT(M)=FMAXT(M)/(-AREA(M))
3760 GOT0(5442,5442,5553),IOPT15
3770 5442WRITE(1;2105)
3780 5550WRITE(1;2106)(M,AREA(M),NFMAXC(M),FMAXC(M),NFMAXT(M),FMAXT(M)
3790&,DMAX(M),D(M),V(M),M=1,P)
3800 BLOWS=0.0
3810 5553IF(DPRIMP.GT.0.0)BLOWS=1.0/DPRIMP
3820 5551UBLOWS(LT)=BLOWS
3830 URUTTL(LT)=RUTOTL
3840 UFMAXC(LT)=FMAXC(P)*AREA(P)
3850C INITIAL U ABOVE IDENTIFIES FIGURES USED IN SUMMARY
3860 GOT0(5552,5552,150),IOPT15
3870 5552WRITE(1;2107)DPRIMP,BLOWS,N
3880 2105FORMAT(/2X,"M AREA(M) N/C SMAX/C N/T SMAX/T"
3890&" DMAX D VELOCITY"/)
3900 2106FORMAT(I4,F8.2,I4,F10.0,I4,F10.2,2F10.4,F10.2)
3910 2107FORMAT(24H PERMANENT SET OF PILE =,F15.8/
3920&27H NUMBER OF BLOWS PER INCH =,F16.8/
3930&19H TOTAL INTERVALS = ,I8)
3940 150CONTINUE
3950 5558D05563M=NSEG1,P
3960 FTMAX(LT)=AMAX1(FTMAX(LT),FMAXT(M))
3970 FCMAX(LT)=AMAX1(FCMAX(LT),FMAXC(M))
3980 IF(FCMAX(LT)-FMAXC(M))5560,5561,5560
3990 5561NCMAX(LT)=M
4000 5560IF(FTMAX(LT)-FMAXT(M))5563,5562,5563
4010 5562NTMAX(LT)=M
4020 5563CONTINUE
4030 5555IF(IOPT11-2)5556,5570,5570
4040 5556IF(DPRIMP-0.001)59,707,707
4050 707IF(BLOWS-60.0)701,701,59
4060 59CONTINUE
4070 WRITE(1;803)CASE,PROB
4080 WRITE(1;804)QPOINT,JPOINT,QSIDE,JSIDE
4090 WRITE(1;805)
4100 D0801J=1,LT
4110 URUTON=URUTTL(J)/2000.
4120 801WRITE(1;802)UBLOWS(J),URUTTL(J),URUTON,UFMAXC(J),FCMAX(J),
4130&NCMAX(J),FTMAX(J),NTMAX(J)
4140 802FORMAT(2X,F7.3,1X,F8.0,"=",F6.0,"T",2X,2F10.0,15,F10.0,15)
4150 803FORMAT(/10X,22H PILE DRIVING ANALYSIS,10X,12H CASE NUMBER,3X,A6/
4160&1H&,9X,15H PROBLEM NUMBER,3X,I3)
4170 804FORMAT(19X,9HQPOINT = F5.2,11X,9HJPOINT = F5.2/19X,
4180&9HQSIDE = F5.2,11X,9HJSIDE = F5.2/)
4190 805FORMAT(2X,"BLOWS/IN. RUTOTAL PT FORCE MAX C STR-",
4200&"SEG MAX T STR-SEG"/)
4210C PLOTTING ROUTINE

```

Figure A1 (sheet 7 of 10)

```

4220 IF(LOPT13-1)5570,5574,5574
4230 5574CALLDRAW(WTOTAL,URUTT,UBLOWS,LT,CASE,PROB)
4240C      END PLOTTING ROUTINE
4250 5570WRITE(1;5572)
4260C      DO 5570 STARTS AT 5120
4270 5572FORMAT(/32X,8H*****/)
4280 5571GOTO5010
4290 END
4300 SUBROUTINEDRAW(WTOTAL,URUTT,UBLOWS,LT,CASE,PROB)
4310 DIMENSIONURUTT(24),UBLOWS(24),YPLT(50),XPLOT(50)
4320 5574YPLT(1)=0.
4330 XPLOT(1)=0.
4340 LTP1=LT+1
4350 DO5573IP=1,LT
4360 YPLT(IP+1)=URUTT(IP)/2000.
4370 5573XPLOT(IP+1)=UBLOWS(IP)
4380 YMAX=YPLT(LTP1)
4390 N2=N2
4400 IF(YMAX.LE.400.)GOTO3
4410 IF(YMAX.LE.800.)GOTO4
4420 IF(YMAX.LE.1600.)GOTO5
4430 IF(YMAX.LE.3200.)GOTO6
4440 3DY=50.
4450 GOTO10
4460 4DY=100.
4470 GOTO10
4480 5DY=200.
4490 GOTO10
4500 6DY=400.
4510 10DX=10.
4520 PPROB=PROB
4521 WRITE(3,100) CASE,PPROB,DX,DY,WTOTAL
4522 DO 25 I=1,LTP1
4523 XPLOT(I)=XPLOT(I)/DX
4524 YPLT(I)=YPLT(I)/DY
4525 25 WRITE(3,101) XPLOT(I),YPLT(I)
4526 100 FORMAT(A6,I4,3F10.2)
4527 101 FORMAT(SX,2F10.3)
4530 RETURN
4540 END
4550 SUBROUTINEDELTC(NPASS,TTDELT,P,W,K,TDELTA,DELTAT,N2)
4560 DIMENSIONW(1),K(1),DELT1(300)
4570 REALK,NPASS
4580 INTEGERP,PLESS1
4590 PLESS1=P-1
4600 N=2*P-1
4610 SUM=0.
4620 TMIN=1.
4630 TDELTA=TTDELT
4640 DELTAT=1./TDELTA
4650 DO1M=1,PLESS1
4660 DELT1(M)=SQRT(W(M+1)/K(M))/19.648
4670 NN=PLESS1+M
4680 1DELT1(NN)=SQRT(W(M)/K(M))/19.648
4690 IF(K(P).GT.0.)GOTO2
4700 DELT1(N)=1.0
4710 GOTO3
4720 2DELT1(N)=SQRT(W(P)/K(P))/19.648
4730 3DO4M=1,N
4740 4TMIN=AMIN1(TMIN,DELT1(M))
4750 IF(TMIN/2.-DELTAT)5,6,6

```

Figure A1 (sheet 8 of 10)

\*OLD LD4TP1  
READY  
\*LIST

10 "LD4/1",6,0,13,1000,1000,0,2,1,1,2,20,3,  
20 0,1710,293,293,293,293,293,293,293,293,293,  
30 1.01E07,8.56E06,8.56E06,8.56E06,8.56E06,8.56E06,8.56E06,8.56E06,  
40 8.56E06,8.56E06,8.56E06,8.56E06,  
50 1,17,12,17,12,17,12,17,12,17,12,17,12,17,12,17,12,  
60 17,12,17,12,  
100 1,14000,15,1,.85,36000,.8,1,1,100000,24,3,11,.1,.15,.05,0,  
110 2,2,0,1,1,  
200 2,14000,15,1,.85,36000,.8,1,1,200000,24,3,11,.1,.15,.05,0,  
210 2,2,0,1,1,  
300 3,14000,15,1,.85,36000,.8,1,1,300000,24,3,11,.1,.15,.05,0,  
310 2,2,0,1,1,  
400 4,14000,15,1,.85,36000,.8,1,1,400000,24,3,11,.1,.15,.05,0,  
410 2,2,0,1,1,  
500 5,14000,15,1,.85,36000,.8,1,1,500000,24,3,11,.1,.15,.05,0,  
510 2,2,0,1,1,  
600 6,14000,15,1,.85,36000,.8,1,1,600000,24,3,11,.1,.15,.05,0,  
610 2,2,0,1,1,  
1000 0,0,0,0,0,

\*OLD LD4TP2  
READY  
\*LIST

10 "LD4/2",6,0,13,1000,1000,0,2,1,1,2,20,3,  
20 0,1710,408,408,408,408,408,408,408,408,408,  
30 1.01E07,1.19E07,1.19E07,1.19E07,1.19E07,1.19E07,1.19E07,1.19E07,  
40 1.19E07,1.19E07,1.19E07,1.19E07,1.19E07,1.19E07,  
50 1,23.86,23.86,23.86,23.86,23.86,23.86,23.86,23.86,23.86,23.86,23.86,23.86,  
60 23.86,  
100 1,14000,15,1,.85,36000,.8,1,1,100000,30,3,.133,.1,.15,.05,0,  
110 2,2,0,1,1,  
200 2,14000,15,1,.85,36000,.8,1,1,200000,30,3,.133,.1,.15,.05,0,  
210 2,2,0,1,1,  
300 3,14000,15,1,.85,36000,.8,1,1,300000,30,3,.133,.1,.15,.05,0,  
310 2,2,0,1,1,  
400 4,14000,15,1,.85,36000,.8,1,1,400000,30,3,.133,.1,.15,.05,0,  
410 2,2,0,1,1,  
500 5,14000,15,1,.85,36000,.8,1,1,500000,30,3,.133,.1,.15,.05,0,  
510 2,2,0,1,1,  
600 6,14000,15,1,.85,36000,.8,1,1,600000,30,3,.133,.1,.15,.05,0,  
610 2,2,0,1,1,  
1000 0,0,0,0,0,

\*OLD LD4TP3  
READY  
\*LIST

10 "LD4/3",6,0,13,1000,1000,0,2,1,1,2,20,3,  
20 0,1710,468,468,468,468,468,468,468,468,468,  
30 1.01E07,1.368E07,1.368E07,1.368E07,1.368E07,1.368E07,1.368E07,1.368E07,  
40 1.368E07,1.368E07,1.368E07,1.368E07,1.368E07,  
50 1,27.36,27.36,27.36,27.36,27.36,27.36,27.36,27.36,27.36,27.36,27.36,  
60 27.36,27.36,  
100 1,14000,15,1,.85,36000,.8,1,1,100000,36,3,.167,.1,.15,.05,0,  
110 2,2,0,1,1,  
200 2,14000,15,1,.85,36000,.8,1,1,200000,36,3,.167,.1,.15,.05,0,  
210 2,2,0,1,1,  
300 3,14000,15,1,.85,36000,.8,1,1,300000,36,3,.167,.1,.15,.05,0,  
310 2,2,0,1,1,  
400 4,14000,15,1,.85,36000,.8,1,1,400000,36,3,.167,.1,.15,.05,0,  
410 2,2,0,1,1,  
500 5,14000,15,1,.85,36000,.8,1,1,500000,36,3,.167,.1,.15,.05,0,  
510 2,2,0,1,1,  
600 6,14000,15,1,.85,36000,.8,1,1,600000,36,3,.167,.1,.15,.05,0,  
610 2,2,0,1,1,  
1000 0,0,0,0,0,

Figure A1 (sheet 9 of 10)



```
4760 SDELTA=TMIN/2.  
4770 TDELTA=1.0/DELTA  
4780 6DO7M=1,N  
4790 7SUM=SUM+DELTA(M)  
4800 N2=4.0*SUM/(2.0*DELTA)  
4810 RETURN  
4820 END
```

READY

Figure A1 (sheet 10 of 10)



## APPENDIX B: NOTATION

$a$	arbitrary stress wave magnitude
$\bar{a}$	particle acceleration
$A$	cross-sectional area, $L^2$
$\bar{A}$	ratio of ram weight to drivehead weight
$\bar{B}$	ratio of hammer impedance to pile impedance
$c$	velocity of wave propagation
$C$	spring compression, in.
$C_m$ max	temporary maximum compression value previously computed
$\bar{d}$	distance from exhaust ports to anvil, $L$
$d_m^*$	value of displacement after $n - 2$ time intervals
$D$	displacement of point mass, in.
$D'$	plastic displacement of point mass, in.
$e$	coefficient of restitution
$E$	Young's modulus, psi
$E_E$	explosive energy of the diesel hammer system which performs useful work, FL
$E_K$	rated kinetic impact energy of diesel hammer, FL
$E_R$	ram output energy, FL
$F$	spring force, lb; force
$\bar{F}$	resultant force
$g$	gravity acceleration, 32.2 ft/sec/sec
$h$	hammer stroke (height of fall), $L$
$h_e$	"equivalent" hammer stroke
$i, j$	node number (may be used as subscript)
$J, J_p$	point resistance damping constant, sec/ft

$J', J_s$  shaft resistance damping constant, sec/ft  
 $K$  pile element spring constant, lb/in.  
 $K'$  soil element spring constant, lb/in.  
 $K_H$  horizontal point spring constant  
 $K_V$  vertical "point spring" constant  
 $\ell$  pile element length, in.  
 $L$  length  
 $m$  subscript denotes pile element  
 $M$  mass  
 $n$  subscript denotes current time interval of computation  
 $N$  exponent of velocity  
 $o$  subscript denoting initial value with respect to time  
 $p$  value of  $m$  subscript for pile tip element  
 $P$  operating steam or air pressure,  $F/L^2$   
 $P_{rated}$  manufacturer's rated steam or air pressure,  $F/L^2$   
 $Q$  quake (maximum elastic soil deformation), in.  
 $Q_p$  elastic quake at pile joint  
 $Q_s$  elastic quake at the pile shaft  
 $r, z, \theta$  coordinate system  
 $R$  element resistance force, lb,  $F/L$   
 $RU$  element maximum static soil resistance, lb  
 $s$  permanent pile set, in.  
 $t$  time  
 $\bar{T}$  pseudoperiod of the ram cushion, sec  
 $T$  element critical time interval, sec  
 $u$  element displacement,  $L$

$\dot{u}$  derivative of displacement with respect to time  
 $\ddot{u}$  second derivative of displacement with respect to time  
 $u_1$  ram displacement  
 $u_2$  drivehead displacement  
 $V$  element velocity, ft/sec  
 $V_R$  initial ram impact velocity  
 $W$  element weight, lb  
 $W_H$  weight of hammer housing, F  
 $W_R$  ram weight, F  
 $x$  coordinate location of a point along the rod  
 $Z$  resultant force on element, lb  
 $\delta$  interface friction angle  
 $\epsilon_x$  strain at a point along the rod  
 $\zeta$  dimensionless time variable  
 $\eta$  hammer mechanical efficiency  
 $\bar{\theta}$  interval of revolution used in the element stiffness formulation  
 $\rho$  mass density, M/L<sup>3</sup>  
 $\sigma_n$  normal stress on pile-soil interface  
 $\sigma_x$  stress at a point on the rod, F/L<sup>2</sup>  
 $\tau$  shear stress on failure plane  
 $\frac{\partial^2 u}{\partial x^2}$  first partial derivative of displacement with respect to location  
 $\frac{\partial^2 u}{\partial x^2}$  second partial derivative of displacement with respect to location  
 $\frac{\partial^2 u}{\partial t^2}$  second partial derivative of displacement with respect to time

$\Delta t$  time increment magnitude used for calculation, sec

$\Delta x$  pile element length

